
Mitigation and Prevention of Lunar Dust on NASA Artemis xEMU Spacesuits

Final Report
December 9, 2020

Course Information MECHENG 450, FA 2020
Instructor Heather Cooper
Team Information Section 003, Team 04
Sponsor Information NIA & NASA
 bigidea@nianet.org

Mihir Gondhalekar mihirg@umich.edu
Chad Parks chadprks@umich.edu
Nikhil Shetty nhshetty@umich.edu
Brian Wang brianwan@umich.edu

CONTENTS

EXECUTIVE SUMMARY	5
PROBLEM DEFINITION AND BACKGROUND	5
An Introduction to the Lunar Dust Problem	5
The Adverse Effects of Lunar Dust on Space Equipment	5
The Adverse Effects of Lunar Dust on Human Health	5
Properties of Lunar Dust	5
Physical Properties of Lunar Dust	7
Chemical Properties of Lunar Dust	8
The 2021 NASA Big Idea Challenge	10
The Detrimental Effects of Lunar Dust on Spacesuits	11
Analysis of Wear on Apollo Mission EVA Spacesuits	11
Mechanisms of Lunar Dust Transport and Interaction in Lunar Conditions	18
Project Goal and Stakeholders	20
BENCHMARKING	21
Electrodynamic Dust Shields (EDS)	21
Work Function Matching Coating	21
PLZT Dust Removal	21
Magnetic Filtration and Microwave Radiation	22
REQUIREMENTS AND ENGINEERING SPECIFICATIONS	23
CONCEPT EXPLORATION	24
Concept Generation	24
Generation Methods	24
Generation Results	24
Concept Development	26

Development Methods	26
Development Results	27
Concept Screening	28
Concept Screening Technique	28
Concept Screening Implementation	29
Solutions Eligible for Concept Selection Stage	30
CONCEPT SELECTION	34
Final Concept Selection Strategy	34
Sticky Mats	34
Boot Brush	35
Electrodynamic Dust Shields (EDS)	36
Efficacy Testing	36
Lunar Dust Simulant	36
Teflon Fabric Simulant	37
Test Box	38
Weighing Scale	39
Efficacy Testing Strategy	40
ENGINEERING ANALYSIS	43
Post EVA Removal Solution Analysis	43
Sticky Mats	43
Boot Brushes	44
Numerical Analysis of EDS Phenomenon	45
Motivation	46
Simulation Strategy	46
Physical Assumptions	48
Proposed Numerical Scheme	49

Limitations of Numerical Scheme	50
Numerical Analysis Findings	51
Power Calculations for EDS Circuit	56
EDS Circuit Analysis	57
RISK ASSESSMENT	58
Failure Mode and Effects Analysis (FMEA) Setup	58
Risk Mitigation Strategies	58
DETAILED DESIGN SOLUTION	59
FINAL DESIGN VERIFICATION	62
Able to Mitigate Small Particles	62
Easily Adoptable by NASA	62
Operable in Harsh Lunar Environments	63
TRL-4 Compliance	63
Durable	63
Cost Effective	63
Minimal Required Operation Time	64
DISCUSSION AND RECOMMENDATIONS	65
Suit Assembly Plan and Materials	65
Cost Comparison of Electrode Material	65
Wearing Procedure	66
Anticipated Project Challenges	66
EDS Challenges	66
Testing Equipment Challenges	67
Materials Challenges	67
Further Expertise Requirements	67
CONCLUSION	67

AUTHORS	69
ACKNOWLEDGMENTS	70
REFERENCES	71
APPENDIX A (IMPORTANT SUPPORTING DOCUMENTATION)	74
APPENDIX B (SUPPLEMENTAL CONTEXT)	86
APPENDIX C (NUMERICAL SIMULATION CODE)	91
APPENDIX D (CONCEPT SCREENING DOCUMENTATION)	96
APPENDIX E (EDS CIRCUIT CONTROLLER CODE)	101

EXECUTIVE SUMMARY

Ever since the start of NASA's Apollo missions, humanity has sought to establish human settlements on the moon. One of the greatest challenges obstructing the path of this dream is the existence of highly harmful dust across the lunar surface. In past Apollo missions, lunar dust has proved to adversely impact lunar instrumentation, habitats, and spacesuits. More concerningly, lunar dust has also shown to cause respiratory and cardiovascular diseases for astronauts. With hopes of bringing humankind back to the surface of the moon as part of the 2024 Artemis missions, NASA is looking to address the problems with lunar dust. The premise of our ME450 senior design project is to develop a strategy to mitigate the damaging effects of lunar dust, specifically on the Artemis xEMU spacesuits which will be used for the Artemis missions. The following report describes Team 4's development of a solution strategy that removes and mitigates lunar dust exposure on xEMU spacesuits.

Identifying solutions that are efficient in removing lunar dust was the primary motivation during the concept generation and concept evaluation processes. Extensive literature review was conducted initially to build an understanding of the problem scope and search existing solutions. By doing so, we were able to justify critical aspects of our solution strategy and parts of the design process. Through communication with NASA and other stakeholders, we were able to derive a full set of requirements and specifications, which helped guide the project to success. The requirements for the solution include being able to mitigate small particles, easily adoptable, operable in harsh lunar environments, TRL-4 compliance, durable, cost effective, and minimal required operation time. With these requirements and specifications in mind, we conducted literature research and concept generation techniques to generate preliminary concept ideas. These concepts were split into two categories, real-time mitigation concepts and post-EVA concepts (extravehicular activity), based on the nature of NASA missions and interactions between astronauts and lunar dust. Through thorough concept selection, we narrowed down the list of concepts to three, sticky mats, boot brushes, and EDS (electrodynamic dust shields). Sticky mats typically retain debris that comes into contact with it, boot brushes are used to mechanically remove dirt or other debris from surfaces, and EDS uses electrostatic forces to expel a repulsive field, pushing away the electrostatically charged lunar dust.

The selected concepts were put through efficacy tests to determine which would have the best efficiency of removing dust, and therefore be the best solution. Through physical testing and virtual simulation, we determined EDS was the best solution for removing and mitigating lunar dust. Afterwards, we performed engineering analysis and risk assessment to create a draft for a detailed final solution, which satisfies all of the requirements and specifications. Due to time constraints and COVID restrictions, a physical prototype of the final solution was not possible to build. The final EDS solution consists of an electrode sleeve that is attachable to the surface areas of the Artemis spacesuits that are more vulnerable to lunar dust, which include the upper arms, forearms, thighs, and calves. The electrode sleeves are constructed of high elasticity ortho-fabric, and will have an EDS mesh sewn into the fabric. The EDS circuit is powered by an AC power supply and generates an electric field across the surface of its electrode mesh. If we are chosen to move forward with the 2021 NASA Lunar Dust Challenge, we will continue work on this solution, particularly with a physical prototype of the proposed final design solution.

PROBLEM DEFINITION AND BACKGROUND

Since the conclusion of the Apollo missions, NASA has been planning to return to the moon's surface. One major barrier to returning - is the presence of lunar dust. It is tiny, abrasive, and adheres to most surfaces. In order to return to the moon safely, a solution must be developed that can mitigate the adherence of lunar dust to spacesuits, equipment, and lunar habitats.

An Introduction to the Lunar Dust Problem

The surface of the moon is covered with fine particles of lunar dust. During the Apollo missions, NASA found that the dust is extremely damaging and abrasive. To make matters worse, lunar dust is able to adhere to almost all surfaces. These properties allow lunar dust to pose several difficulties for any astronauts attempting to explore the lunar surface.

The Adverse Effects of Lunar Dust on Space Equipment. The dust can damage the astronauts' spacesuits and equipment while performing extravehicular activities (EVA). In addition, due to the dust's adhesive nature, it is very easy for astronauts to carry unwanted dust after EVAs are performed. If the dust is not removed after an EVA, it can cause damage to spacecraft, the internal habitats, and any technology or equipment that is exposed. It can disrupt sensors and potentially cause equipment failure, resulting in millions of dollars going to waste and causing the failure of lunar missions.

The Adverse Effects of Lunar Dust on Human Health. Despite all of these threats, perhaps the most dangerous problem is that lunar dust can be detrimental for an astronaut's health. Due to its small size, it is easy for astronauts to inhale. This can damage their lungs and allow dust to enter the bloodstream. A study by researchers at the University of Tennessee analyzed the impact of different size ranges of lunar dust on humans. While they concluded that the bulk of the particles were found to be drivers in serious respiratory system issues, including high-risk lung fibrosis, they also shockingly discovered that the extremely small particles towards the lower end of the size distribution ($< 0.1 \mu\text{m}$ in diameter) were capable of entering the human bloodstream and triggering a reduction in hemoglobin levels due to chemical reactions between the particles and Fe^{3+} [1].

A quote from Eugene Cernan, an astronaut on the Apollo 17 mission, sums up the problems lunar dust poses: "One of the most aggravating, restricting facets of lunar surface exploration is the dust and its adherence to everything no matter what kind of material, whether it be skin, suit material, metal, no matter what it be and its restrictive friction-like action to everything it gets on." [2]. For these reasons, it is crucial that the lunar dust problem is properly dealt with and solved for the NASA Artemis exploration missions in 2024. This paper will outline our solution to the lunar dust problem and provide an in-depth analysis of its properties.

Properties of Lunar Dust

Before understanding what sort of impact lunar dust has on lunar exploration missions, it is imperative to understand the physical and chemical properties of lunar dust. These properties will give us more insight into why lunar dust is considered to be one of the biggest hindrances to astronauts, and why its interaction with space equipment, lunar habitats, and other aspects of space travel is an important problem today.

Physical Properties of Lunar Dust. One of the most important properties of lunar dust is that the particles are not naturally found with uniform size. When talking about the size (diameter) of lunar dust particles, researchers typically refer to a size distribution. In all of the research on lunar dust, the particles are always assigned a certain mean, which is then placed within a range of size values. From this range and mean, values for standard deviation and skew of the size distribution can be obtained. These variables together give a somewhat complete description of the size range of a lunar dust sample. Since most research tends to analyze clumps of lunar dust particles, it is fitting to represent the individual particles within these clumps as having a certain mean diameter along with a standard deviation around this mean. Looking at lunar dust particles individually, however, we see that these size ranges can spread across a large spectrum, with most particles falling into a diameter range of 0.1 μm to 50 μm [1]. The image below shows an example size distribution obtained from a lunar dust sample from the outer surface of an Apollo 17 spacesuit's ITMG layer.

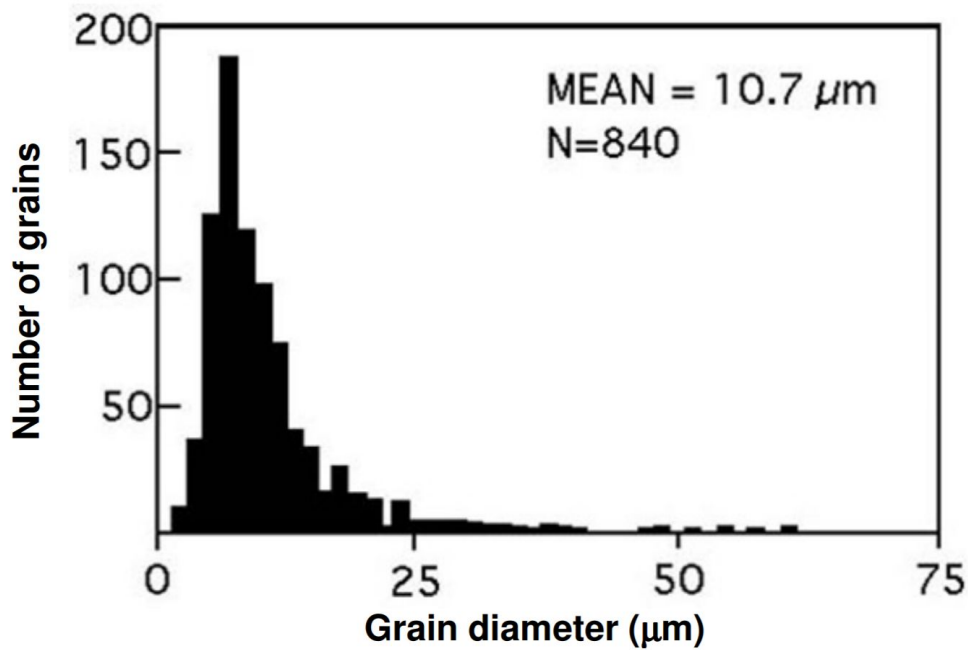


Figure 1. Size distribution of lunar dust particles obtained from the outer surface of an Apollo 17 spacesuit ITMG layer through adhesive tape extraction process [3].

From this distribution, we see that the majority of particles that were obtained from this sample agglomerated towards the lower end of the size spectrum, making the distribution highly right-skewed. This is unfortunately one of the reasons why lunar dust can tend to be easily transferable and very dangerous to humans.

Along with the size distribution of lunar dust, many researchers have also attempted to characterize the physical topography of singular lunar dust particles. Analyzing these lunar dust particles in clumps is not necessarily useful for analyzing each particle's surface structures, so researchers had to depend on SEM technology to obtain well-refined results. In simple terms, lunar dust particles are formless and tend to come in a variety of geometries. A study in 2008 by the University of Tennessee obtained lunar dust samples from various Apollo missions and characterized each sample based on its aspect ratio and surface roughness. The study found most lunar dust particles within the samples to be highly angular, jagged, and irregular in form [1]. They once again were required to construct a distribution when analyzing these factors in order to capture the full range of properties for the lunar dust samples. For each particle, the aspect ratio was measured by finding the ratio between the particle's short axis and its long axis. The bulk of the distribution was situated within the values of 0.5 to 0.8 for most of the samples, indicating the fairly long nature of the particles. Analogously, surface roughness was characterized by a complexity factor, which was calculated by dividing the ratio of the particle's perimeter by the perimeter of an optimally fit ellipse. Most particles possessed a complexity factor of 1.25, suggesting that they were fairly angular and jagged in geometry [1].

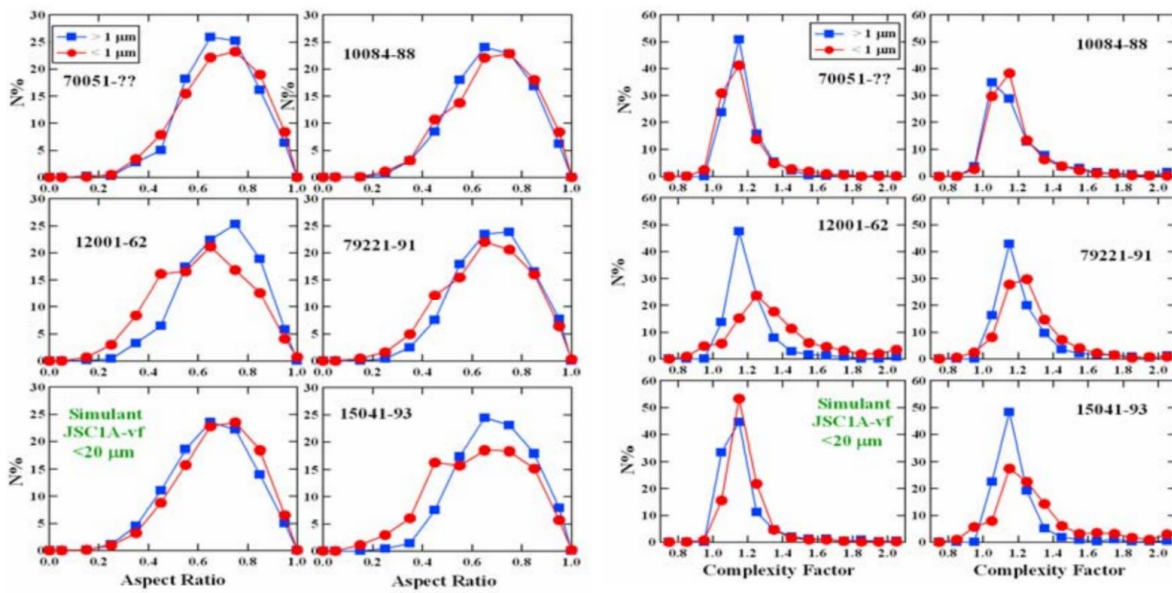


Figure 2. Graphs on the left represent aspect ratios for each lunar dust sample investigated. Aspect ratio here is defined as the ratio between a particle's short axis and its long axis. Graphs on the right represent complexity factors for each lunar dust sample investigation. Complexity factor is a measurement of surface roughness and is the ratio between a particle's real perimeter and its optimal ellipse's perimeter [1].

Chemical Properties of Lunar Dust. While the physical properties of lunar dust mentioned above indicate that the particles are quite dangerous, research on the chemical decomposition of lunar dust has come to show why lunar dust is fatal in more than just a physical sense. The same study from above by the University of Tennessee performed chemical decomposition analysis on the same strains of lunar dust and recovered the following breakdown data.

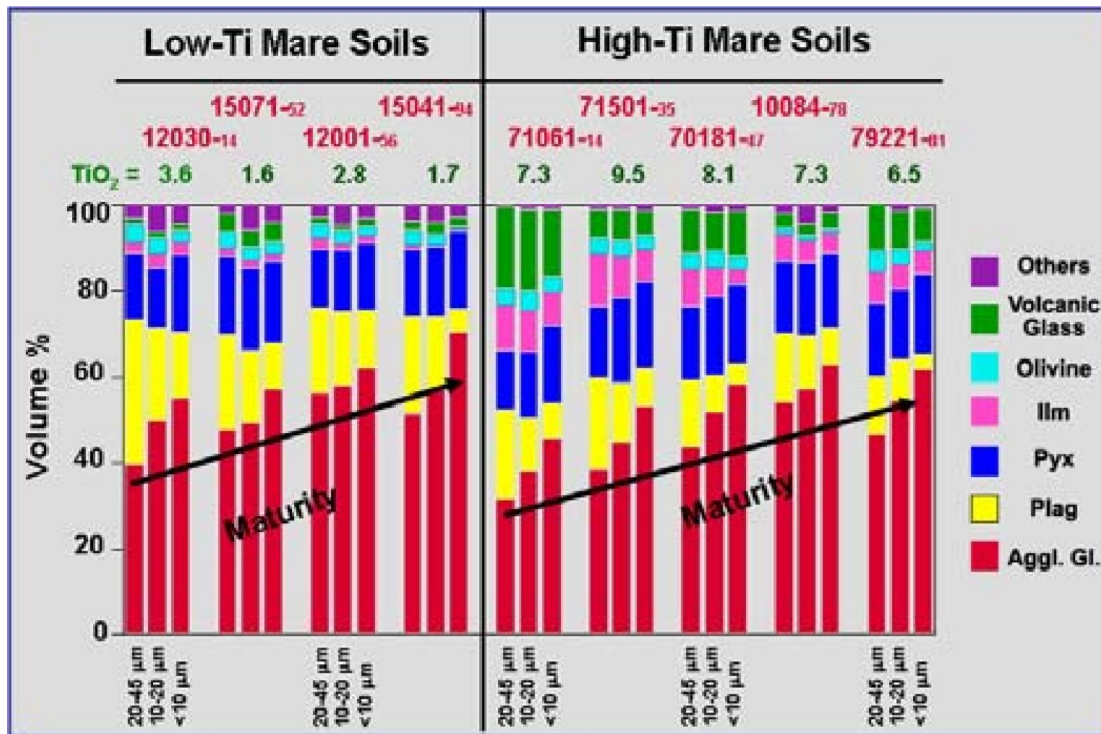


Figure 3. Modal percentage (by volume) of mineral substances found in several samples of lunar dust particles. “Aggl. Gl.” stands for agglutinitic glass, “Pyx.” stands for pyroxene, and “Plag.” stands for plagioclase [1].

From the above figure we see that the majority of the lunar dust samples, once decomposed, produced agglutinitic glass, plagioclase, pyroxene, and several other minerals in trace amounts. The substances which were the most abundant in these decomposed samples, however, were the agglutinitic glass, plagioclase, and pyroxene. It was also found that with higher levels of agglutinitic glass, there were also higher levels of nanophase metallic iron present. Dust particles with mean diameters of 10 µm or under were found to have roughly 80% by volume worth of agglutinitic glass in the chemical composition. From this, the study inferred that fully respirable lunar dust particles of diameters smaller than 2.5 µm contain more than 80% by volume of agglutinitic glass and nanophase metallic iron, both of which are highly toxic to humans [1].

Furthermore, relationships between the physical structure of these lunar dust particles and their chemical toxicity provide deeper insight into why lunar dust particles are destructive in nature, and highlight the urgency of the lunar dust problem. Research has shown that smaller lunar dust particles tend to possess more irregularities in structure due to the presence of vesicles, mounds, and bumps. These structures increase the effective surface area of these particles, making them much more reactive than if they were globular in structure [1]. This increased reactive surface area coupled with the presence of toxic minerals

in the chemical composition is the overarching reason why inhalation of lunar dust particles can be extremely hazardous to crew.

This section only details through a narrow body of research conducted on lunar dust particles, but even with this evidence it is obvious that lunar dust does not behave like ordinary dust particles one would expect to interact with on Earth or Mars. Lunar dust is much more irregular and complex, and the research done on samples has shown the repercussions of interacting with lunar dust to be much more fatal. Studying the properties of lunar dust will allow research groups to deeply understand by what mechanisms lunar dust can interfere with all things space related, and it is only with this knowledge that these groups can then evaluate these mechanisms and propose solutions.

The 2021 NASA Big Idea Challenge

The 2021 Big Idea Challenge from NASA explores the lunar dust concept and the many challenges it poses to space exploration, as established by the problem description in this report. With the abundance of evidence regarding the detrimental nature of lunar dust, NASA is proposing a challenge in which they are asking engineering, scientists, and researchers around the globe to investigate the current situation of lunar dust interactions with various facets of space exploration, and propose a solution or strategy which can be used to mitigate or even alleviate the lunar dust problem for the future of space travel. The challenge itself is very open-ended; however, it is segmented into four sub-challenges which each attribute to a different challenge that is associated with lunar dust. This table below introduces the four sub-challenges of the 2021 Big Idea Challenge from NASA and illustrates the problem each sub-challenge is aiming to resolve.

Table 1. List of sub-challenges from the NASA 2021 Big Idea Challenge [4].

Sub-Challenge Number/Title	Sub-Challenge Description
#1. Landing Dust Prevention and Mitigation	To protect from plume/surface interactions which may result in damaged landers and nearby surface assets.
#2. Spacesuit Dust Tolerance and Mitigation	To limit dust adherence to spacesuits and other deleterious effects to its subsystems.
#3. Exterior Dust Prevention, Tolerance, and Mitigation	To protect lunar surface systems or preclude dust from entering habitats and landers.
#4. Cabin Dust Tolerance and Mitigation	To clean habitable volumes and their interior surfaces, which helps prevent dust from making it back to Gateway and Orion when the lander returns to lunar orbit from the surface.

In order to determine which lunar dust challenge would be the most applicable and feasible to complete in regards to the time frame of the project and various other external conditions, we constructed a Pugh

matrix evaluating these various conditions with each challenge. Note that this design project was conducted during the SARS-CoV-2 outbreak of 2020, meaning that larger-than-normal restrictions were imposed on us during our execution of the design process. The Pugh matrix below lists the four different sub-challenges along with the different factors which were evaluated and their respective weights.

Table 2. Pugh matrix of the four 2021 Big Idea Challenge sub-challenges.

		Challenges			
Criteria	Weights	#1	#2	#3	#4
Feasibility	5	0	1	-1	1
Availability of literature	4	0	1	0	0
Easily virtualizable	3	0	0	0	0
Level of interest	2	0	1	0	0
Level of urgency	2	0	1	1	-1
Total Score		0	13	-3	3
Rank		3	1	4	2

From this Pugh matrix, it is evident that the sub-challenge our team decided to focus on for this project is the #2, Spacesuit Dust Toleration and Mitigation challenge. The fact that this specific issue with lunar dust has been researched the most, poses one of the highest levels of urgency, and is yet the most feasible and easily testable issue makes it the clear choice for the 2021 Big Idea Challenge. The remainder of this Problem Definition and Background portion of the report will discuss specifically the threats that lunar dust particles pose on the functionality and lifetime of spacesuits and why this in turn could lead to adverse health impacts on the astronauts in mission.

The Detrimental Effects of Lunar Dust on Spacesuits

Many research groups in the past have taken the initiative to analyze spacesuit samples from various Apollo missions and study what sorts of impact lunar dust particles can have on the lifetime and functionality of these spacesuits. Spacesuits are an essential asset to space exploration, as they don't only protect the astronauts from the harsh extra-terrestrial conditions that they otherwise would not survive in but also provide several other resources to assist astronauts during extravehicular activities (EVA). In accordance with this, also understanding the various mechanisms through which lunar dust is transferred onto spacesuits is integral in obtaining more knowledge about the problem at hand.

Analysis of Wear on Apollo Mission EVA Spacesuits. An important study on the impact of lunar dust on spacesuits was published by researchers from NASA in 2009. In this study, researchers from NASA inspected A7L/A7LB spacesuits that were worn during EVA from the Apollo 12, 16, and 17 missions [3].

These spacesuits were found to be constructed from multi-layered fabrics, with each layer having its own purpose in the holistic spacesuit system. These layers were obviously inherent to the Apollo 12, 16, and 17 mission spacesuits, but highlights the fact that all spacesuits used in these missions were composed of multiple layers for enhanced protection and robust functionality. The layers found in the Apollo 12, 16, and 17 spacesuits can be seen in the table below.

Layer Sequence (relative to surface)	Material	1st-Level Function	2nd-Level Function	Description
1a	Teflon® cloth (T-164 8.5 oz woven Teflon® fabric)	Abrasion resistance	Flame resistance	Used for extra abrasion resistance on selected areas: knee, waist, elbow, and shoulder
1b	Teflon®-coated filament beta cloth (beta 4484)	Flame resistance	Abrasion resistance	Provided continuous outer fabric flame and abrasion resistance
2	Aluminized Kapton® film/beta marquisette* laminate	Thermal radiation protection	Thermal cross section	Provided thermal and micrometeoroid protection
3	Aluminize Mylar®	Thermal radiation protection		
4	Non-woven Dacron®	Thermal spacer layer		Provided thermal protection
Repeat 3				
Repeat 4				
Repeat 3				
Repeat 4				
Repeat 3				
Repeat 4				
Repeat 3				
Repeat 2				
5	Rubber-coated nylon (ripstop)	Inner liner	Contact layer with the TLSA	

Figure 4. Material sequence for spacesuit ITMG fabric layering [3].

Additionally, each of these layers is woven in nature, meaning that the entire fabric layer was created from the intertwining of singular weave structures. The researchers obtained three different spacesuit samples, one from each Apollo mission investigated, and performed a study in which their goal was to identify the main cause of wear in these spacesuits throughout the duration of their respective missions. They utilized several analysis techniques to determine the concentration of lunar dust particles found on specific areas of the spacesuits. These techniques included adhesive tape extraction, optical microscopy, scanning electron microscopy (SEM), and X-ray fluorescence spectroscopy. Optical microscopy was first used to identify areas of the spacesuit with the highest concentrations of lunar dust to a certain resolution.

The tape extraction procedure was then used to extract a certain sample of lunar dust particles from these areas of highest concentration [3]. This method was shown to be the least destructive method of obtaining lunar dust samples. After obtaining the lunar dust sample on the adhesive, the researchers would then conduct SEM imaging tests and X-ray fluorescence spectroscopy on these samples to determine the distribution of lunar dust particles found and their chemical signatures [3].

This tape extraction procedure would be an indicator of how easily removable lunar dust is from the spacesuits. As we know from above, spacesuits are multi-layered in nature, and the small magnitude of lunar dust particles suggests that they could in theory penetrate through several layers of the spacesuit depending on the weave size and other factors. The researchers also ran X-ray fluorescence spectroscopy on these tape samples to determine the relative amount of lunar dust found in the area as well as the chemical decomposition of the strains [3]. A diagram of the process flow is shown below.

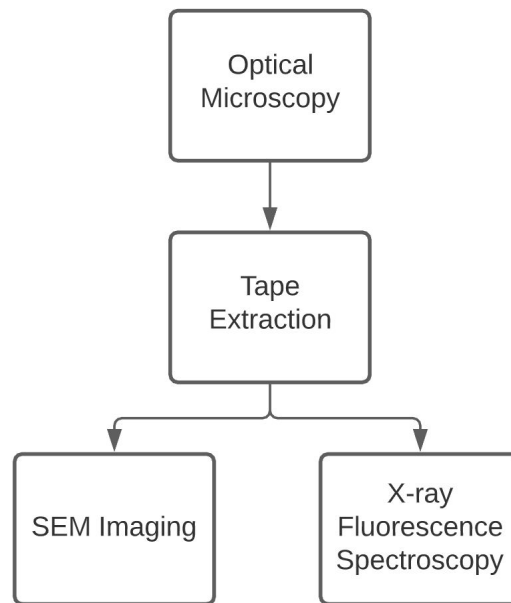


Figure 5. Process flow diagram of research conducted on lunar dust concentrations on Apollo 12, 16, and 17 EVA spacesuits.

The results from the study revealed critical information and provided deep insight into how lunar dust particles interacted with the Apollo mission spacesuits and why these interactions were not only a problem for spacesuit functionality but also posed threats to astronauts in both EVA and intravehicular (IVA) conditions. Firstly, the optical microscopy study showed that the anterior leg, upper torso, and forearm areas of the Apollo spacesuits seemed to possess the highest concentration of lunar dust particles after EVA [3]. The image below is from the Apollo 17 spacesuit, and it's clearly visible that the dark, ashy areas of the spacesuit represent the areas of highest lunar dust concentration.



Figure 6. Standard imaging of anterior and posterior positions of Apollo 17 EVA spacesuit. Areas of highest lunar dust concentration are shown as dark grey patches near the leg, upper torso, and forearm areas. Bare schematics with ovals represent lunar dust sampling locations for tape extraction procedure.

We also see that the areas with the darkest grey hue are found mostly near the leg and torso area of the spacesuit, although there are also certain areas near the forearms which have this dark hue. This result seems absolutely logical, as the majority of EVA are performed with astronauts walking around the surface of the moon, suggesting that particles are most easily adhered to the areas of the spacesuit closest to the moon's surface [3].

The results from the SEM imaging tests show how the lunar dust particles are distributed along the inspected spacesuit layers. These tests were performed on the Apollo 12 spacesuits. Along with obtaining images from the spacesuits used during the actual mission, the researchers also contaminated clean non-flight Apollo 12 spacesuit samples with lunar dust simulant and performed SEM imaging on these samples to determine whether the wear patterns were consistent with the true spacesuit samples. This allowed the researchers to isolate wear from lunar dust particles from any other potential sources of wear and abrasion. After conducting these tests, the researchers were able to retrieve the following SEM images for the actual Apollo 12 spacesuits used during EVA [3]. The image below shows a patch sample from the left knee area of the spacesuit, which was identified to possess one of the highest levels of lunar dust concentration from the optical microscopy test.

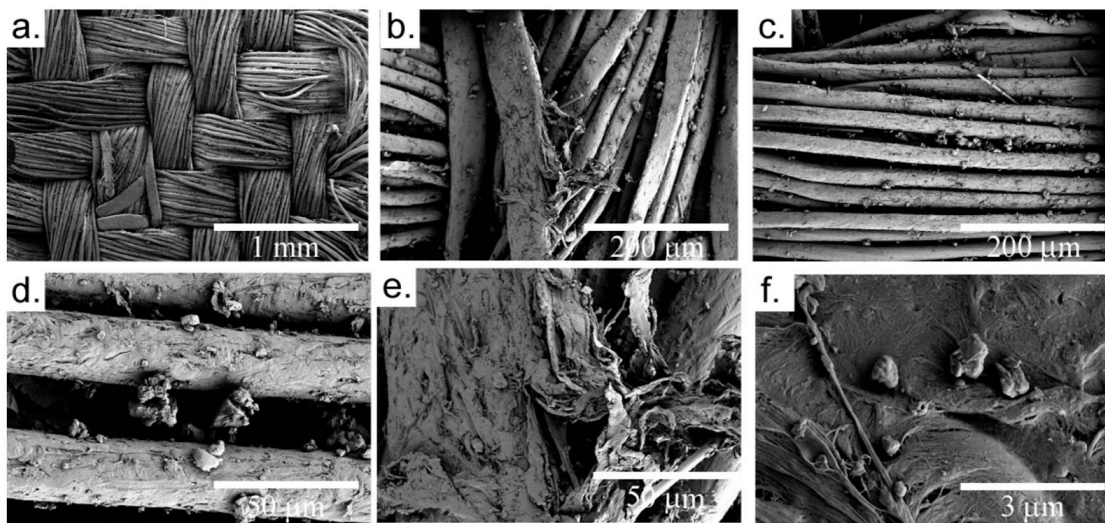


Figure 7. SEM images of outer Teflon layer of left knee fabric patch from Apollo 12 EVA spacesuit. Scale at the bottom right of each image represents image resolution [3].

The images progress from low resolution to high resolution. We can see how the lower resolution images don't provide much information about the presence of lunar dust particles due to the length scale of observation being too high. However, as the resolution is increased to the order of 1-10 μm, the lunar dust particles are clearly distinguishable from the fabric fibers. The researchers also provided side-to-side comparisons of the left knee patch and the artificially contaminated patch from the lab. This can be seen in the figure below.

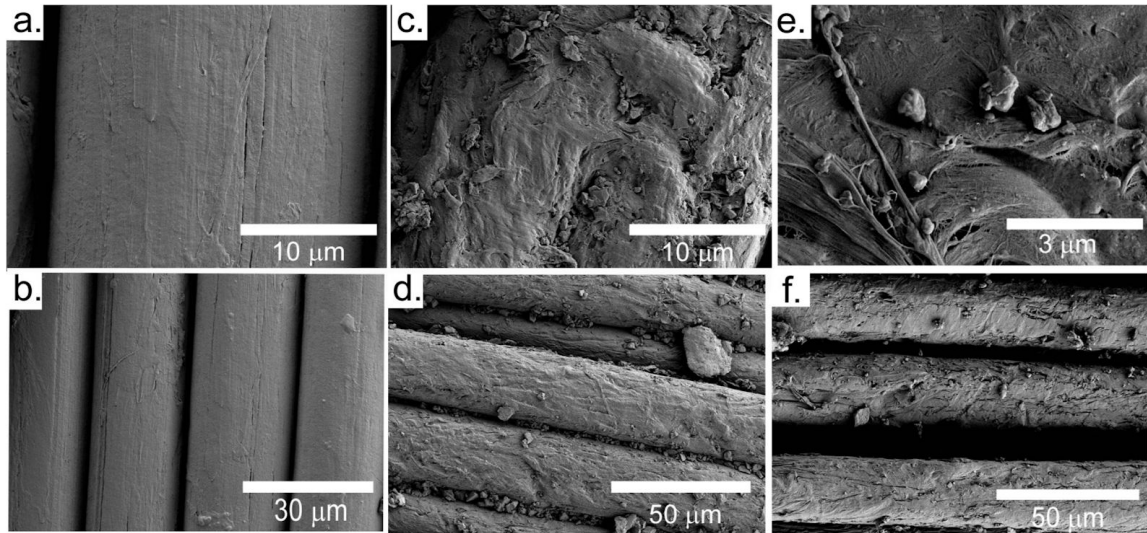


Figure 8. SEM images of three different spacesuit patch configurations. Images a) and b) show the non-flight swatch that was not exposed to any particulate matter. Images c) and d) show the non-flight swatch which was artificially impregnated with lunar dust simulant. Images e) and f) show the same Apollo 12 spacesuit left knee patch from Figure 7 above [3].

These images once again provide a very clear distinction between unexposed fabrics and exposed fabrics. The low- and high-resolution images of the unexposed fabrics show a very clean fabric structure that is unfrayed. However, the images of the artificially contaminated fabric and left knee patch from the Apollo 12 spacesuit (at the same resolutions as those of the unexposed fabric) clearly show the damaged fabric structure as caused by the formation of frays and gaps in the fabric weaves. Additionally, the irregular “spherical” structures seen in between the weaves are the lunar dust particles trapped in the fabric. These images proved that even though wear due to contact with other surfaces and particulates is common, it is the wear from the jagged and abrasive nature of lunar dust particles which also leads to a clearly identifiable destruction in spacesuit structure.

The final portion revolved around X-ray fluorescence spectroscopy analysis on the tape samples. Tape samples were obtained from the arm, lower torso, and leg areas of the Apollo 17 space suit sample. In all three samples, it was found that upwards of 80% of the particles were composed of pyroxene, agglutinitic glass, and plagioclase feldspar, indicating that they were indeed constituents of lunar dust particles. This 80% roughly corresponded to a lunar dust particle count of 840 across the three samples. This value, along with results from SEM, were used to conclude that the majority of the particles were under 10 μm in diameter. However, the median diameter of these lunar dust particles were around 8 μm , suggesting the distribution was fairly right skewed [3]. The composition breakdown of each mineral can be found in the bar chart below.

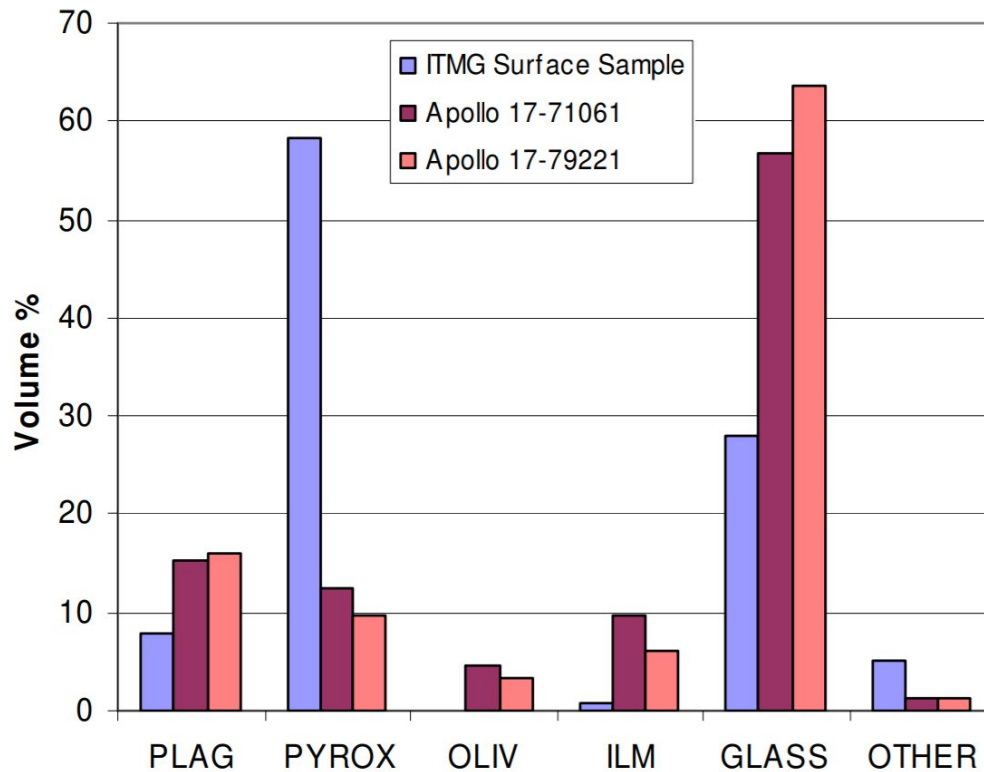


Figure 9. Modal percentage (by volume) of different mineral substances in tape-extracted lunar dust particles from Apollo 17 ITMG spacesuit outer-layer fabric. Both this sample and past research shows the abundance of agglutinitic glass, pyroxene, and plagioclase present in lunar dust particles [3].

One final important piece of information that the adhesive tape sample test provided in the study is the fact that the majority of the lunar dust particles in the most highly contaminated areas of the spacesuit fabric were very easily removable with the tape. This suggested that the majority of the larger-diameter lunar dust particles were simply clinged onto the outer layer of the spacesuit during EVA.

Smaller-diameter particles were found in deeper layers of the spacesuit, but the majority of them were situated on the top layer [3]. The reason this phenomenon was so concerning to the research group is because it suggested that any vigorous shaking of the spacesuit could lead these surface-level particles to be transferred into the atmosphere. After conducting EVA, astronauts enter into certain lunar habitat chambers with their spacesuits on and then dismantle all components and remove their spacesuit.

However, while this happens, astronauts are required to physically move the spacesuit around, and actions like these can cause the atmosphere to be contaminated with these macroscopic lunar dust particles found on the surface.

With this research paper, it is highly evident that lunar dust is an immediate problem when observing its interactions with spacesuits. EVA spacesuits especially can get very contaminated in several areas, and the lunar dust particles in these areas either stay clinged to the surface layer or can penetrate into deeper layers of the suit and inflict damage to the internal fabric weave structures. One additional thing to note is

that although this research study successfully identified ways in which interaction with lunar dust particles can be detrimental to space suits, it failed to account for how these interactions actually occurred. To be able to conceptualize solutions to this problem, we must first be able to pinpoint the different mechanisms through which lunar dust particles interact with these high concentration areas of spacesuits.

Mechanisms of Lunar Dust Transport and Interaction in Lunar Conditions. Lunar dust is capable of adhering to a wide range of different surfaces and can do so through several modes, although there are two very significant ones. For fairly large lunar dust particles ($> 50 \mu\text{m}$ in diameter), it was found that electrostatic attractions are predominant, but for smaller particles ($< 50 \mu\text{m}$ in diameter), van der Waals forces were found to be the main driver. However, it was also discovered that lunar dust particles are constantly charged due to the lunar atmosphere, therefore making electrostatic charging the dominant mechanism behind lunar dust adhesion in nearly all size regimes [5].

A study was conducted by researchers from the NASA Goddard Space Flight center in which they sought to explore the different mechanisms through which lunar dust interacted with astronauts' spacesuits as they conducted EVA. Firstly, the study divided the various mechanisms of lunar dust interaction it researched into mechanical and electrostatic mechanisms. In mechanical terms, lunar dust particles have shown to be fairly "barbed" and irregular in structure, and this is the reason why they're so easily able to penetrate through spacesuit fibers [2]. A quote from Apollo 12 astronaut Alan Bean perfectly illustrates this issue, as he states that "dust tends to rub deeper into the garment than to brush off" [2]. Although the previous study discussed in this section of the report notes that most of the larger lunar dust particles were easily removable with minimal effort through the tape extraction process, it did not acknowledge the possibility of extremely small lunar dust particles being able to penetrate through several layers of spacesuit fabric.

While the mechanical means of interaction does seem quite critical to the interaction of lunar dust particles with spacesuits, most of the larger scale lunar dust particles are able to interact with spacesuit fabric through electrostatic means. There are a couple of ways in which lunar dust particles can obtain excessive charge, with several of them being exposure to solar wind plasma, photoionization, and triboelectric charging. The moon's surface is often exposed to solar winds, and the geometric structure of the moon tends to cause wakes aft of the flow, which is what is responsible for the creation of large electric fields on the lunar surface. Furthermore, for roughly a quarter of its orbit, the lunar surface is also exposed to the Earth's magnetosphere's tail, which can also cause an electric imbalance and lead to the creation of large electric fields [2].

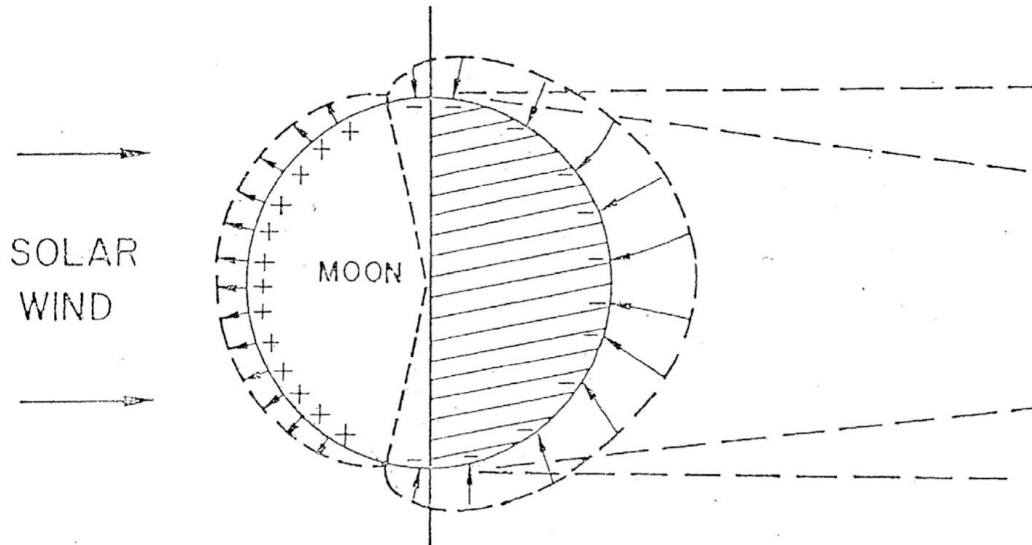


Figure 10. Global-scale charging of lunar surface due to solar wind interactions. Wakes aft of flow are represented by stretched out diagonal lines aft of moon [2].

The final mechanism through which lunar dust particles are able to acquire their charge is through triboelectric effects. This form of electrostatic charge acquisition is not as common as the ones explained above, but it has been replicated under relevant lunar conditions and has shown to impact the charge distribution around lunar dust particles quite significantly. The lunar dust regolith is fairly low in conductivity, which is what allows lunar dust particles to retain their charge once they obtain it. Triboelectric charging would occur when multiple lunar dust particles of varying contact potential rub against one another and transfer this charge through frictional effects [2]. Laboratory experiments have shown that an individual particle of lunar dust with a diameter of roughly $50 \mu\text{m}$ can acquire up to a charge worth $\sim 10^5$ electrons just through triboelectric effects [2].

With these methods of electrostatic transfer, lunar dust particles are capable of clinging onto spacesuits during EVA with ease. The question of how these particles physically move through the atmosphere to then adhere to the spacesuits is still something that not much research has been done on. However, several studies have proposed methods for how and why lunar dust can make its way onto spacesuits. A very common explanation relates simply to how astronauts walk on the lunar surface and conduct EVA [3]. Due to the rarefied nature of the lunar atmosphere, there aren't any surrounding atmospheric gases present to pacify the reactive nature of lunar dust. When astronauts walk on the lunar surface, they tend to kick up lunar dust regolith as they walk, therefore creating a means through which lunar dust particles can adhere to their spacesuits, and that too in various regions. These dust particles aren't kicked high up, so it makes sense that this is the reason behind why there are high lunar dust concentrations near the leg and upper torso. However, a few studies have proposed a model known as the dynamic dust fountain model to explain how lunar dust can get up to the arm area of a spacesuit [2].

As discussed above, the lunar surface essentially develops a sheath layer in which an electric field develops. Lunar dust particles which get charged then accelerate through this sheath layer (depending on the sign of the charge). After this short acceleration, the particles act like normal ballistic objects and travel a parabolic trajectory until they reach the surface again. This process then repeats periodically. A diagram depicting the dynamic dust fountain model is shown below.

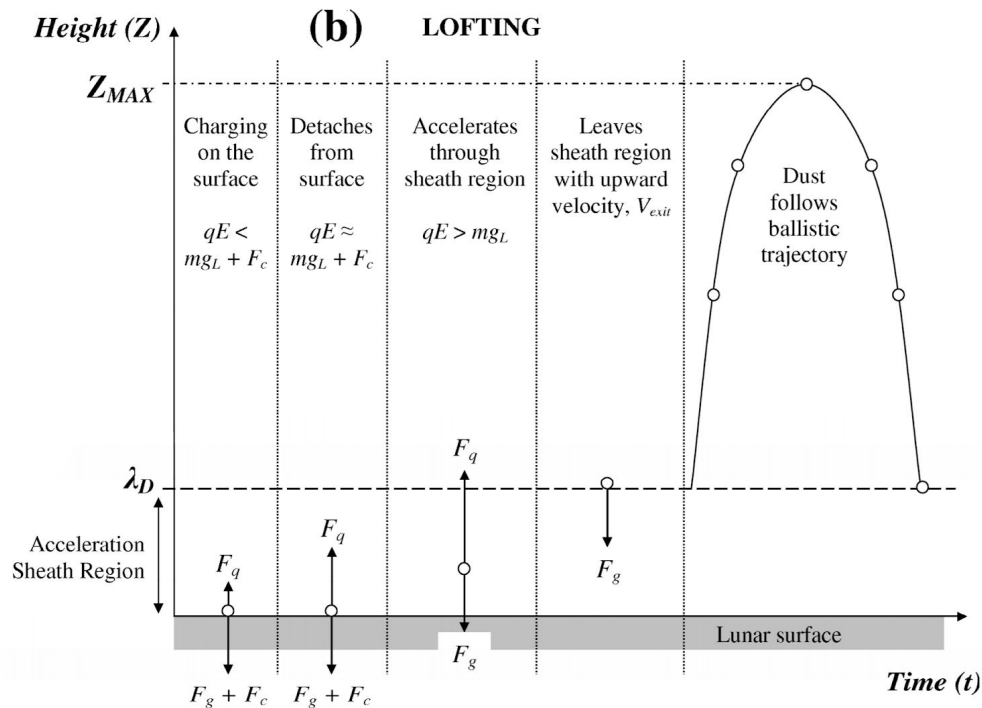


Figure 11. Evolution of lunar dust particle position as a function of time according to the dynamic dust fountain model [6].

The dynamic dust fountain model explains why the lunar atmosphere in general tends to contain large lunar dust clouds every now and then. These lunar dust clouds can act as a huge inhibitor to progress during EVA and also serves a logical explanation as to why high concentration lunar dust patches have been found near the arm and torso area of Apollo spacesuits.

Project Goal and Stakeholders

The goal of this project and the NASA challenge is to provide a solution that can mitigate and prevent the accumulation of lunar dust, specifically on spacesuits. As the challenge was proposed by NASA, they are the primary stakeholders in this project. Specifically within NASA, the main stakeholders will be the engineers, managers, and technicians working for the Artemis program. Furthermore, the stakeholders we anticipate will be the most concerned with our project will be the Artemis astronauts, who will be using the technology while on the moon's surface.

In addition to NASA, several other entities may be involved with our project and will become stakeholders in the future. One such entity would be the University of Michigan. Should we win the competition, the research group responsible for executing the ideas proposed in our project will become stakeholders. Other entities that could become involved are any private companies that partner with NASA for the Artemis program, such as SpaceX, BlueOrigin, or Boeing.

BENCHMARKING

Benchmarking was crucial in helping give context to the problem, showing the history of the lunar dust problem, and providing ideas for future concept exploration. In order to properly benchmark, several existing technologies and ideas were researched during our literature review. A great deal of research was performed on lunar dust mitigation techniques, spanning a broad spectrum of solutions. The solutions that were found were used for both benchmarking and to help inspire the concept exploration phase.

Electrodynamic Dust Shields (EDS)

The most popular mechanism is Electrodynamic Dust Shields (EDS). EDS is an active mechanism that acts real-time during the time of mission. EDS is a fabric-embedded mechanism, and uses a series of electrodes to generate an electrostatic field. Multiphase AC voltage signals are applied to the electrodes structure, pushing particles away from the surface of the electrode array. EDS has an efficient rate of 80%-95% reduction of dust from material [7].

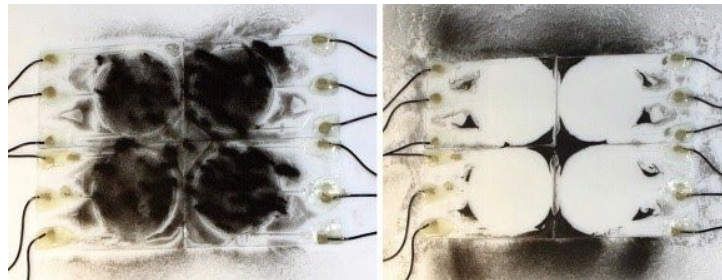


Figure 12. Before and after image of lunar-dust-laden fabric cleaned using a small-scale EDS implementation

Work Function Matching Coating

A popular passive solution, which has been used in conjunction with EDS, is work function matching coating, which is an application of the space suit's fabric material that matches the work function of the positively charged dust particles, effectively neutralizing the charge between the dust and the surface, decreasing the dusts' ability to stick to the surface [8].

PLZT Dust Removal

Other past solutions include PLZT dust removal, magnetic filters, and microwave radiation, which are all active mechanisms. The PLZT dust removal, or the photovoltaic effect of lanthanum-modified lead zirconate titanate, is an efficient mechanism that cleans solar panels via electrostatic travelling waves.

Dust particles are lifted off of surfaces by the electrostatic force caused by these waves, and are in turn absorbed by an aluminum plate called the PLDR. On a 320 mm by 125 mm surface, the PLZT dust removal mechanism can achieve 95% dust removal [9]. A diagram of the PLZT can be seen below in figure 11.

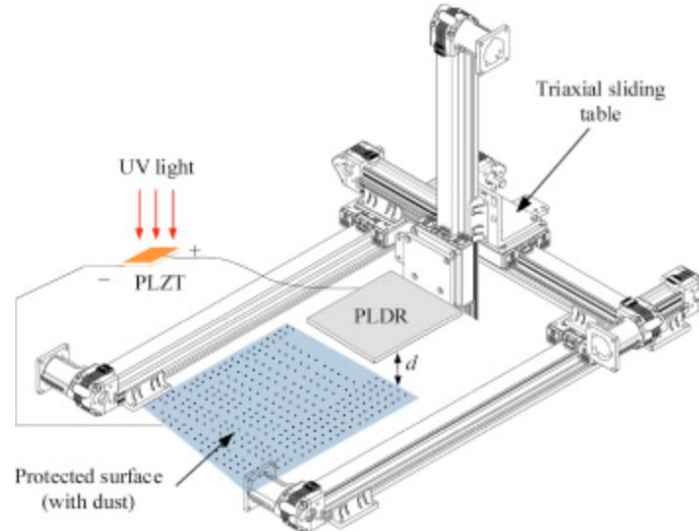


Figure 13: Diagram of a PLZT Dust Removal, note the PLDR plate used to capture dust and the electric circuit used to generate the electrostatic travelling waves.

Magnetic Filtration and Microwave Radiation

Other miscellaneous mechanisms include solutions that are involved in post-mission cleaning. Lunar dust is composed of many different ionized metals, namely SiO_2 , Al_2O_3 , and FeO [10]. As a result, magnetic filters that screen for specific metals can pull large amounts of dust away from surfaces. In addition, there have been studies showing that the radiation that a kitchen microwave emits is capable of melting lunar dust, which would remove the lunar dust from space suits [11]. Both of these mechanisms are active post-mission, instead of during the middle of activity.

Table 3. Lunar dust mitigation technology benchmarking matrix.


	EDS	Work Function Matching Coating	PLZT Dust Removal	Magnetic Filter	Microwave Radiation
Mass (kg)	5	1	5	5	20
Cost	\$100	\$100	\$100	\$75	\$200
Time	10-15 minutes	10-15 minutes	10 minutes	5 minutes	30 seconds
Efficiency	80% - 95%	80-85%	95%	70%	50%

REQUIREMENTS AND ENGINEERING SPECIFICATIONS

Design constraints were provided by NASA as part of the 2021 Lunar Dust Challenge. Extensive research was performed in order to fully understand the constraints and to derive a more thorough list of requirements and specifications.

First, the solution must be able to manage and mitigate small, abrasive dust and small particles. As per the NASA constraints, the specification for this requirement states that the solution must mitigate particles ranging in diameters from 0.5 μm to 50 μm [4]. Next, the solution must be easily adoptable by NASA meaning it should be low mass, small size, low power, non-flammable, non-toxic, and easily transportable [4]. This proved to be one of the more elusive requirements. The derived specifications are based on an air filtration system used onboard the ISS [13]. Based on this filtration system, it was decided that the mass should be less than or equal to 6 kilograms, the dimensions should be less than or equal to 50 cm (length, width, and height), and the solution should have a Toxic Hazard Level 0 as specified by NASA JSC26895 Guidelines. Another requirement is that the solution must be operable in the harsh lunar south pole environment. To meet this requirement it was decided that the solution must be able to operate within a temperature range of $-243\text{ }^{\circ}\text{C}$ to $-49\text{ }^{\circ}\text{C}$ and at a pressure of approximately 10^{-5} bar [13]. These conditions are typical on the surface across the surface of the moon. Next, the solution must reach TRL 4 readiness level. This requirement means that the solution must be validated in a laboratory environment. Furthermore, the solution must be durable. This requirement was not provided by NASA, but was added in order to meet the NASA constraint that requires the designed solution to survive multiple day/night cycles on the south pole of the moon. Each lunar cycle is approximately 29.5 days while the average Artemis mission should last approximately 26 to 42 days [14]. It was thought to be appropriate that the solution should be operable for a minimum of 2 lunar cycles totalling approximately 60 days [13]. The next requirement states that the solution must be cost effective. Again, while vague, this was driven by the NASA constraints. The maximum amount of awarded funding from NASA is \$180,000, therefore the derived specification states that the solution must not exceed \$180,000 [4]. The final requirement is that the solution should minimize required crew time for use. To derive an appropriate specification, research was completed to determine the average amount of time required to clean a spacesuit after an EVA. This process was determined to be around 10 minutes based on the ISS EVA Checklist [15]. Based on this it was determined that the solution should take no more than 15 minutes to remove lunar dust from the exterior of a spacesuit.

The complete table of the requirements and specifications can be found in Figure 12 below. It should be noted that the highest priority requirements and specifications are arranged in descending order. Each specification is testable and justified by research of the topic. Additionally, a column was added that states whether the requirement and accompanying specification is required or desired.



Priority	Stakeholder Requirements	Engineering Specifications
Required	Able to manage and mitigate small, abrasive dust and small particles	Mitigates particles of the order of 0.5-50 μm
Required	Easily adoptable by NASA (low mass, small size, low power, nonflammable, nontoxic, easily transportable etc.)	Mass \leq 6 kg Dimensions: L \leq 50 cm, W \leq 50 cm, H \leq 50 cm NASA JSC 26895 Guidelines: Toxic Hazard Level 0
Required	Operable in harsh lunar South Pole environments	Operating Temperature Range: -243 $^{\circ}\text{C}$ to -49 $^{\circ}\text{C}$ Operating Pressure: 3×10^{-5} bar
Required	Must reach TRL 4 Readiness Level	Solution must be validated in a laboratory environment
Required	Durable	Withstand \geq 2 lunar day/night cycles
Required	Cost Effective	< \$180,000
Desired	Minimize required crew time for use	Operation time \leq 15 min

Figure 14. Requirements and engineering specifications.

CONCEPT EXPLORATION

Concept exploration served as a crucial part of creating effective and suitable ideas based on the problem definition, requirements, and specifications. This phase also served as the groundwork for future plans, such as concept selection and solution development. During this process, we explored the solution space using different ideation techniques, developed some of our solutions using design heuristics, and used a structured approach to effectively evaluate our finalized concepts. The process of concept generation, concept development, and concept screening are detailed below.

Concept Generation

The first step in the concept exploration process was the concept generation phase, where our team generated multiple preliminary design ideas to be looked at during the concept generation process. This is discussed in detail in the following sections.

Generation Methods. Based on our problem definition, we classified our solutions into two categories: real-time dust mitigation which occurs during extravehicular activities (EVA), and post-EVA dust removal which occurs after EVA. Afterwards, we brainstormed and developed ideas under each category. Using these two categories as the starting nodes of our “tree”, we leveraged mind-mapping and divergent thinking to build branches off of these starting nodes, establishing hierarchy in our ideas. In addition, we iterated through several ideas at once to create “links” between ideas, further generating related concepts.

Generation Results. Through these concept generation techniques, we generated around 50 ideas. The formation of our concept tree and the relations between ideas are shown in figure 15 below. The key

concept solutions, which were first tier solutions in the mind-mapping tree, that we considered for the rest of the concept exploration phase are shown in table 4 below. Some of the key concept solutions include EDS, hand-held devices, bunny suits, storage lockers, sticky mats, ultrasonic vibrations, and “licking” technology.

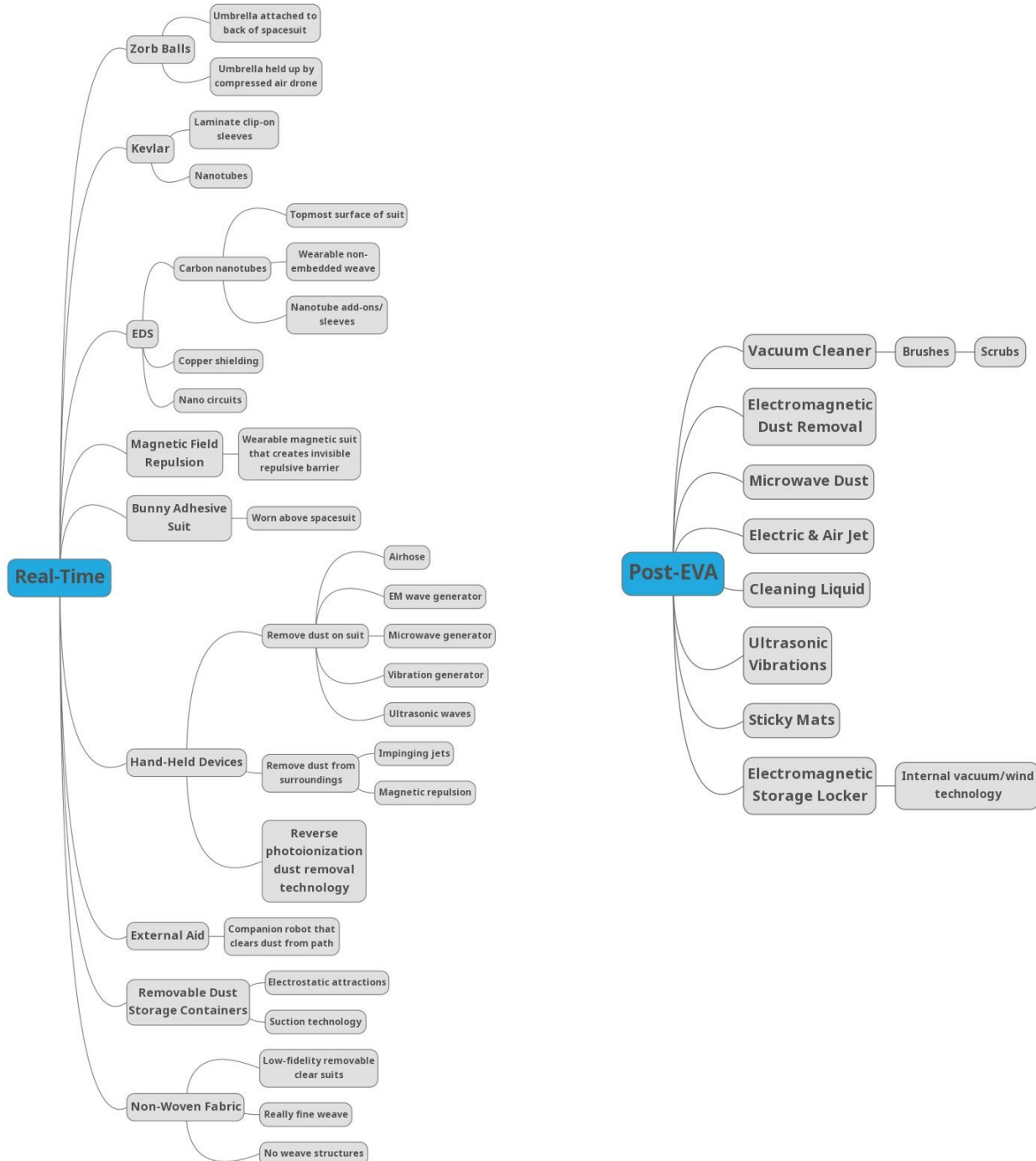


Figure 15. Mind-map representations of our concept generation, split into real-time and post-EVA categories.

Below is a table which lists the first tier concepts generated from the mind mapping session that was performed.

Table 4. Table of first tier concepts generated, listed respectively under each overarching category. Other ideas stemmed from these in our mind-mapping tree.

Real-Time Dust Mitigation	Post-EVA Dust Removal
EDS	Storage locker
Hand-held devices	Sticky mats
Bunny suits	Ultrasonic vibrations
Removable dust storage containers	Cleaning liquid
Different fabric options	Electric and air jet
Zorb balls	Microwave radiation
External aid	Magnetic filter
	Vacuum cleaner
	“Licking” technology

Concept Development

For the concept development phase of the concept exploration process, design heuristic cards were used to further develop four of the most promising ideas. These ideas were determined to be the most because each had previous test data to build upon with further development. The process of developing these ideas is discussed in detail in the following sections.

Development Methods. Once around 50 concepts had been generated through brainstorming and mind-mapping, a subsection of the most promising ideas were selected and further developed. These ideas included electrostatic dust shields, real time dust storage containers, storage locker with electrostatics and vibrations, and adhesive bunny suits.

To further develop these ideas, the method of design heuristics was selected. When compared to the other concept development techniques, it was decided that design heuristic cards were the most applicable to our generated concepts, as many of them did not share common parts or features. This aspect would have made a development technique like morphological analysis challenging to implement. Eight total heuristic

cards were selected including: incorporate user input, scale up/down, roll, mimic natural mechanisms, attach product to user, layer, change surface properties, and utilize opposite surface.

Development Results. For EDS, the first idea, and the user input design heuristics card, it was thought that an on/off switch could be incorporated into the suit to activate and deactivate the EDS. For the scale up/down card, the generated idea was to make an EDS that covered the entire spacesuit. Next, for the roll card, it was thought that EDS could be integrated into mats/sleeves that would fold/roll over various portions of the spacesuit. For the layer card, the generated idea was to stack the EDS circuit layers in the spacesuit layers to increase the overall effectiveness. Finally, for the utilize opposite surface card, it was thought that EDS could be attached to both the internal and external layers of the spacesuit to increase overall effectiveness.

For the second idea, real time dust storage canisters, and the user input design heuristics card, it was thought that a button could be pressed to activate/deactivate the canister storage system. For the scale up/down card, the generated idea was to use a backpack or larger container to store the captured lunar dust. Next, for the utilize the opposite surface card, it was thought that dust canisters could be coated with an adhesive material which would capture dust on the exterior of them. For the attach product to the user card, the generated idea was to attach canisters to the spacesuit with a plug-socket configuration. Finally, for the layer card, it was thought that canisters could be daisy-chained to one another to increase lunar dust storage capacity.

For the third idea, a storage locker with electrostatics and vibrations, and the user input design heuristics card, it was thought that the space suit could be automatically removed with the aid of a user interface. For the scale up/down card, the generated idea was to use a series of smaller sub-lockers for glove/helmets/or other detachable pieces of the space suit. Next, for the roll card, it was thought that the locker could rotate to produce a centrifugal force that would flick the dust off the spacesuits. For the mimic natural mechanisms card, the generated idea was to use high-frequency low amplitude vibrations for dust removal. Next, for the layer card, it was thought that a layered dust trap could be used in the locker to catch additional dust particles. For the change surface properties card, the generated idea was to coat the locker in a material that would attract the dust particles. Finally, for the utilize opposite surfaces card, it was thought that some surfaces of the locker could generate an electric field to attract dust particles while others could produce ultrasonic vibrations to shake dust off the surface of the space suit.

For the fourth and final idea, adhesive bunny suits, and the user input design heuristics card, it was thought that the bunny suit could function like a jumper for ease of use. For the scale up/down card, the generated idea was to use bunny suit sleeves in areas of high dust accumulation such as the arms and legs. Next, for the roll card, it was thought that a roll-on like bunny suit material could be applied to the exterior of the space suit before an EVA. For the mimic natural mechanisms card, the generated idea was to use natural adhesives that work in extreme cold conditions. Next, for the layer card, it was thought that multiple layers of bunny suits could be used for EVAs. For the change surface properties card, the generated idea was to coat the bunny suit in a dust resistant material. Finally, for the utilize opposite surfaces card, it was thought that reversible bunny suits could be used.

Concept Screening

In order to further narrow down our fully-developed solution space from the concept development phase, we derived a set of filters which were used to evaluate each concept and determine if they qualified to remain in our final list of solutions for further consideration. This process would then allow us to focus on just one or two solutions when creating our detailed design for the final solution.

Concept Screening Technique. We first created a set of seven filters, and each of these filters was derived directly from our stakeholder requirements and engineering specifications. Below you will find a table of the filters that were used and a brief justification as to why they were considered as important filters in the concept screening process.

Table 5. List of filters used to narrow down solution space in the concept screening phase.

Filter	Justification of Filter Consideration
Preliminary (gut) check filter	<ul style="list-style-type: none"> ● Selected as main method of filtering based on alignment of solution with requirements and specifications ● Purpose is to mass filter a large portion of solutions at once
Complexity and scope filter	<ul style="list-style-type: none"> ● Selected to filter out solutions that we perceive are too complicated to either research due to a lack of literature or prototype and test due to limited knowledge
Monetary restrictions filter	<ul style="list-style-type: none"> ● Selected to filter out solutions that would exceed NASA’s budget for the 2021 Big Idea Lunar Dust Challenge ● Directly derived from Stakeholder Requirements [6] → “Cost effective”
Practicality filter	<ul style="list-style-type: none"> ● Selected to filter out unrealistic solutions that we believe cannot be practically implemented to function in the conditions provided by the challenge ● Directly derived from Stakeholder Requirements [3] → “Operable in harsh lunar south pole environments”
Foreseeable effectiveness filter	<ul style="list-style-type: none"> ● Selected to filter out solutions that would potentially be ineffective and would not holistically accomplish the goal of lunar dust mitigation on spacesuits ● Directly derived from Stakeholder Requirements [1] → “Able to manage and mitigate small, abrasive lunar dust particles”
Ease of use filter	<ul style="list-style-type: none"> ● Selected to filter out solutions that we perceive as being too difficult for the astronauts to use while exploring the lunar surface and conducting EVA ● Directly derived from Stakeholder Requirements [7] → “Minimize required crew time for use”

Durability/robustness filter	<ul style="list-style-type: none"> Selected to filter out solutions based on short-term and long-term robustness, durability, and lifetime Directly derived from Stakeholder Requirements [5] → “Durable”
------------------------------	---

Afterwards, we took our list of potential solutions from the concept development stage and applied these screening filters to generate our final list of solutions for future consideration. The filtration process was conducted one filter at a time instead of applying multiple filters at once. Each filter was applied one at a time to each solution from the development stage. Solutions which did not pass the criteria imposed by the first filter were immediately ruled out and not considered for the remaining six filters. Solutions which did pass the criteria imposed by the first filter were then considered for the next one. This was done for every filter, and throughout each step we noticed the solution space decrease in size and converge to a few solutions by the end of the seventh filter. This process flow is illustrated in the graphic below:

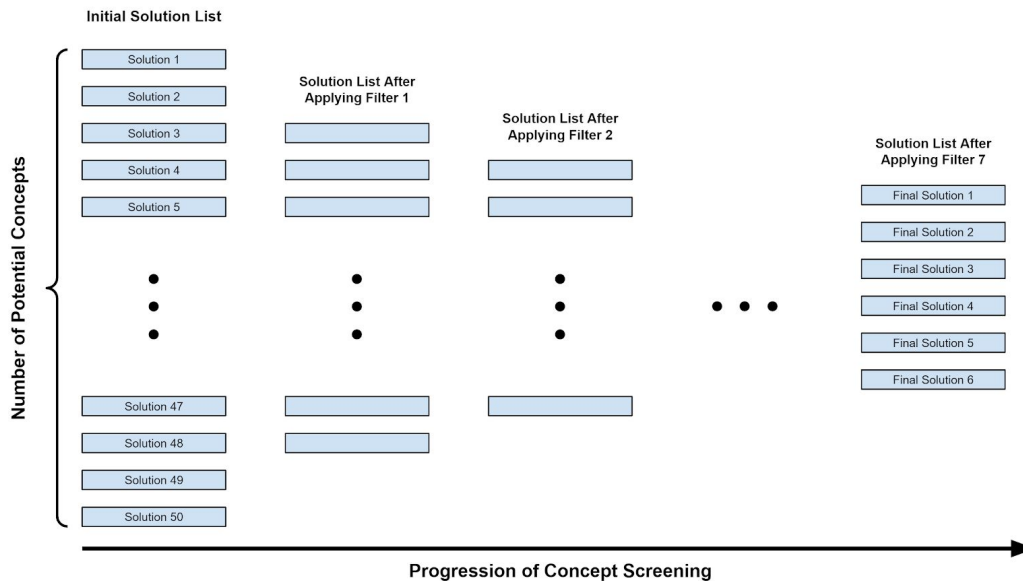


Figure 16. Flowchart depicting the concept screening approach which was implemented.

Concept Screening Implementation. All of the solutions devised from our concept generation and development phases were drafted in an online document in a hierarchical bullet format. This allowed us to efficiently represent our potential solutions while still preserving the connections we established in the concept generation stage. Then, we color coded our screening filters so that we would retain all the information about why a specific solution was ruled out during this process. After defining these on our document, we then went through each solution one-by-one and evaluated each of them with the first filter. The first filter was selected to be the preliminary (gut) check filter. This was the easiest filter to use and successfully nullified a large portion of possible solutions from our list. All of the solutions which did not pass through this filter were highlighted with the appropriate color code for that filter and crossed out from the list.

We then applied this same routine for the rest of the filters. Approaching the concept screening phase this way ensured that everyone on the team fully understood why certain solutions did not qualify for further consideration and for what reasons. It also allowed us to reflect on our decisions for each filter rather than further complicating the process by applying all filters simultaneously. Below is a pre- and post-screening comparison image which depicts how this strategy was implemented digitally.

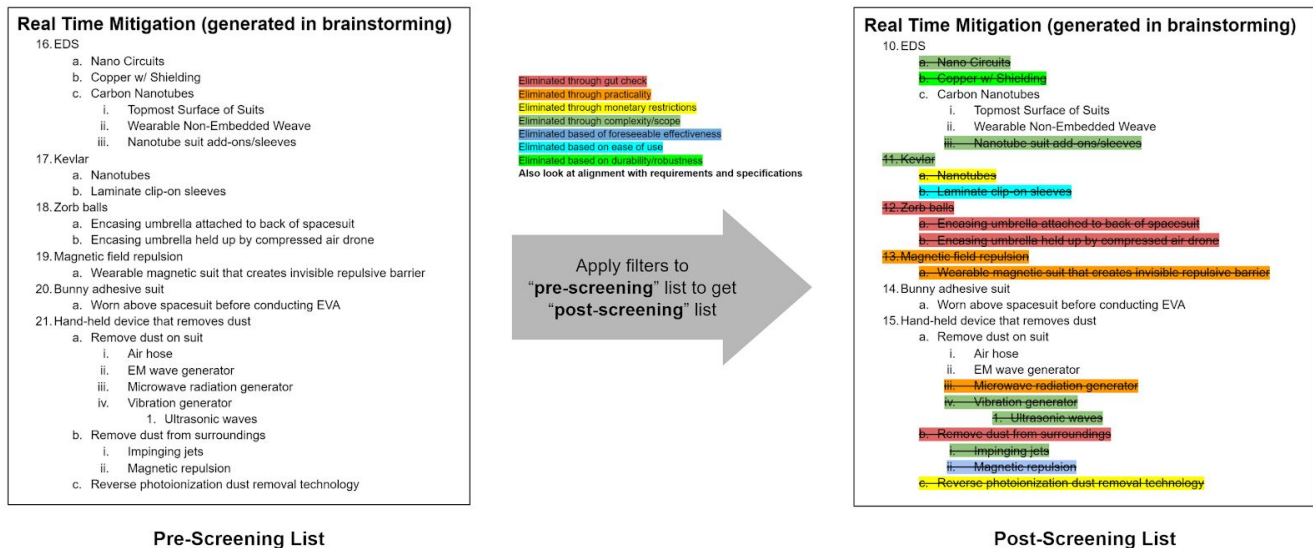


Figure 17. Diagram depicting how the concept screening filter process was implemented to our concepts from the generation and development phases

The complete concept screening document can be found in Appendix D. The difference in the pre-screening solution space and the post-screening solution space is very clear in terms of what we are considering for the future. All of the decisions we made during the screening process for each filter were supported either with logical judgement from the team members or with sources from our literature review. This ensured that through each step of the screening process, we made informed decisions collectively as a team that wouldn't adversely impact us in the solution development stage later on. After completing the screening process, we were successfully able to narrow down our number of solutions from fifty possible ones to just six, which are then considered in the concept selection stage.

Solutions Eligible for Concept Selection Stage. Six total potential solutions remained after our first few rounds of concept screening. Four of the solutions fell under the "Post EVA Removal" category, while the other two fell under the "Real Time Mitigation" category. The solutions are listed and explained below.

Post EVA Removal Solutions
Vacuum Cleaner (Strain, 2020)

The vacuum cleaner will be a hand held device (similar to everyday devices we use) that uses suction to suck dust particles off the spacesuit. The vacuum cleaner will be a simple and easy to use solution. However, the vacuum cleaner may be inefficient and ineffective while in lunar conditions.

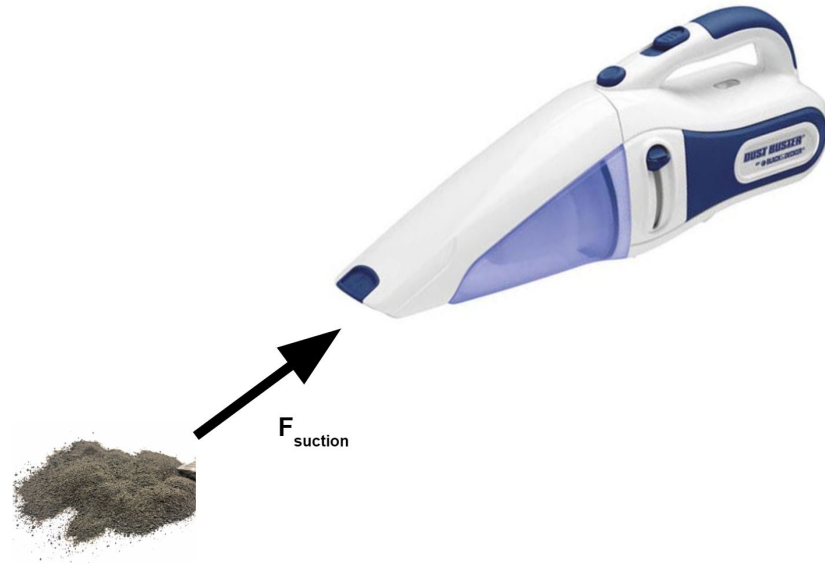


Figure 18. Image of vacuum cleaner hose [19][20].

Hand Held Electrostatics Device (Jiang et. al., 2019)

The hand held electrostatic device will be a device that utilizes electrostatics to neutralize the charge on dust particles and remove them from the space suit. The device is a high tech solution with a high expected effectiveness. However, the device may require a lot of power and could be complex.



Figure 19. Image of a hand-held electrostatic sprayer, designed to spray electrostatic charge to clean surfaces [16].

Hand Held Electrostatics + Air Dust Removal Device (Jiang et. al., 2019)

The hand held electrostatic + air dust removal device utilizes both the technology of the electrostatic removal device and an air hose to remove particles off the spacesuits. Like the solution above it, the device will be high tech, robust, and have an even higher expected effectiveness. It is also expected that the device will require a lot of power and will be complex.



Figure 20. Image of air hose assembly and hand-held electrostatic sprayer [16][18]

Sticky Mats (Penny, 2020)

Sticky mats will be similar to sticky mats used on Earth today which work by capturing particles off the bottom of spacesuit boots. Sticky mats are cheap, simple, and easy to use solutions that can be easily integrated on spaceships and lunar habitats.



Figure 21. Image of a conventional sticky mat.

Real Time Mitigation Solutions

EDS with Carbon Nanotube Electrodes (Manyapu et. al., 2019)

The EDS with Carbon Nanotubes can either be embedded on the top layer of the suit or be a wearable/detachable system. The EDS and carbon nanotubes will prevent dust particles from attaching to the surface by neutralizing the charge on dust particles. The EDS & carbon nanotubes are high tech and have a high expected effectiveness. Embedding the solution in the space suits will be hard for integration

but will be easy for the astronauts to use. Conversely, making an attachable solution will be easy for integration while being harder to use.

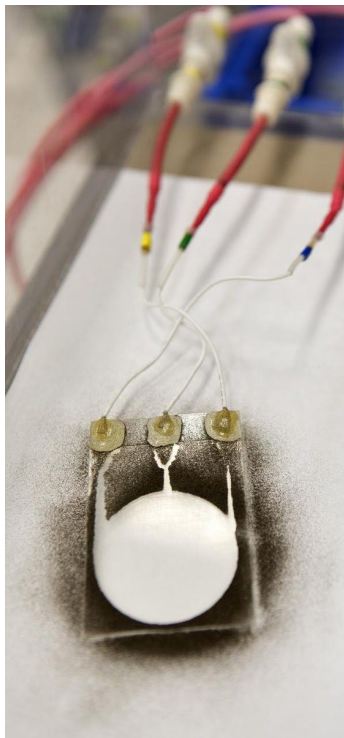


Figure 22. Image of an electrostatic dust shield with carbon nanotubes embedded. The image shows dust being “shaken” off of the surface of the paper [17].

Bunny Suit with Outer Adhesive Layer (Mahoney, 2019)

Bunny suits are exposable, outer layer suits that cover the entire space suit. They are disposable and will have a layer of adhesive that will catch the dust particles. Post EVA, the astronauts will remove the bunny suits and dispose of them. They are low tech, low cost, and easy to use. They may be hard to remove after use however.



Figure 23. Image of a conventional bunny suit [20].

CONCEPT SELECTION

This section details the steps we have taken and the steps we plan on taking to select a specific solution for our project. Two ideas from the “Real Time Mitigation” solution category and four ideas from the “Post EVA Removal” solution category had survived all of the previously discussed solution filters. Our final solution, which is to be submitted to NASA, will either be one or a combination of several of these final six solutions. The next steps of our project will be to continue performing preliminary efficacy testing and solution analysis to help us determine our final solution.

Final Concept Selection Strategy

Due to material constraints, project time constraints, and regulatory constraints regarding in-person activity, we decided to perform a revised concept screening on our six remaining solutions and retained three of them: sticky mats, boot brushes, and electrodynamic dust shields (EDS). This was done on the grounds of being feasible for us to continue testing and developing. To select our final concept, we first built prototypes/models for these three concepts that passed the concept screening stage. Afterwards, we built testing equipment to perform efficacy testing, and ran efficacy tests on our prototypes/models. We then evaluated the test results, and will select the best concept based on the maximum efficiency of lunar dust removal.

Three trials were conducted for the solutions. The solutions will be ranked according to the percentage of dust removed/mitigated, with the ‘winner’ being the solution that removed/mitigated the highest percentage of dust. However, any solution that is able to remove at least 80-85% of the dust on the teflon will be considered as a pass and will not be eliminated.

Furthermore, solutions will be analyzed and sorted by the part of the spacesuit they are able to clean. For example, sticky mats may only be able to clean the bottom of the astronauts’ boots. Even if it is an efficient solution, something else will have to be used to clean or keep the rest of the body clean. Solutions that work synergistically to keep the entire space suit clean while still maintaining proper efficiency could be combined into a single, final solution.

Finally, solution prototypes that can work together without interfering and are, however, underperforming could also be combined into a single solution in the hopes of increasing the overall efficiency of the system. In the case that every single solution underperforms, the solution prototypes will be combined and tested together in hopes of achieving the necessary 90% dust removal/mitigation efficiency.

Sticky Mats. The sticky mats prototype was purchased from Amazon, and is a traditional sticky mat with strong water-based adhesive coating, made out of PVC material. The sticky mats weigh 18.1 ounces, and have dimensions of 18” x 36” x 1”. The plan is to use sticky mats to capture lunar dust from the bottom of spacesuit boots, and will act as a “Post EVA Removal” solution. Samples of sticky mat squares will be cut and placed within a test box for efficacy testing.



Figure 24. Picture of sticky mat prototype ordered from Amazon.

Boot Brush. The boot brush prototype was purchased from Amazon, and is a small nylon bristle brush. The brush weighs 0.774 ounces, and has dimensions of 2.2” x 1.1” x 3.2”. The plan is to use the broot brush to brush off lunar dust from different areas of spacesuits, including boots, and will act as a “Post EVA Removal” solution. For efficacy testing, we used the boot brush to brush off lunar dust simulant from the fabric simulant.



Figure 25. Picture of boot brush prototype ordered from Amazon.

Electrodynamic Dust Shields (EDS). EDS is a mechanism that depends on the creation of travelling waves in order to force particles that are statically charged to trace a certain trajectory. We currently have not acquired a prototype or digital model of EDS, but know the critical specifications of an operating EDS system. An EDS prototype would require high voltage AC signals from 700 - 900 V, frequencies on the order of 10 Hz, and power output from 2 - 4 W [26]. Either copper electrodes or carbon nanotubes thread would be used for the EDS mesh. We are currently working with experts to find the necessary electrical hardware components with appropriate specifications that we could use to construct an EDS system.

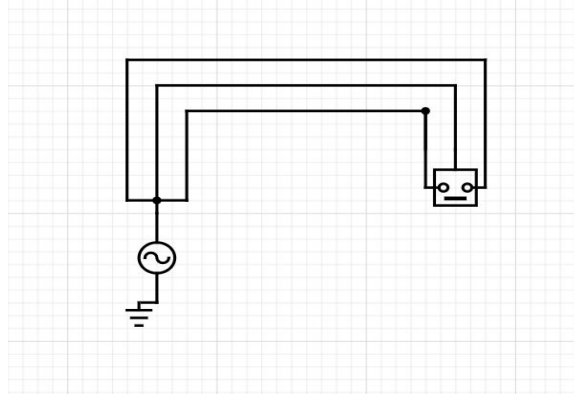


Figure 26. Picture of a simple EDS electrical circuit.

Efficacy Testing

The first step to determining the final solution is to set up efficacy tests and create the prototypes of our solutions. The next is to physically perform the tests and analyze the data. The solution, or combination of solutions that perform the best will then be evaluated and selected. The five main items needed for testing are the following: a prototype of the solution, lunar dust simulant, xEMU teflon fabric simulant, a test box, and a scale.

Lunar Dust Simulant. The simulant used to emulate lunar dust for our efficacy testing was the LMS-1 Lunar Mare Simulant, which was acquired from the Class Exolith Lab from University of Central Florida. The bulk density is 1.56 g/cm^3 , the particle size range is between 0-1 mm, and the mean particle size is 63 microns. The mean particle size is a little higher than the range specified in the specs and reqs, but this simulant was the best simulant of lunar dust we could find that was publicly available.



Figure 27. Picture of LMS-1 Lunar Mare Simulant, packaged in an air-tight bag.

Teflon Fabric Simulant. Two different varieties of Teflon fabric simulant were acquired to emulate the outer layer of the xEMU spacesuits that will be used on future Artemis missions. The first one weighs a total of 60 g, and has dimensions of 15” x 25” x 0.005”. The second one weighs a total of 110 g, and has dimensions of 20” x 16” x 0.01”. The Teflon simulant will be cut up during testing to better reflect geometries of human body surfaces and the constraints given by our test box and scale.

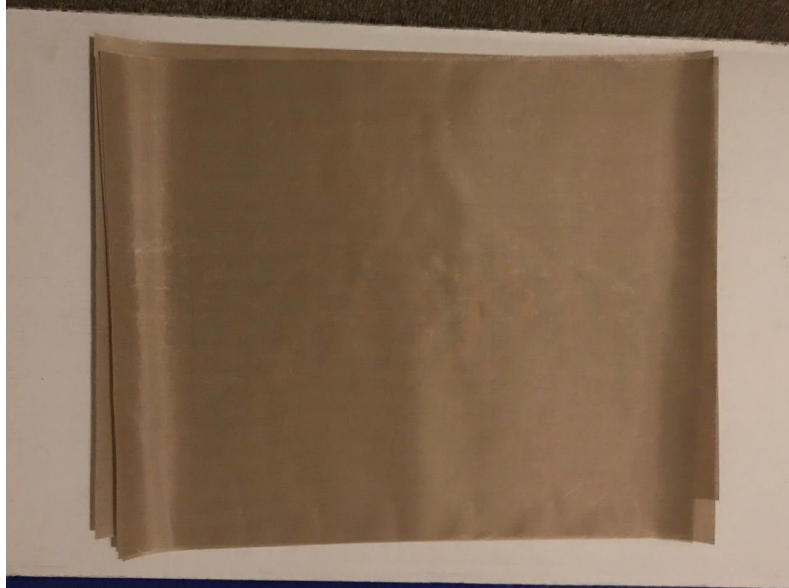


Figure 28. Picture of Teflon fabric simulant, laid out to show a fully flat surface.

Test Box. The test box used for efficacy testing was manufactured by our team and Charlie from University of Michigan Department of Mechanical Engineering machine shop staff. The box is a 1' x 1' x 1' box to contain solution prototypes and LMS-1 simulant during efficacy testing. It consists of an aluminum steel frame, manufactured from square tube stock and welded by Charlie from the machine shop. It is enclosed on all faces with acrylic plexiglass plates, and has a magnetic hinged door to keep the efficacy testing sealed inside during testing, ensuring no leakage occurs out the front face door. The box has circular holes on the side faces for handling the testing inside the box with glove-clad hands, for both the post-EVA removal solutions and real-time mitigation solutions. There is an opening on the back face of the box for electrical equipment, particularly the electrical equipment and hardware for EDS. A formal manufacturing plan for this test box can be found in Table A1 of Appendix A. These materials and design were chosen for a number of reasons. First, we needed the test box to be strong and durable in a number of conditions to be suited for vacuum and cold chamber testing. Next, the acrylic plexi was chosen so tests could be performed visually. Lastly, the box was designed in such a way to meet the primary need of not sharing the same air with the lunar dust simulant, as it is very dangerous to human health. Figure 29 below shows the finalized test box CAD design with a front-face view. Figure 30 below shows the bill of materials (BOM) for the test box, where the test box budget is a little over \$100.

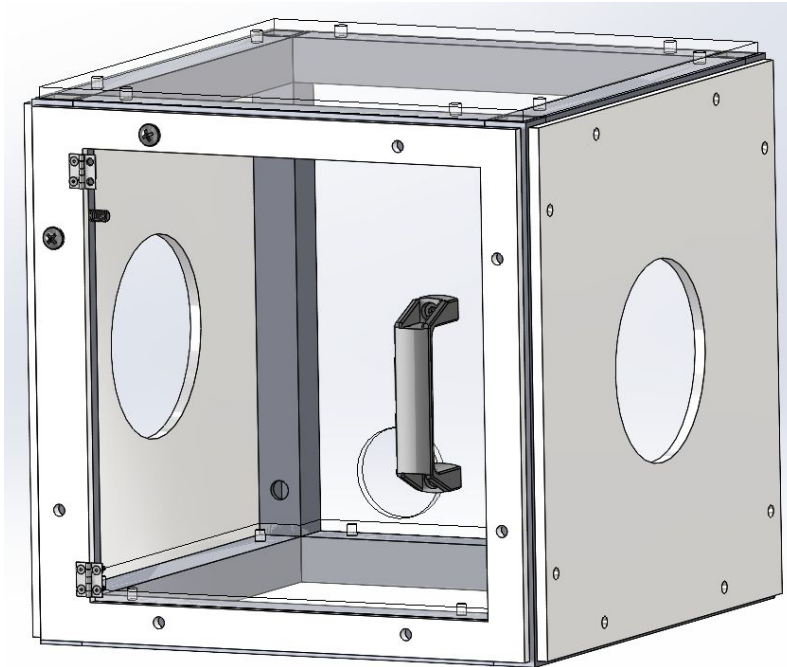


Figure 29. Finalized CAD of test box, shown from front-face view.

Below is a screenshot of the current bill of materials for the text box.

Test Box BOM					
Item (R - Further Research, Y - Ordering in progress, G - Acquired)	Function	Quantity	Projected Price	Actual price	Source
Aluminum Square Tube Stock	Box Frame		\$0.00	\$ -	ME Machine Shop
Plastic Handle	Front Door Handle	1	\$3.90		McMaster
Surface mount hinge	Front Door hinges	2	\$1.53		McMaster
Black-Oxide Alloy Steel Hex Screw	Hinge fasteners	8 (1 pack of 25)	\$6.09		McMaster
Nuts for hinge screws	Hinge fasteners	8 (1 pack of 100)	\$1.00	\$ 14.05	McMaster
Acrylic	Side Panels	6	\$12.98 (6 total)	\$ 95.28	Amazon
95263A546	Phillips Head Screws Hardware	50	\$13		McMaster
90592A016	1/4-20 Nuts	50	\$11		McMaster
UXglove Chem resistant	Box gloves	1	\$10		Amazon

Figure 30. BOM for test box.

Weighing Scale. The scale used for efficacy testing was the Mettler Toledo Excellence Plus XP56 scale. The scale was found in the research lab of Andrea Poli, mechanical engineering staff at the University of Michigan, who allowed us to use his scale for testing. The scale is extremely high-resolution, with a low weight capacity. The max weight the scale can handle is 52 g, and the precision is 0.001 mg. This will be used to weigh the fabric simulant and lunar dust simulant during testing. As the scale is very high-resolution, it is also very sensitive to commotion in the nearby atmosphere, so we had to be very careful in regards to making sudden movements around the scale when weighing our test samples. We decided to use a scale with high precision and low maximum weight due to the impracticality of testing a full scale boot.

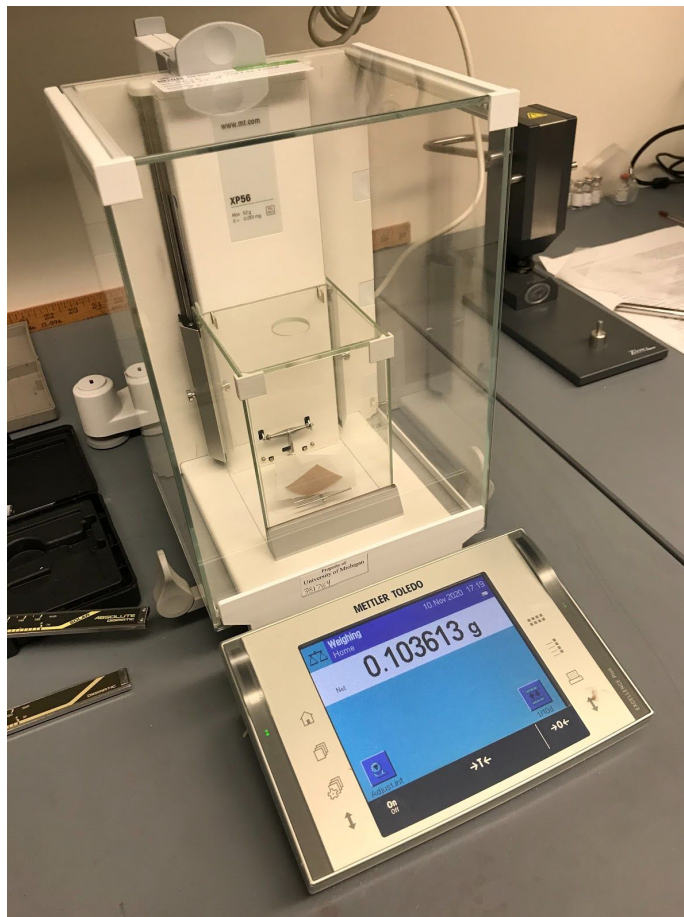


Figure 31. Picture of the Mettler Toledo scale weighing a cut-out piece of Teflon fabric simulant.

Efficacy Testing Strategy

Currently, the plan is to use LMS-1 as the simulant for lunar dust for our tests. This simulant has successfully been purchased, verified, and is close to the simulant specs provided by NASA. The outermost layer of a xEMU space suit is Teflon fabric. The simulant for this fabric has been purchased. A 1' x 1' x 1' box made of aluminum square tube stock and acrylic plexiglass has been manufactured as the test stand. Efficacy testing was split into categories: “Post EVA Removal” solutions and “Real-Time Mitigation” solutions.

Tests for the two “Post EVA Removal” solutions were done physically with the use of the lunar dust simulant, fabric simulant, test box, and scale. Both of the test plans for sticky mats and boot brushes were written in Excel spreadsheets and distributed to each team member so everyone was on the same page. These detailed testing plans can be found in Tables A2 and A3 in Appendix A. For each “Post EVA Removal” solution, three trials were performed so that we had more data and could account for variability in testing procedure and results. We initially weighed the Teflon fabric simulant in a 3-D printed plastic tray and set that as our baseline weight. Afterwards, we added some LMS-1 lunar dust simulant to the fabric simulant, and weighed that on the same tray to determine the mass of lunar dust added. Then we

applied our solution, sticky mats or boot brushes, to the fabric + dust configuration for a set amount of time to remove the dust as best as possible. This was done within the test box to control any external factors and to safely recollect the removed dust post-testing. Once the solution was applied satisfactorily, the cleaned fabric sample was weighed again, with the difference in weights providing us the amount of dust removed during testing. Thus, we were able to calculate the percentage of dust removed, representing the efficiency of the solution, and recorded these values.

During the physical testing of the “Post EVA Removal” solutions, some challenges arose with our testing procedures that may have affected the consistency and variability of our tests. For the purpose of weighing the Teflon fabric simulant and dust simulant, we 3D-printed a plastic tray for each trial, with a total of six plastic trays for the three sticky mat trials and the three boot brush trials. This was done because the lunar dust simulant could contaminate a plastic tray after each trial, so we wanted a clean tray for each new trial. However, this introduces some variability in results because each tray for each trial is not the same, and therefore will have slightly different weights. In addition, the amount of dust added to the fabric simulant each time was not the same, and this may have added variability to the results. We could not confirm that we added the same amount of dust every time because of the fine nature of the lunar dust simulant; we could not measure out an amount of lunar dust and then sprinkle it onto the fabric. Instead, we printed an extra plastic tray that contained 50 mg of lunar dust, and pressed the fabric into the tray to gather as much dust as possible. By using a tray with the same set amount of dust for each trial, we combatted the inherent variability of the testing procedure as best we could. Finally, there was also variability in the actual application of the sticky mats and boot brush. For the application of sticky mats, we placed the fabric simulant on top of the simulants with the face with lunar dust on it facing the sticky mats, and then applied 3.3 lb to the top side of the fabric simulant with weights. We set the weights on top of the sticky mats and fabric for 20 seconds each, so that each trial stayed consistent with the solution application. For the boot brush, we applied the solution to the fabric with dust on it for 20 seconds. However, we can accurately replicate the human behavior and force of hand-brushing the fabric simulant for each trial, and tried our best to control those factors to reduce variability.

The proper amount of force to apply to the teflon when applying the LMS-1 and when cleaning it with the sticky mat was found to be 3.3lbs. The force of 3.3 lbs was calculated using the following equation:

$$F_{teflon} = \frac{1.6 * 1.6 * (W_{astronaut} + W_{xEMU})}{6 * 72}$$

In the equation, the total weight of an astronaut wearing an xEMU is found to be 498 lbs, as the astronaut’s weight was approximated to be 180 lbs and the weight of an xEMU was found to be 318 lbs. Dividing the total weight by 6 gives the astronaut’s weight on the moon. Finally, the total area of the astronaut’s boots were approximated to be 72 in² while the area of the teflon square was 256 in². When contaminating it with LMS-1, we made sure to be slightly over 3.3 lbs so as to get more dust to stick to the teflon. Conversely, when cleaning it with a sticky mat, we made sure to apply slightly less than 3.3 lbs so that our data was more conservative.

Given time, material, and regulation constraints, we may not be able to perform physical testing on the “Real Time Mitigation” solution, EDS. We are currently looking into using different types of simulation software, such as computational fluid dynamics software, to simulate the effect EDS would have on lunar dust to determine the efficiency of the solution. In the event that we are able to perform physical testing with EDS, we are looking into building an EDS system of our own using a microcomputer, DC power supply, mosfets, voltage transformer, resistors and capacitors. If we were to physically construct an EDS system, we would subsequently write a testing plan for testing. This plan would look similar to that for the “Post EVA Removal” solution plans, except the applied solution would be that of EDS, and it would be integrated with the fabric simulant from the beginning of testing.

Overall, efficacy testing involves finding the percentage of dust simulant removed from the fabric simulant using different solution prototypes. The solution prototype will be weighed and placed in the test box. LMS-1 will be showered and directed at the fabric, and the mass of the dust added will be measured. The solution prototype will then be used to clean the dust, and the cleaned fabric will then be reweighed. These values will be inputted into an excel spreadsheet that calculates the percentage of dust that has been cleaned by each solution for multiple trials, along with error calculations for key components. Solutions that can remove 80-85% of the dust simulant will be considered as a pass. The solution with the highest dust cleaning efficiency will be chosen as the final solution. If none of the solutions pass the efficiency rate threshold of 80-85%, multiple solutions will be combined and tested in hopes to achieve at least 90% dust removal efficiency. Below is a flowchart explaining our final concept selection procedure moving on in a consolidated manner.

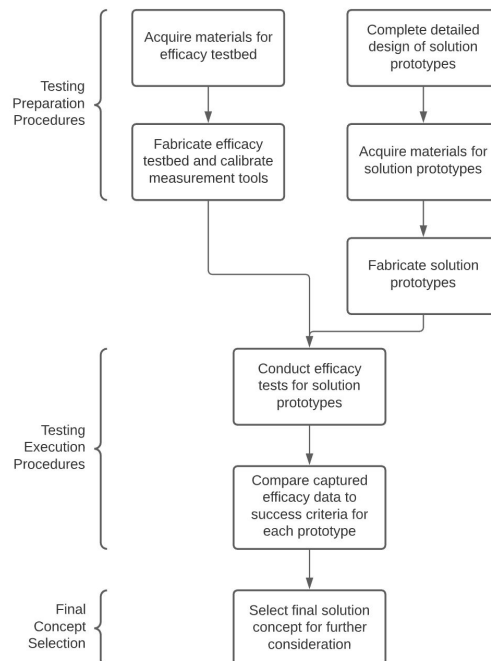


Figure 32. Flowchart depicting the steps procedure used to narrow down to final solution for development.

ENGINEERING ANALYSIS

This section covers in detail the processes used to objectively analyze and compare the three potential solutions. The cleaning efficiency and test results for boot brushes and sticky mats are discussed and evaluated in detail. Additionally, the process of modeling and approach to the creation of a physical EDS circuit and power supply is covered.

Post EVA Removal Solution Analysis

In order to determine if sticky mats and boot brushes are viable solutions, tests were conducted on the two solutions to measure their efficiency in removing lunar dust. As explained in the test plan for these efficacy tests, the mass of the system (which includes the testing tray, teflon, and sometimes LMS-1) were measured and recorded three times throughout the tests. The three recorded measurements were the “baseline fabric mass” (just a testing tray and a clean piece of teflon), the “dirty fabric mass” (after the teflon was dipped in LMS-1), and the “cleaned fabric mass” (after the teflon was cleaned using a specific solution). After recording the raw data, the solution’s efficiency was calculated using the following equation:

$$\text{Efficiency} = \frac{(\text{Dirty fabric mass} - \text{Baseline fabric mass}) - (\text{Cleaned fabric mass} - \text{Baseline fabric mass})}{\text{Dirty fabric mass} - \text{Baseline fabric mass}} * 100\%$$

Sticky Mats. A table of the sticky mat dust removal efficiencies is shown below in Figure 33.

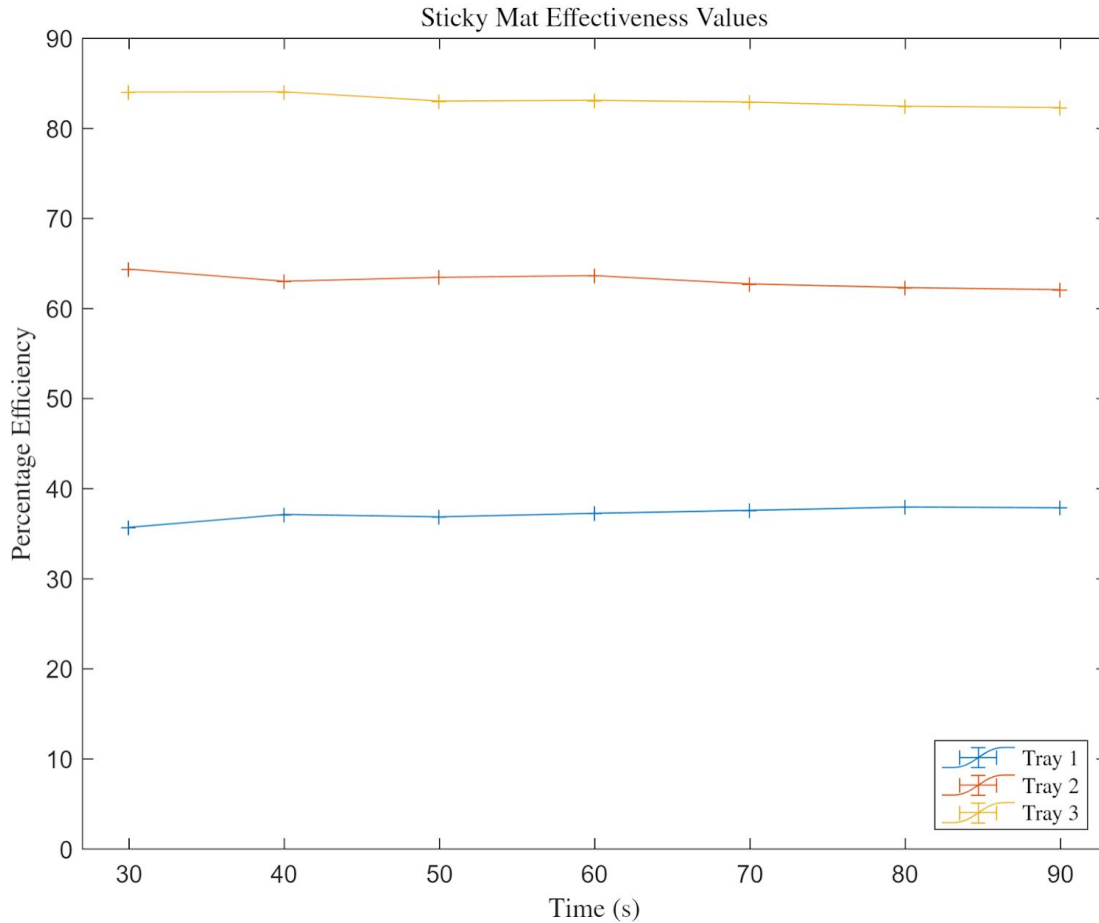


Figure 33. The percent efficiency of removing lunar dust using boot brushes graphed as a function of time. Note that the precision and accuracy errors of the weighing scale are miniscule and are therefore not visible at this scale.

The average efficiency was calculated to be 37.2% for tray 1, 63.1% for tray 2, and 83.1% for tray 3. Two of the efficiencies are too low and do not meet our requirement of being at least 80% efficient even when taking error into account. However, tray 3 had an efficiency that met our requirements and as a result, sticky mats will be kept as a solution that could be further developed for our final solution.

Boot Brushes. A graph of the boot brush dust removal efficiencies measured over time is shown below in Figure 34.

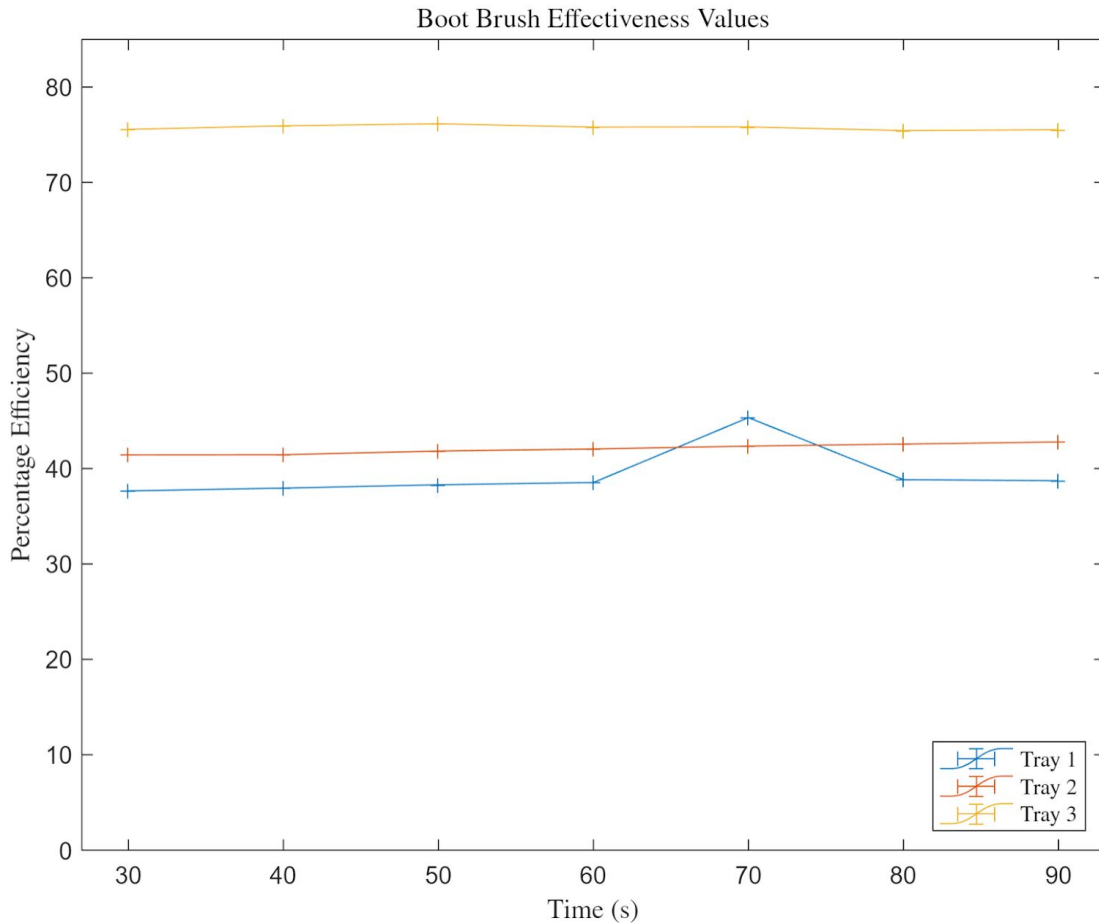


Figure 34. The percent efficiency of removing lunar dust using boot brushes graphed as a function of time. Note that the precision and accuracy errors of the weighing scale are miniscule and are therefore not visible at this scale.

The average efficiency was calculated to be 39.3% for tray 1, 42.1% for tray 2, and 75.7% for tray 3. Unfortunately, these efficiencies are too low and none meet our requirement of being at least 80% efficient even when taking error into account. Only 1 tray reached an efficiency close to 80%, however this anomaly can be explained by the fact that the teflon in tray 3 was brushed for a longer period of time than the other two. This was an error in testing procedures, but due to the limited amount of lab time the test was unable to be repeated.

Numerical Analysis of EDS Phenomenon

In order to understand the fundamental physics behind electrodynamic dust shields (EDS), we decided to implement a numerical scheme that would allow us to visualize the impact of the governing forces from EDS on simulated lunar dust particles. This scheme would allow us to construct a particle tracker algorithm which would allow us to observe the competing effects from the various EDS forces on a randomized lunar dust particle sample.

Motivation. It should be noted that the goal of this numerical simulation is not to entirely replace the initial intent of physically prototyping a representative EDS circuit. Performing analysis on the solution method would instead provide us with a higher level of insight into the mechanisms behind the solution. Furthermore, the results can be used as a potential parameter tuning tool that would be relevant once a physical prototype of our EDS solution has been constructed. One of the pieces of literature about EDS which we benchmarked even explicitly claims that attempting to numerically simulate a full-scale electrodynamic dust shield on a realistic computational grid is not at all feasible and would not be fully representative of the real-world phenomenon if attempted [23]. Doing so would require high-memory solvers which could take a long time to develop to a certain degree of accuracy. This is partly due to the highly erratic nature of lunar dust particles and their unpredictable affiliation with different surfaces. Therefore, we are completely aware that our simulations would also need to be greatly simplified for the same reasons. However, developing such a tool is still necessary in providing us with critical insights that may assist us in formulating a more reasonable physical prototype configuration for the future, if one cannot be constructed due to COVID restrictions.

Simulation Strategy. Electrodynamic dust shields leverage the electrostatic and dielectrophoretic forces resulting from a spatially varying electric field to incite repulsive motion in lunar dust particles [23]. These lunar dust particles are to be initialized at a certain position in the computational domain, and once the electric field is activated, we will be able to visualize the trajectory it takes as a result of the competing forces acting on it. This serves as the main strategy of our simulation. The equations for the electrostatic (1) and dielectrophoretic (2) forces sourced from the EDS are shown below.

$$\langle \underline{F}_{dep} \rangle = 2\pi\epsilon_m r^3 Re\{\underline{K}(\omega)\} \nabla E_{rms}^2$$

$$\underline{F}_e = q\underline{E}$$

Note that both the dielectrophoretic and electrostatic forces are dependent on the electric field produced by the EDS. This piece of information will be critical for us when conducting this analysis.

For a singular dust particle, one can then write a force balance to show the competing effects of the above two forces from the EDS and the gravitational force. For this simulation, we assume that there are negligible viscous and pressure drag effects on the lunar dust particles (will be justified in Physical Assumptions). We will also assume a 2D simulation for simplicity. Assuming that we are interested in this particle's movement in two dimensions, we can draw a free body for this single dust particle, as seen below.

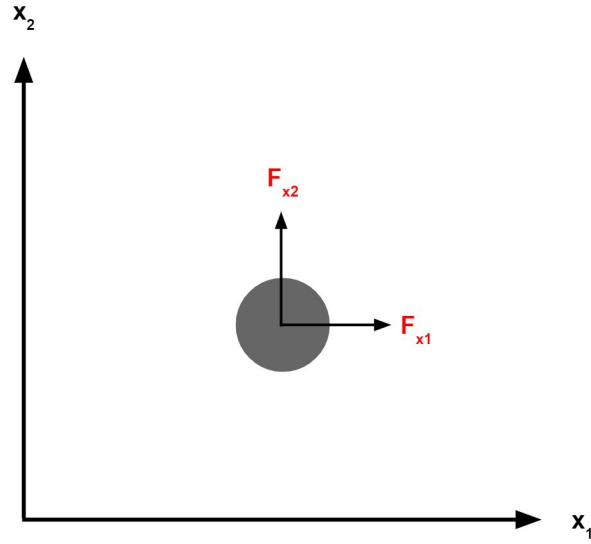


Figure 35. The grey sphere in the center represents a lunar dust particle. Note that direction of forces placed on the body is arbitrary at first and can change depending on sign of force value.

In the free body diagram above, F_{x1} is the force imparted on the particle in the x_1 direction and F_{x2} is the force imparted on the particle in the x_2 direction. Accounting for the electrostatic and dielectrophoretic forces on the particles, we can represent the forces on the three axes using Newton's laws of motion.

$$ma_{x_1} = qE_{x_1} + 2\pi\epsilon_m r_p^3 \text{Re}\{K(\omega)\} \frac{\partial E_{rms}}{\partial x_1}$$

$$ma_{x_2} = qE_{x_2} + 2\pi\epsilon_m r_p^3 \text{Re}\{K(\omega)\} \frac{\partial E_{rms}}{\partial x_2}$$

Once these equations are derived, we can then define our computational domain, which will act as the region in which the lunar dust particles conduct activity. Note that this computational domain will be 2-dimensional, as we are interested in seeing how the electric field from EDS can affect the trajectories of the lunar dust particles in all three dimensions. Once our computational domain is defined, we can proceed to issue a random clump of lunar dust particles on the horizontal plane of our computational domain at $t = 0$ (t is our simulation time variable). Each particle within this clump will be assigned the same dimensions, mass, and charge. We can then instantaneously activate our simulated electric field from the EDS and iteratively compute the new positions of each lunar dust particle until the value of time we wish to stop at. After we halt the simulation at our end time, we can observe the new position of all the particles and compute a numerical "efficiency" of the electric field. The advection of each lunar dust

particle will be found by doubly-integrating the acceleration as a result of the forces, more of which will be discussed in the Proposed Numerical Scheme section. Below is a side-by-side comparison of what an example particle tracker simulation would achieve in 3 dimensions.

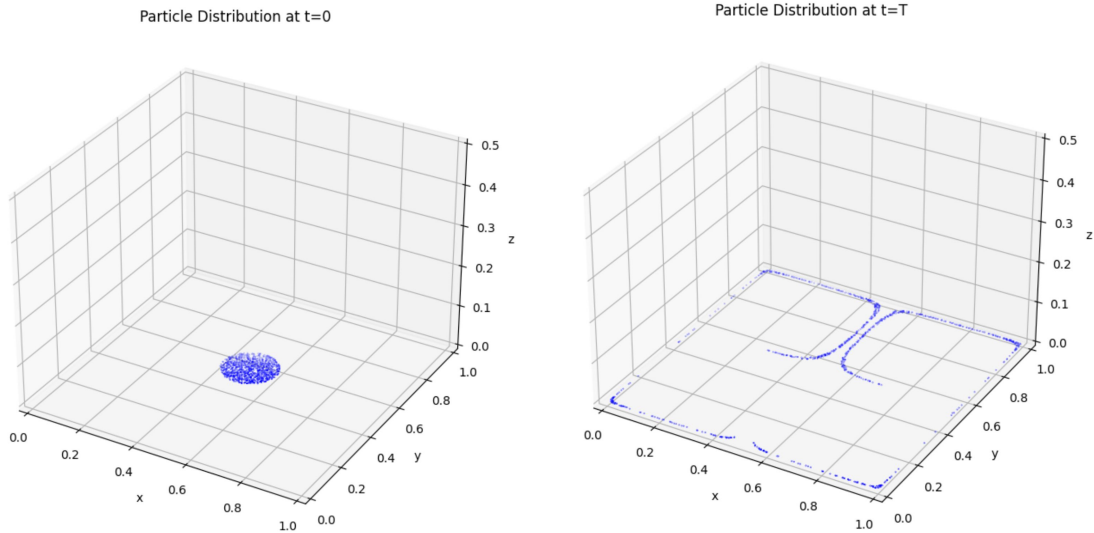


Figure 36. Image on the left shows particle distribution at $t = 0$. Image on the right shows particle distribution at some time $t = T$ after the external force field is activated.

Note how earlier we derived a link between the dielectrophoretic and electrostatic forces and electric field of the EDS. With this particle tracker strategy, we will be able to examine how varying one parameter of the EDS electric field at a time will affect the force balance on the particles. This will then, in turn, inform us on how the particle trajectories and numerical EDS “efficiency” change as a result.

Physical Assumptions. Since the numerical analysis strategy we wish to employ is solely meant to provide us with insight about the fundamental driving mechanisms behind the forces surrounding EDS, we have the freedom to make certain assumptions, as long as they are justified given the simulation conditions. Below is a table which lists the assumptions made and justifications for why they are reasonable given the nature of the problem.

Table 6. List of simplifying assumptions for EDS numerical simulation

Assumption	Justification
No viscous or pressure drag faced by particles	Viscous effects dominate at very small length scales, so pressure drag is immediately neglected Due to lack of atmosphere on moon, viscous drag can also be neglected
Electric field is spatially and temporally varying	Main driver of dielectrophoretic force is gradient

	<p>of electric field squared (∇E_{rms}^2), so electric field must vary spatially for gradient to exist</p> <p>The electric field also has a characteristic frequency (ω), which means it must be temporally varying.</p>
Neglect intermolecular forces and collisions	<p>Goal of simulation is to analyze general trends in particle trajectory, so no need to over-complicate with particle-particle interactions</p> <p>Neglecting inter-particle interactions make simulation considerably cheaper</p>
Assume all forces go through center of mass of particle	Can neglect unimportant effects due to moments
Uniform 2D computational domain	Reduces unnecessary simulation complexity

These assumptions will allow us to considerably reduce the complexity of our solution while still ensuring our results are tractable. Neglecting the effectiveness of these assumptions would mean that we wish to numerically simulate a costly real-world full-scale EDS implementation, which isn't the original motivation for the development of this analysis, as mentioned earlier.

Proposed Numerical Scheme. In order to numerically simulate the evolution of our governing equations for each particle (listed earlier), we are required to discretize the equations in time. There are several robust numerical schemes which can be used to achieve this, and one of the most widely used ones is the Euler time marching method, also known as [24]. The Euler scheme allows users to take a set of nth-order differential equations and convert them to a linear system of 1st-order equations. In our case, our two nth-order differential equations are the results we obtained from the force balance analysis on a lunar dust particle, shown below.

$$m\ddot{x}_1 = qE_{x_1} + 2\pi\epsilon_m r_p^3 Re\{K(\omega)\} \frac{\partial E_{rms}}{\partial x_1}$$

$$m\ddot{x}_2 = qE_{x_2} + 2\pi\epsilon_m r_p^3 Re\{K(\omega)\} \frac{\partial E_{rms}}{\partial x_2}$$

Note that we simply replaced the acceleration variable a with \ddot{x} in order to create our three 2nd-order differential equations. Note that the $K(\omega)$ term in these equations is the Clausius-Mossotti relation and has a dependence on the relative permittivities of the lunar dust particles and the lunar atmosphere it is in

and on the frequency (ω) of the external electric field [23]. We can then proceed to apply an order reduction to the above equations to give us the linear system of equations of motion we wish to solve in our computational domain.

$$\dot{x} = u \quad \text{and} \quad \dot{u} = \frac{q}{m} E_x + \frac{2\pi\epsilon_m r_p^3}{m} \text{Re}\{K(\omega)\} \frac{\partial E_{rms}}{\partial x}$$

$$\dot{y} = v \quad \text{and} \quad \dot{v} = \frac{q}{m} E_y + \frac{2\pi\epsilon_m r_p^3}{m} \text{Re}\{K(\omega)\} \frac{\partial E_{rms}}{\partial y}$$

Note for the above equations that we replaced (x_1, x_2) with (x, y) just for ease of notation. Additionally, (u, v) represent the particle velocities in the x and y directions, respectively.

We can then take the above system of reduced-order differential equations and discretize them in time using the Euler time-marching scheme. The Euler scheme is a very stable and accurate time-marching scheme under small timestep values. As long as the scheme operates within a timestep threshold, which is often dictated by some characteristic frequency in the system, it will provide reliable results. Additionally, for a simulation like this, the Euler scheme is fairly easy to implement and has a small overall time and memory cost. In order to ensure that all major particle behaviors are being captured through the simulation, however, we need to ensure that the time step chosen for the time-marching is smaller than the frequency of the external electric field. Therefore, if we wish to observe the impact of the EDS's frequency on the trajectory of lunar dust particles, then we will need to have small enough time steps to ensure that all effects are preserved.

Limitations of Numerical Scheme. As with any numerical simulations and schemes in existence, there are certainly limitations that one must consider. The point of a simulation is not to precisely mirror effects noticed in the real world, but being cognizant of the simulation's limitations will allow us to form the basis for further research. Below is a table which lists the biggest limitations of our numerical simulation and what impact they could have on our results.

Table 7. List of limitations of EDS numerical simulation

Limitation	Justification
Problem must be greatly simplified to reduce computational complexity	Can mask certain aspects of the problem which may be important for real world experimentation
Strategy does not account for inter-particle interactions	Such forces may have a non-negligible impact on trajectory, electrostatically-speaking
Very large particle populations may lead to high	May not provide easily-attainable results for large

memory and time overhead	number of simulations
--------------------------	-----------------------

Although these limitations exist in our numerical simulation, we would once again like to reiterate that this effort is to develop a greater understanding of the physics behind electrodynamic dust shields with hopes of gaining more insight into the problem at hand. The limitations listed above will indeed have an impact on our results, but we expect these impacts to be outweighed by the usefulness of the simulation in helping us design and prototype our physical EDS circuit.

Numerical Analysis Findings. The goal of this numerical simulation was to further our understanding of the governing forces behind EDS and determine what parameters can be influenced to impact the trajectory of lunar dust particles. In order to run the simulation, the system of linear equations presented in the Proposed Numerical Scheme subsection above were first discretized using the Euler scheme to give us the below set of equations.

$$x^n = x^{n-1} + \Delta t u^n$$

$$y^n = y^{n-1} + \Delta t v^n$$

$$u^n = u^{n-1} + \Delta t \left[\frac{q}{m} E_x + \frac{2\pi\epsilon_m}{m} \text{Re}\{K(\omega)\} \frac{\partial E_{rms}}{\partial x} \right]$$

$$v^n = v^{n-1} + \Delta t \left[\frac{q}{m} E_y + \frac{2\pi\epsilon_m}{m} \text{Re}\{K(\omega)\} \frac{\partial E_{rms}}{\partial y} \right]$$

After the equations were discretized, the values for each constant and a representation for the external electric field had to be determined. The list of constants used for this simulation can be found in the table below. Note that all of these constants were taken from sources [23] and [25].

Table 8. Numerical values for governing constants used in numerical simulation.

Constant	Value
Dielectric permittivity of atmosphere (ϵ_m)	8.85e-12 [C ² N ⁻¹ m ⁻²]
Dielectric permittivity of particle (ϵ_p)	8.85e-11 [C ² N ⁻¹ m ⁻²]
Electrical conductivity of atmosphere (σ_m)	0 [S m ⁻¹]
Electrical conductivity of particle (σ_p)	6e-15 [S m ⁻¹]
Particle diameter (r_p)	63e-6 [m]

Particle bulk density	1.56e-6 [kg m ⁻³]
Particle charge density	3.3e-6 [C m ⁻³]

All other constants were derived from the above base list. Once the constants above were defined, the numerical grid was defined and a random clump of particles was imposed at the center of the numerical domain. The domain was chosen to be 1 unit by 1 unit in size, and the particles were distributed in a small circle of radius 0.1 units right at the center of the domain, as shown in the image below.

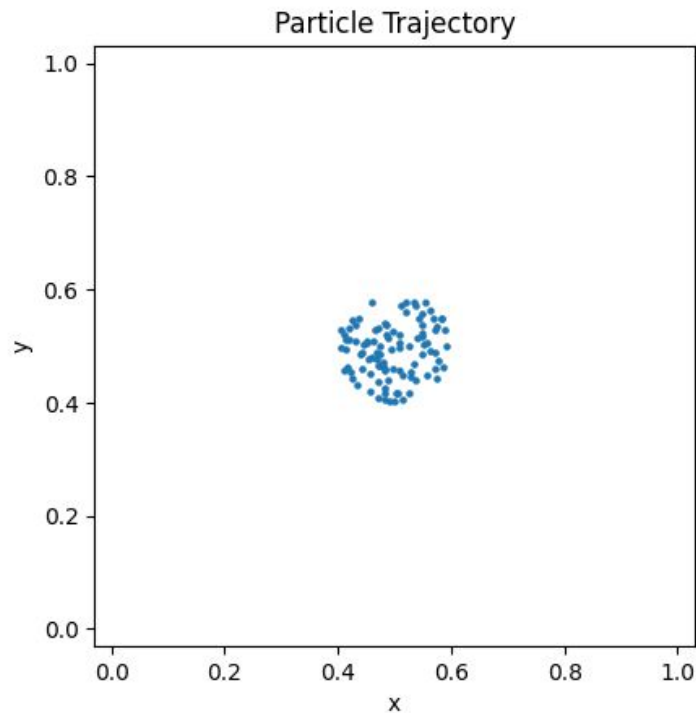


Figure 37. Depiction of numerical grid at start of simulation. Note that the particles are confined with a small circle at the center of the domain.

To ensure the simulation wouldn't take a large time to run, a relatively small amount of particles (~100) was chosen to be imposed at the start. The value for timestep was chosen to be 0.005. Assuming that the time scale for the simulation is in seconds, this timestep value is indeed smaller than the frequency of the external field used in experiments from previous literature, which is roughly 10 Hz [22]. The period was computed to be 0.1 seconds from this frequency, so the timestep was realized to be comfortably within its acceptable range. The final time for the simulation was set to be 2000. This is a relatively large value with respect to the timestep, and this ensured that a steady state solution was reached in all iterations of the simulation.

The final setup step before running the simulation was determining a representation for the external electric field. For simplicity, the electrical field was chosen to be represented by a canonical Taylor-Green function, which is given by the set of equations below [27].

$$E_x = \sin(2\pi x) \cos(2\pi y)$$

$$E_y = -\cos(2\pi x) \sin(2\pi y)$$

The partial derivatives of the above equations were taken to obtain the electric field gradient terms in the dielectrophoretic force equations. These equations are shown below.

$$\frac{\partial E_x}{\partial x} = 4\pi \cos^2(2\pi y) \sin(2\pi x) \cos(2\pi x)$$

$$\frac{\partial E_y}{\partial y} = -4\pi \cos^2(2\pi x) \sin(2\pi y) \cos(2\pi y)$$

A series of simulations were then run to determine the impact of two parameters particularly on the dielectrophoretic force, as that was the more complicated of the two forces to understand. From the above derived equations, we noted that the dielectrophoretic force is a function of several constants as well as the electric field's gradient and effective frequency (from the AC signal). Therefore, the simulations were run to note the impact of these two parameters on the particle trajectory. For both sets of simulations, the particle trajectories were tracked from time $t = 0$ until the last timestep $t = 2000$ (as defined above). At the final timestep, the simulated "effectiveness" of the EDS was calculated by finding the percentage difference in the number of particles remaining after the simulation ended and the number of particles at start (100). Note that these effectiveness values are inevitably going to be different from experimental values found in literature.

To determine the impact of electric field AC signal frequency on the trajectory of lunar dust particles, the simulation was run for frequency values of 0.001, 0.01, 0.1, 1, 10, 100, 1000, 10000, with all values prescribed in Hz. Corresponding "effectiveness" values were calculated and then plotted as a function of nondimensional frequency values. The results are shown in the figure below.

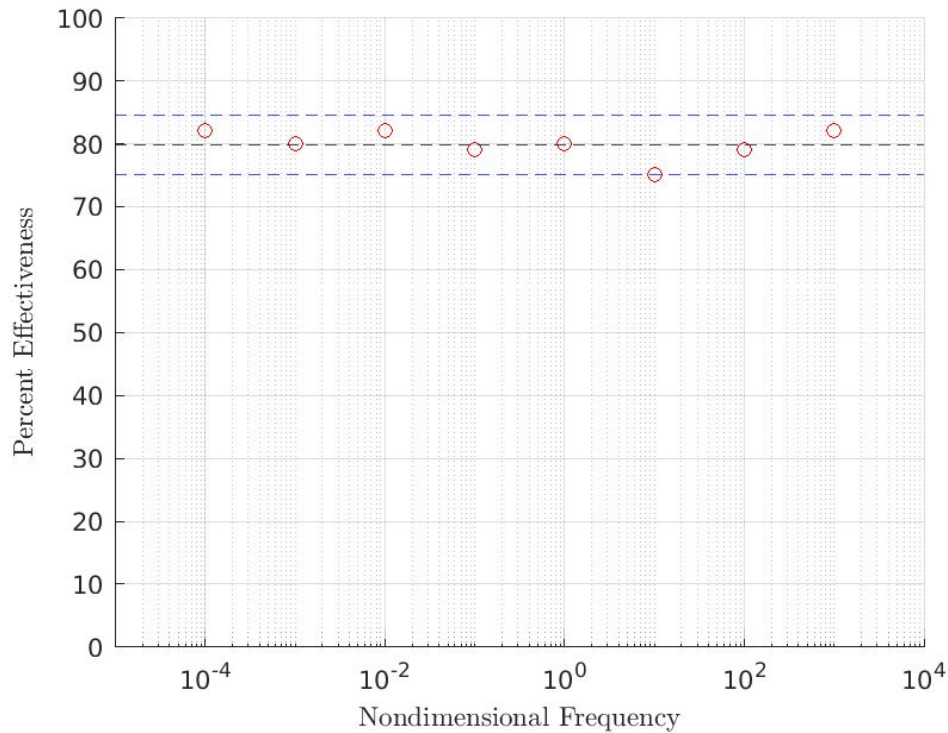


Figure 38. Percent effectiveness as a function of nondimensional frequency. Black line represents average of effectiveness values and blue lines represent 95% confidence interval band. Visible variance is primarily due to randomness in initial particle cluster.

From the above plot we can see that regardless of the frequency used in the simulation, the effectiveness values are statistically coherent, as they all fall within the same band of values. This result shows us that when developing an EDS prototype, the frequency of the AC signal used to generate the electric field will not significantly impact the mitigation effectiveness of the prototype. This could explain why several of the papers observed in the literature review of this report use a standard 10 Hz frequency wave for their experiments [22]. Furthermore, it can be stated with confidence that this frequency-independence is indeed correct, as a prior research paper from NASA mathematically showed that the $Re\{K(\omega)\}$ term of the dielectrophoretic force has very little dependence on frequency due to the intrinsic characteristics of lunar dust [23].

The second goal of the simulation was to determine the impact of the electric field magnitude and that of its gradient on the particle trajectory. The unary electric field was determined from the Taylor-Green equations shown previously, and the calculated “effectiveness” from this electric field was set to be the baseline. Then, this electric field was scaled by factors of 0.01, 0.05, 0.1, 0.5, 1, 5, 10, 50, and 100, and corresponding “effectiveness” values were calculated and plotted in a nondimensional manner. The results are shown in the figure below.

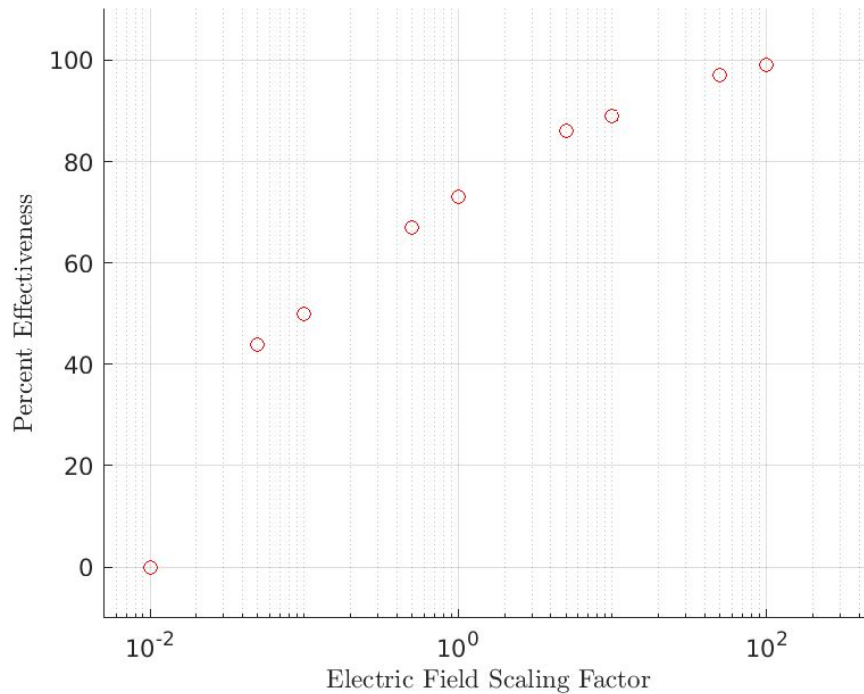


Figure 39. Percent effectiveness as a function of electric field scaling factor. Note that the geometry of the resulting trend isn't of huge interest here.

Note that as the electric field is scaled, a much more noticeable trend develops regarding effectiveness. This result posits that the dominating factor which can alter particle trajectory in an EDS is the spatial magnitude of the electric field and its gradient. We note from the plot above that for larger values of electric field, the lunar dust particles are ejected from the area of interest with high effectiveness, whereas for smaller values of electric field, the lunar dust particles are barely ejected from the area of interest. These observations could also indicate that the effects of EDS operate much faster for larger electric fields. This requirement for a larger electric field was quite an important finding when performing theoretical developments of our EDS section (discussed in the next section).

We would once again like to reiterate that the variability in these results is in part due to the randomness of the initial clump of particles imposed on the numerical domain. This randomness serves as a logical explanation for the variation noticed in the frequency study. The trend noticed in the electric field strength study, however, was much more significant and clearly was not a result of randomness in initial particle distribution. It should also be noted that the limitations in this numerical simulation force it to be simplified, which could mask other useful information for prototyping an EDS circuit. These simulations, however, involve much more mathematically intense closures and generally require more computationally intensive methods. Additionally, nearly all of the papers which were studied in our literature review performed stringent simplifications to reduce the complexity of their simulations, especially considering the erratic nature of lunar dust. Furthermore, due to time constraints, it was extremely difficult to procure the necessary knowledge required to run a much more realistic simulation of EDS and therefore was

simplified to a considerable extent. More detailed information regarding the electric field generated from an EDS circuit would be needed to improve the accuracy of the simulation. If our solution proves to be viable for the future, then there will definitely be an interest in developing more complex simulations with the aid of official resources from our stakeholders.

Finally, the simulation videos for each case study can be found at https://drive.google.com/drive/folders/14ufsF_XWEraSgsDJe8sqBT0nHw4p3FDL?usp=sharing, and the code for the simulation can be found in Appendix C.

Power Calculations for EDS Circuit

After the initial concept generation stage, one of our primary goals was to manufacture and test an EDS solution. As the project progressed, EDS began to look less and less feasible. The primary reason for this was due to the lack of a suitable power supply. The original specifications for a power supply capable of powering an EDS circuit were taken from the paper *Electrostatic Cleaning System for Removing Lunar Dust Adhering to Space Suits* [22]. The results in this paper showed the best EDS cleaning rates were realized with a high voltage, low alternating current, low frequency power supply. The voltage required to perform at the highest cleaning rates, in this case 75-80%, was directly related to the characteristic length between the electrodes of the EDS circuit. This relationship is approximate as the dielectrophoretic force ($|F_{dep}|$) in the overall EDS system balance. This approximation was published in *History and Flight Development of the Electrodynamical Dust Shield* [23] as:

$$|F_{dep}| = V^2/L^3$$

In the above equation, F_{dep} represents the dielectrophoretic force produced by EDS, V represents the voltage through the electrodes, and L represents the gap between each adjacent electrode. This relationship was verified through the results of the *Electrostatic Cleaning System for Removing Lunar Dust Adhering to Space Suits* paper [22]. In this paper, the researchers had to supply 2000 V to the EDS circuit with an electrode gap length of 1.2 mm to reach the 75-80% cleaning rate. They then lowered the gap to 0.6 mm and only had to supply 900 V to reach the same cleaning rate. The change in voltage with the lower gap in the research article was higher than expected in theory by roughly 27% but still provides physical proof that decreasing the electrode gap allows far lower voltages to be used to achieve similar cleaning rates. Furthermore, we found from our numerical solutions (described in the section prior to this) that the only electric field parameter which has a significant impact on lunar dust particles under the effect of EDS is the electric field (and its corresponding gradient) strength. Recalling from first principles that the electric field is proportional to supplied voltage, we can therefore conclude that the EDS can be most improved by altering this voltage. The voltage-electrode dependence shown above can be used with this fact to develop a safe yet effective EDS prototype, more of which will be discussed below.

This realization provides the groundwork to develop an EDS that is safer and more efficient than previous EDS systems. It is believed that an EDS circuit with an electrode gap of 0.3 mm can be created with a 3D printed grid and thin copper electrodes. Theoretically, the electrode gap should only require 250 to 350 V if the $|F_{dep}|$ values from the studied research paper are held constant. Due to real-world dissipative

effects, the voltage required will be on the higher end of this spectrum, but this is still around 3-4 times lower than our initial proposed voltage range. Additionally, this breakthrough should allow for a power supply to be constructed from a microcomputer, DC power supply, MOSFETs, voltage transformer, and a handful of off-the-shelf resistors and capacitors. A potential schematic for this is shown in Figure 37 below.

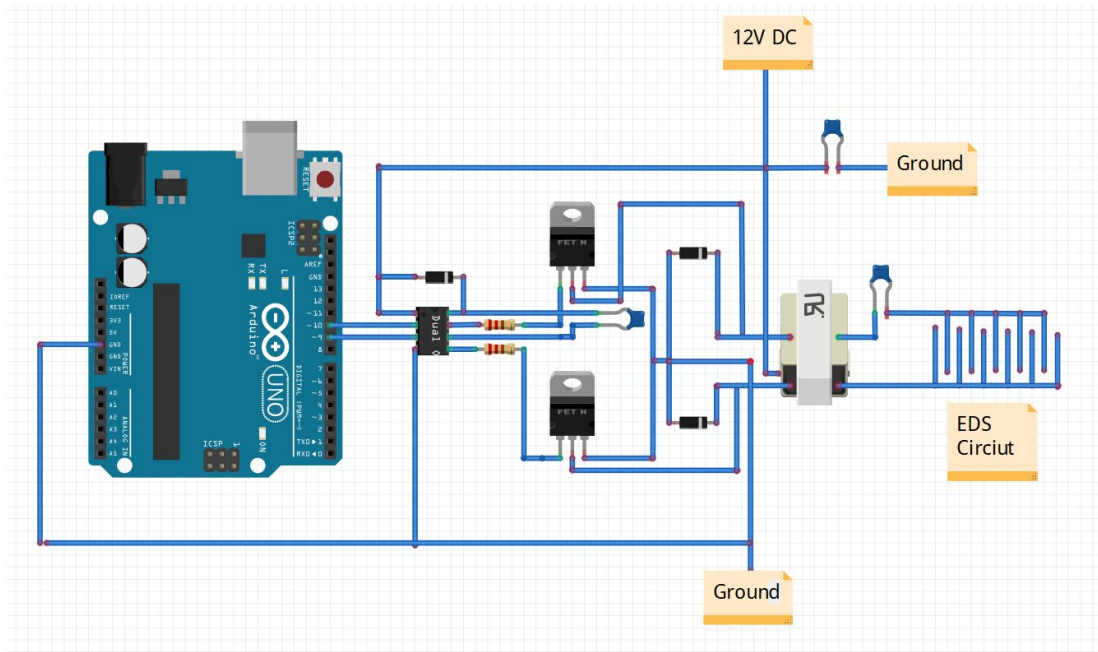


Figure 40. Circuit diagram of simple single phase DC to AC inverter

EDS Circuit Analysis

After the preliminary circuit was designed, the appropriate components were ordered and the circuit was constructed. Due to time limitations and COVID restrictions, only one one day of lab testing was able to be completed. During this testing, the circuit was powered and troubleshooted.

First, an oscilloscope was used to measure the digital signals at the output of pins 9 and 10 on the arduino. The code running to create this output was adapted from open source code and is shown in Appendix E. Both pins were programmed to output modulated PWM signals based on a sinusoidal waveform. These outputs were offset to provide both the peak and trough of the desired sine wave. These low power signals were then fed into a mosfet driver used to switch the gates of the mosfets. Due to a suspected failure of the mosfet driver, the desired output was never achieved.

Though unable to generate a 230 VAC power signal during testing, meaningful insights into the complexities and challenges associated with high voltage power circuits necessary for powering EDS were still gained. Going forward, if more testing can be performed, a signal generator will be used to provide a smooth switching signal to the MOSFET driver.

It should be noted that the 230 VAC output from the sourced transformer is below the theoretically desired voltage range of 250-300 VAC. The selected transformer was the most suitable choice as it nearly met this range and was available for rapid procurement. In the future, a custom transformer could be developed that is capable of outputting 300 VAC.

RISK ASSESSMENT

To ensure that our final design solution poses as few risks as possible once implemented on NASA Artemis missions, risk analysis on various subsystems of the developed solution was performed. The implemented strategy was a failure mode and effects analysis (FMEA), with each failure corresponding to a different subsystem of the final solution.

Failure Mode and Effects Analysis (FMEA) Setup

To automate the calculation of risk probabilities for each failure mode, an FMEA spreadsheet was designed and utilized to assess each solution subsystem. When performing FMEA on a system, one is required to identify various modes of failure for each part, determine potential effects on the system from the mode, attribute each mode to a root cause, and list the various methods of detecting the mode. Each mode effect is given a severity rating (S) from 1-10, where 1 signifies a negligible impact on the system, while 10 signifies a very repercussive impact. Each root cause is given an occurrence rating (O) from 1-10, where 1 means that the root cause is very unlikely to occur while 10 indicates a very probable occurrence of the root cause. Finally, each mode detection method is assigned a detectability number (D) from 1-10, where 1 suggests that the detection method can be very easily used to identify the failure mode, while 10 indicates that the method is virtually useless in detecting the failure mode. For each mode-effect-cause-detection combination, a risk probability number (RPN) is calculated by finding the product of the severity, occurrence, and detection numbers for that combination. The highest RPN values typically indicate combinations which are very severe, very likely to occur, and not easily detectable, which present to the designer the subsystems which need to be assessed for risk mitigation. After identifying the highest risk combinations, potential solutions were presented in hopes of reducing either the severity or occurrence or increasing the detectability of the combination. Finally, new RPN values and risk reduction percentages were calculated with these solutions in mind. The detailed FMEA spreadsheet with the corresponding values and descriptions can be found in Appendix A Figure A1.

Risk Mitigation Strategies

The highest RPN values from the original FMEA spreadsheet were identified and then assessed for risk mitigation. High RPN values typically indicate mode-effect-cause-detection combinations which are very severe, very probable to occur, and not easily detectable, which present to the designer the subsystems which need to be assessed for risk mitigation. After identifying the highest risk combinations, potential solutions were presented in hopes of reducing either the severity or occurrence or increasing the detectability of the combination. Finally, new RPN values and risk reduction percentages were calculated with these solutions in mind. A secondary spreadsheet with just the highest risk failure modes along with the proposed risk mitigation strategies and corresponding rectified RPN values can be found in Appendix A Figure A2. Note that several of these risk mitigation strategies acted as drivers for some of the features

present in our developed solution whereas other strategies (specifically the solutions to overheating and diagnostic interfaces) are to be addressed in future developments of this solution.

DETAILED DESIGN SOLUTION

Although full EDS efficacy testing was unable to be completed, we decided to move forward with it as the primary solution for the mitigation of lunar dust on xEMU spacesuits. This decision was made based on the theoretical calculations and results of past EDS implementations uncovered in our literature review. Our proposed final solution consists of an electrode sleeve that can be rapidly integrated into the surface of xEMU space suits that are prone to the highest level of lunar dust accumulation. These areas include the upper arms, forearms, thighs, and calves, as these were noted by literature as the most vulnerable areas of the spacesuit to lunar dust contamination [3]. A simplified schematic of this solution can be seen below in Figure 41.

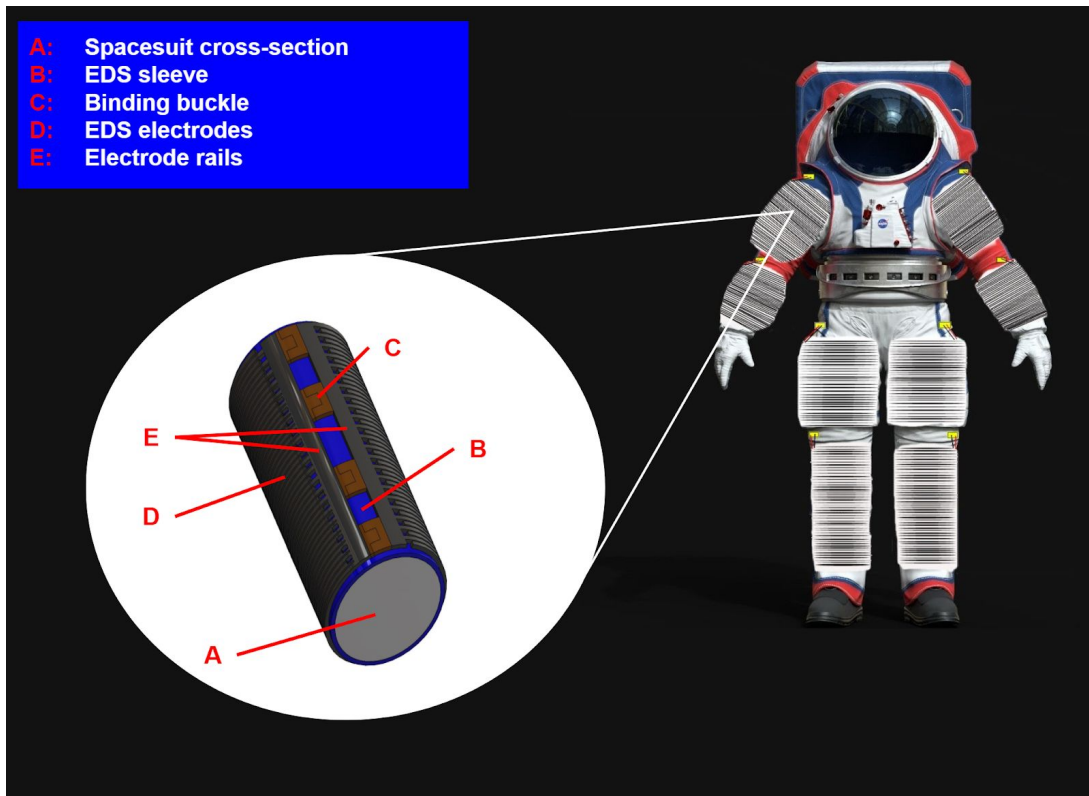


Figure 41. Schematic of developed solution design along with descriptions of important components.

The electrode spacing dimension for this electrode configuration can be found in the schematic for Figure 42 below.

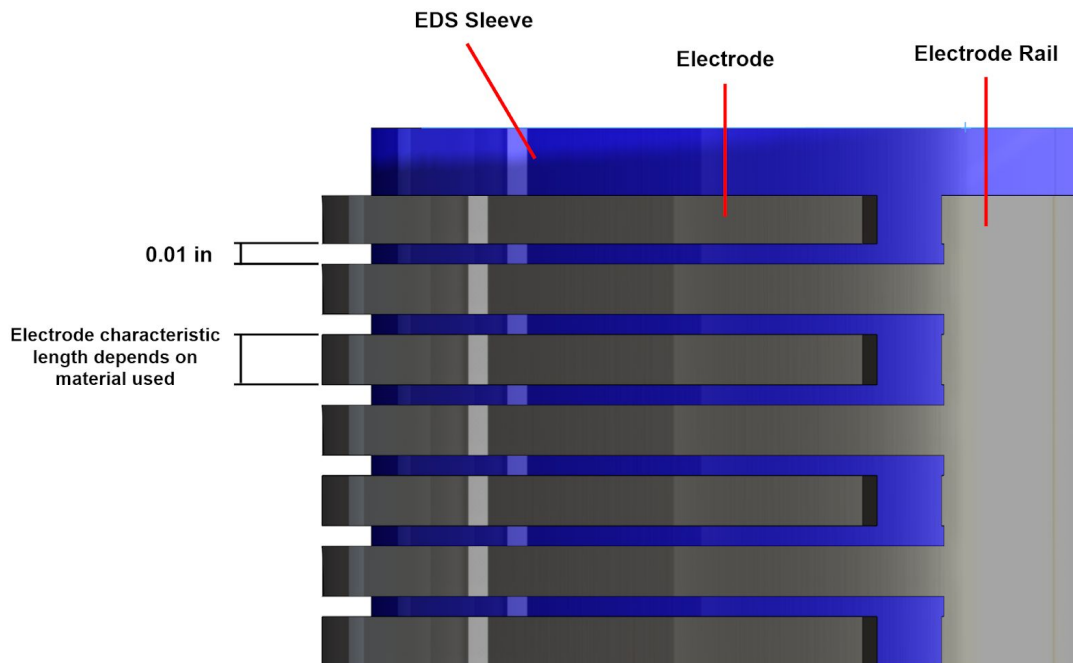


Figure 42. Relevant dimensions for EDS sleeve design.

The sleeves are to be constructed of a high elasticity ortho-fabric similar to the existing outer layer of NASA xEMU suits. The EDS mesh will be sewed into the fabric in a grid structure using 0.3 mm (0.01 in) gaps between adjacent electrodes (as derived in the Power Calculations for EDS section). The electrodes could potentially be enameled copper wire or carbon nanotube thread. Both materials serve as effective electrodes, but each carry drawbacks that will be discussed further in the Final Design Verification section of this report. Additionally, a segmented and fastenable solution utilizing multiple sleeves was selected in order to avoid stress in the electrodes (as discussed in the FMEA), improve ease of use, mitigate poor adhesion between each end of the sleeve (as discussed in the FMEA), and avoid modifying any fabric layers of the existing xEMU suits. Furthermore, the reason the electrodes were chosen to span along the length of the sleeves in a patterned hoop-like configuration was to ensure that the rails for either set of electrodes were adjacent to one another. As can be seen in Figure 41, the EDS sleeve rails are denoted with the letter E, and in a hoop electrode configuration, the two rails would be in proximity to one another. This would ensure that the wires providing the AC signal to the rails can be coupled through some physical means of fastening, therefore reducing the risk of entanglement or wire strain. This is another issue which was found to be apparent from our FMEA.

In accordance with the requirements and specifications this solution is expected to meet or exceed all design requirements and specifications. The proposed EDS grid geometry should easily be able to mitigate small lunar dust particles while only consuming 30 W of power. Additionally, the power supply designed to power the EDS will be relatively small and should be fairly easy to integrate into the existing xEMU power pack. The dimensions of the prototype circuit were roughly 5" x 3" x 1". This volume could

be further reduced by creating a circuit PCB that has a purpose-driven microprocessor instead of using a standalone microcontroller. A CAD model of a potential circuit packaging solution can be found in figure 43 below.

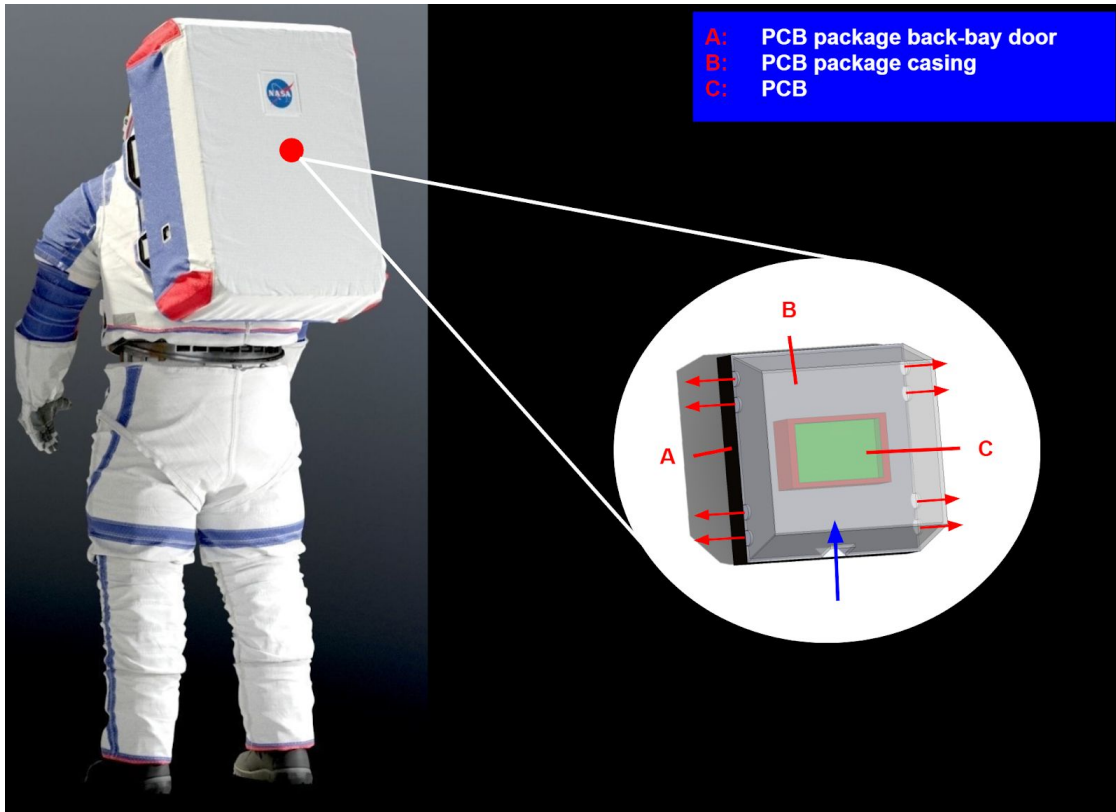


Figure 43. Schematic depicting electronic PCB packaging mechanism. Red arrows represent wires connecting PCB output to EDS sleeve rails. Blue arrow represents power input from the spacesuit battery.

Another important concept in the final proposed design is the wiring harness strategy. To ensure that the PCB circuit for the EDS sleeves is secured at the back of the spacesuit, it will be mounted onto a board, which will then be able to accommodate a casing used to seal the circuit from the external environment. In the diagram above in Figure 43, there are circular holes present in the casing to allow for wiring to route from the PCB to the electrode rails on the EDS sleeves. There is also a larger hole present on the bottom of the casing which is meant to feed in the power source wiring to the PCB. In order to ensure these holes do not defeat the purpose of a protective circuit casing, it is recommended that internal wire connectors from the PCB be press-fitted into the holes. These connectors can then be joined with longer wires which will then supply the AC signal to each EDS sleeve. This casing subsystem will then be attached onto the rear of the spacesuit.

It is also noteworthy to mention why our design solution leverages the use of external EDS “sleeves” which will be worn by the astronauts. Another alternative to this solution would be integrating micro-scale EDS circuits into existing xEMU spacesuit architecture. This solution would undoubtedly be

the more aesthetic of the two and would not require additional add-on mass during missions. However, integrating our EDS electrodes into the layers of the spacesuit would require us to alter the existing spacesuit design. This alternative will not be as easily adoptable by NASA, which is one of our requirements, and would require much more effort with regards to manufacturing and integration. Furthermore, utilizing an external system would ensure modularity, and with the usage of fastenable EDS sleeves and elastic ortho-fabric, we can ensure that this solution is functional for a wide range of spacesuit dimensions. The modularity of this solution also means that it is a reusable one. A spacesuit-integrated EDS circuit would remain bound to one spacesuit, while an external solution like EDS sleeves can be transferable from one spacesuit to another if required. These sleeves can also be cleaned after use and could potentially be reused for more than one mission cycle. Hence, for all the above reasons, it is clear why an externally-mounted solution for lunar dust mitigation on spacesuits is preferred, at least in the scope of this project.

FINAL DESIGN VERIFICATION

Once the final design is physically created, verification is necessary to make sure the final solution satisfies the requirements and specifications derived at the beginning of the design process and to demonstrate the different qualities of the solution. Various different verification methods will be used to certify that all requirements and specifications were satisfied. To re-hash, the requirements for the concept solution are as follows: able to manage and mitigate small particles, easily adoptable by NASA, operable in harsh lunar South Pole conditions, TRL-4 compliance, durable, cost effective, and minimal required operation time.

Able to Mitigate Small Particles

The EDS must be able to mitigate the accumulation of dust particles that are between 0.5 - 50 μm in diameter. Successful EDS efficacy testing in vacuum chambers using a dust simulant with a mean particle size less than 50 μm (such as the JSC-1A simulant) will verify that the solution is able to mitigate small particles and meets the specification. A test plan for efficacy testing the EDS can be found in appendix A4.

Easily Adoptable by NASA

In order for the solution to be easily adoptable for NASA, three different specifications must be met. The first is that the solution must weigh less than 6 kg. To ensure this specification is met, the complete EDS (including its power supply, harness, circuits, electrodes, sleeves, etc..) will be weighed on a scale. The next specification is that the length, width, and height of the solution must be less than 50 cm. While the EDS will certainly be larger than the specified dimensions while being worn by the astronauts during EVA, it only needs to meet the specifications when being transported to and from the moon on the spaceship. To ensure the specification is met, all parts of the EDS must fit in a 50 x 50 x 50 cm box. The final specification is that the solution must be toxic hazard level 0 according to NASA JSC 26895 guideline. None of the anticipated components of the EDS are toxic and all materials used in the EDS will be checked and verified by the said NASA guideline.

Operable in Harsh Lunar Environments

As the EDS is a real-time mitigation solution, it must properly function in the harsh South Pole lunar environment. It must be operable in a temperature range of -243 °C to -49 °C and withstand a pressure of 3×10^{-5} bar. To ensure it can operate in these conditions, the EDS will be efficacy tested in similar conditions. The vacuum chamber will be able to provide the necessary pressure and can be subjected to cryogenic conditions and temperatures to simulate these conditions. If the EDS is still able to mitigate the accumulation of at least 85%-90% of the dust, the specifications will be met.

TRL-4 Compliance

To ensure the solution is TRL4 ready, the EDS must be ready to be tested and validated in a laboratory environment. This includes hardware qualifications, software qualifications, and exit criteria. A more detailed description of TRL protocols can be found in Appendix A Figure A4. For hardware qualifications, a low fidelity prototype must be built and operable to demonstrate basic functionalities in critical test environments, and performance predictions must be made relative to the final operating environment. For software qualifications, critical software components must be integrated and functionally validated for operability with hardware in relevant environments, and performance predictions must be made relative to the final operating environment. For exit criteria, the documented test criteria must be in agreement with analytical predictions, and relevant environments must be detailed. To verify this requirement, the EDS system will be tested in a vacuum chamber lab environment with all of the hardware and software components for the prototype integrated. We will proceed to document the functionalities of the hardware and software components, and determine how the system would operate in the final operating environment based on the environment conditions set during lab testing.

Durable

Unfortunately, it is difficult to test the durability of the solution within a reasonable timeframe. In order for the EDS to be deemed as durable, it must be able to withstand two lunar cycles, which equates to 60 earth days. The EDS must be operable for each of the 60 days and must maintain its average measured efficiency. To verify the durability of the solution, the EDS will be used every day, for 60 days straight without substantial maintenance. If its functionality and efficiency remains somewhat constant, it will be deemed as durable. If this is not possible due to time constraints, the EDS will be used every day for as many days as possible, and the functionality and efficiency data will be analyzed to see if the EDS system is durable.

Cost Effective

The total amount of money awarded for developing a solution is at most \$180,000. Based on our calculations and prediction, the total cost of a suit is \$237.55. A breakdown can be found in Table 9 below. This cost is lower than the allotted \$180,000 so the solution should meet the cost effective requirement. It should be noted that copper wire is currently selected to be the base material of the electrodes as it is much cheaper than CNT thread. However, we are still considering using CNT for a potential hybrid design. The main advantage of CNT over copper wire is that it can withstand higher stresses and hypothetically provides a more efficient EDS. CNT could potentially be used in areas that experience high hoop stresses and areas with greater dust accumulation.

Table 9. Budget breakdown for a bundle of EDS sleeves. Note that a bundle consists of eight sleeves, two for each appendage. The cost for copper wire was taken from Table 10.

Component	Quantity	Total Cost
47 nF, 400V Capacitor	1	\$16.99
4800 μ F, 16V Capacitor	1	\$7.99
10 μ F, 16V Capacitor	1	\$8.49
1N4001 Diode	3	\$4.28
IRFZ44N MOSFETs	2	\$6.75
Arduino Uno	1	\$23.00
IR2301PBF MOSFET Driver	1	\$6.70
DC Power Supply	1	\$54.00
HM4118-ND Transformer	1	\$10.76
100 Ohm Resistor	2	\$5.53
36 AWG Copper Wire with Enamel	3	\$26.07
PTFE Fiberglass Fabric	1	\$66.99
TOTAL		\$237.55

Minimal Required Operation Time

When the xEMU suit is fully finished and the EDS ready to be implemented, the astronauts will do a run through of equipping and powering the EDS. They will be timed starting from when they start setting up the EDS on the spacesuit to the time when the EDS is fully powered and ready to use. Specifically, they will be timed while they pull on all 8 sets of sleeves, buckle up and connect all of the electrodes, connect all the electrodes to the main power supply, and finally turn on and power the EDS. If they take less than 15 minutes to perform all of these actions, the solution will have met the specification. It should be noted however that this requirement is desired and not required, so if the astronauts take a little longer to set up and power the EDS, the solution will still be considered valid. Below is a verification/compliance table which consolidates these testing criteria.

Performance Statistic	Measurement Unit	Needed Value	Requirement	Performance Met?
Dust Mitigation	% Dust Mitigated	≥ 90	Needed	
Low Weight	Kg	< 6 kg	Needed	
Small Size	cm	L & W & H ≤ 50 cm	Needed	
Non - Toxic	-	Non-Toxic (according to NASA JSC 26895)	Needed	
Operable in Lunar Environment	°C	-243 °C to -49 °C	Needed	
Operable in Lunar Environment	bar	3 x 10 ⁵ bar	Needed	
TRL4 Readiness	-	Ready	Needed	
Durability	months	Lasts 2 months	Needed	
Cost Effective	\$	< \$180,000	Needed	
Ease of Use	min	< 15min	Desired	

Figure 44. Verification/compliance table for our proposed EDS sleeve solution.

DISCUSSION AND RECOMMENDATIONS

The next steps in the project after finishing vacuum chamber efficacy testing is to create a plan for integrating the EDS system onto the xEMU suit. In this section, we will outline the assembly plan along with the materials needed, the anticipated cost to develop an EDS per suit, the wearing procedure, and further expertise needed to complete the project.

Suit Assembly Plan and Materials

The primary materials used on the spacesuit will be the electrodes producing the EDS, the power supply, copper wiring, carbon nanotubes (CNT) (just for future consideration), and the buckles (made of plastic). The higher level assembly plan is as follows. First, the CNT/copper will be cut to size according to the xEMU arm/leg circumference. Next, the electrodes will be attached to the ortho fabric, along with the buckles. Finally, the power supply will be attached and implemented into the xEMU spacesuit, and will be attachable to the 8 sections of the EDS. The power supply will be integrated with the rest of the xEMU functions and will act be attached to the rest of the EDS circuits before extravehicular activity (EVA).

Cost Comparison of Electrode Material

As explained in the previous segment, there are two primary materials being considered for the electrodes in the final proposed EDS sleeve solution. The following table (Table 10) details the price of both of the materials, the amount of each material used for all 8 EDS sleeves, the overall cost and usage of each when implemented in our solution.

Table 10. Cost comparison between carbon nanotube thread and copper wire for proposed total EDS sleeve system.

EDS Sleeve Location	Length of suit section (in)	Diameter (in)	Fabric Needed (A) in ²	Linear ft of electrode material (for 2 of each)	Total Cost CNT Thread (\$1,300/32.8084 ft)	Linear Cost Per Foot Copper Wire (\$8.69/3708 ft)
Forearm (X2)	8	4	100.5309649	1030.7555	40842.65463	2.462916324
Upper Arm (X2)	9	6	169.6460033	1787.955	70845.92665	4.190218163

Thigh (X2)	12	8	301.5928947	3221.69883	127656.5904	7.550313601
Calf (X2)	12	4.5	169.6460033	1755.621458	69564.74244	4.114441875
				Cost of Electrodes For Full System:	\$ 308,909.91	\$ 18.32

As seen from the table, the CNT thread is much more expensive than the coated copper wire. If each suit were homogenous and made of one specific material, the copper suit would be around \$20 and the carbon nanotube would be around \$300,000. Unfortunately, using an EDS that utilizes a full CNT solution will not meet our cost effective requirement as a full CNT suit will cost upwards of \$300,000. This is much greater than our limit of \$180,000. While copper is much more inexpensive, it may be more robust to develop a hybrid solution that utilizes a specific combination of copper and CNT. The advantage of using CNT over copper is that it can handle a higher hoop stress and provides a more effective EDS. Currently, this idea is being further developed and will be considered in the future.

Wearing Procedure

In total, there are 8 wearable sections of the EDS: the two forearms, the thighs, the shins, and the upper arm. First, the astronauts will wear the arm sections of the EDS. Before wearing their space suit gloves, they will pull the upper arm section of the EDS over their arms and attach them to the main circuit. Next, they will pull over the forearm sections and secure each of the buckles. After securing the upper-body portions of the EDS, the astronauts will wear their gloves. Then, they will pull up the thigh sections of the EDS and attach it to the main circuit while ensuring the upper body circuit is working properly. Finally, they will wear the calf portions of the EDS and attach them to the major circuit. After everything is secured, the astronauts will put on their boots and be ready for EVA.

Anticipated Project Challenges

The root of the majority of our challenges comes from the limitations posed by COVID-19. Starting Wednesday November 18th, all of the on-campus labs have been shutdown, making it difficult to create prototypes and conduct additional efficacy tests. In addition, our data from NASA is very limited and it has been difficult to find the equipment that will work with our test plans.

EDS Challenges.

We foresee many difficulties when it comes to creating, testing, and analyzing an EDS prototype. In order to have a working prototype, we require a power supply that can provide at least 300V, a frequency output of 10Hz, and a power output of 30 W. It has been difficult finding a power source with these specifications, and as a result, we are currently researching alternative methods for reaching the necessary outputs. As explained, we are looking into the possibility of creating our own AC power supply, but this may be difficult to accomplish given the restrictions on students handling devices with voltages greater than 48V. We are currently talking with industry experts about the feasibility and safety of using this

setup. In addition, we anticipate it will be difficult to test the EDS even if we are successful in creating a working prototype due to the new university shut down order in the state of Michigan.

Testing Equipment Challenges. As mentioned in the previous section, gathering the equipment needed to power an EDS properly will be challenging. In order to test an EDS properly, the dust must be showered on the suit in a vacuum. Finding a vacuum chamber on campus that could be used for testing has also been difficult. The chambers on campus that are accessible are either too small and cannot accommodate real time mitigation solutions. Finally, the last equipment challenge we face is the limited size of the XP56 scale. We have managed to work around this limitation for our first set of efficacy tests involving post mitigation solutions. However, we will still need to find a way to fit an EDS on a 1.6” x 1.6” square piece of teflon fabric which could be potentially problematic.

Materials Challenges. Unfortunately, NASA is unable to disclose in depth information on the xEMU suits that will be used by astronauts on the Artemis missions. As a result, there is very limited information on the internet and even fewer products available for consumers that could potentially simulate the xEMUs. As far as we know, the outer layer of the spacesuit is made of some sort of teflon. Furthermore, we have found no information on the material used on the astronauts’ boots. So far, we have purchased two different varieties of teflon fabric in hopes that they are suitable for emulating an xEMU outer layer.

Further Expertise Requirements

The main issue we face as a team is insufficient knowledge in the field of electrical engineering. It is difficult to predict the efficiency and effectiveness of our EDS circuit in harsh lunar conditions. In addition, it is difficult to work out the specifics of each of the EDS sleeves and how it will attach to the main power supply. Gaining support from electrical engineering experts for this project will help us ensure that our EDS works properly in any condition. Furthermore, looking back at the risk assessment which was performed on this system, it will be necessary to ensure that the further developed solution can mitigate all the identified risks. Unfortunately, due to resource and knowledge restrictions and constraints, a few of the more complicated risk mitigation solutions from the risk assessment were not implemented in our current proposed solution and will therefore need to be considered in future iterations. Finally, it would also be necessary to utilize this further expertise to address the challenges our project faced throughout the semester.

CONCLUSION

This report includes an in-depth description of Team 4’s ME450 senior design project, Mitigation and Prevention of Lunar Dust on NASA Artemis xEMU Spacesuits. The report covers literature review of existing technologies and problem scope, and the project’s deliverables. Our project’s primary objective is to develop a concept solution that is capable of removing and mitigating lunar dust off of xEMU spacesuits during lunar missions. Initial concept solutions generated and selected from literature review, concept generation techniques, and concept selection techniques include sticky mats, boot brushes, and EDS. After narrowing down to these three concepts, efficacy testing was performed to determine the best concept to move forward with in concept development and verification. Efficacy testing was done through a combination of physical prototype testing and simulation analysis. Through efficacy testing and project

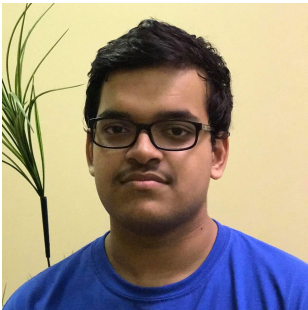
constraints, we decided to move forward with EDS as the final solution. Due to time constraints and restrictions due to COVID-19, further physical testing with EDS was not possible. However, we were able to create a finalized design concept for EDS integration with xEMU spacesuits that satisfy the requirements and specifications laid out by NASA. Detailed engineering analysis, risk assessment, and the detailed design solution are provided to describe the finalized solution's planned functionalities and characteristics. After ME450, we will submit the proposal to NASA with this solution in mind. If our project is chosen by NASA for the 2021 Lunar Dust Challenge and funding is awarded to us, we will continue to work on the finalized EDS solution physically on campus with the university facilities suitable for testing and verification. This report also describes challenges faced during the semester, as well as anticipated future challenges that may occur moving forward with the project.

AUTHORS



Mihir Gondhalekar

Mihir Gondhalekar is a senior at the University of Michigan pursuing a major in Mechanical Engineering. He was born in Flint, Michigan but grew up in Grand Rapids, Michigan. He really enjoys playing sports, video games, and mechanical engineering. He is also really interested in the space industry.



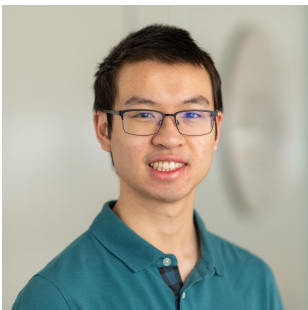
Nikhil Shetty

Nikhil Shetty is a senior at the University of Michigan pursuing a major in Mechanical Engineering and a minor in Computer Science. He is originally from India but was born and raised in Kuwait. Nikhil is currently serving his fourth year on the M-Fly SAE Aero Design Team and had the opportunity to lead the Manufacturing subteam last year. Outside of class and extracurriculars, Nikhil loves to play trivia, watch soccer, and make music.



Chad Parks

Chad Parks is a senior at the University of Michigan pursuing a major in Mechanical Engineering. He was born in Gladstone, a small town in Michigan's Upper Peninsula. He is a second year member of SaNima, a Bluelab sustainability club. In his free time he enjoys cycling, running, and exploring the outdoors.



Brian Wang

Brian Wang is a senior at the University of Michigan pursuing a major in Mechanical Engineering and a minor in Computer Science. He was born in Edison, New Jersey and grew up around Princeton, New Jersey. He has been part of University of Michigan's ASME chapter for four years, and is currently on the executive board. Outside of academics he enjoys playing soccer, video games, breakdancing, and travelling.

ACKNOWLEDGMENTS

We would first and foremost like to thank Professor Heather Cooper, our ME 450 instructor for providing us with endless support throughout the semester. Without her continuous efforts, this project would not have been possible. We would also like to thank our faculty advisor, Professor Jesse Capecelatro, for assisting us in a variety of different ways regarding the technical aspects of our project. His expertise in particle-laden flow came to be very useful during the engineering analysis phase of our design project, specifically the EDS numerical analysis portion. He also played an integral role in helping us prepare the necessary documents required for our NASA 2021 Big Idea Challenge proposal. On a similar note, we would like to thank Dr. Mark Moldwin for reviewing the administrative aspects of our project and acting as our state space grant representative for the Big Idea Challenge. We would like to thank Andy Poli for providing us with a safe laboratory environment for testing during the SARS-CoV-2 pandemic. His knowledge in power electronics also proved to be crucial in our exploration of a physical EDS prototype. We would also like to thank Dr. Jon Van Noord from the CLaSP department for his guidance regarding options for vacuum chamber testing in the near future. Finally, we would like to acknowledge Charlie Bradley and Jonathon Yenkel from the Mechanical Engineering Machine Shop for assisting us in manufacturing our testing apparatus.

REFERENCES

- [1] Y. Liu and L. A. Taylor, "LUNAR DUST: CHEMISTRY AND PHYSICAL PROPERTIES AND IMPLICATIONS FOR TOXICITY," *Lunar and Planetary Institute*, 2008. [Online]. Available: <https://www.lpi.usra.edu/meetings/nlsc2008/pdf/2072.pdf>. [Accessed: 29-Sep-2020].
- [2] T. J. Stubbs, R. R. Vondrak, and W. M. Farrell, "IMPACT OF DUST ON LUNAR EXPLORATION," *NASA*, 2002. [Online]. Available: https://www.nasa.gov/centers/johnson/pdf/486014main_StubbsImpactOnExploration.4075.pdf. [Accessed: 2020].
- [3] J. F. Lindsay, "Lunar Dust Effects on Spacesuit Systems," *Lunar and Planetary Institute*, 2009. [Online]. Available: https://www.lpi.usra.edu/lunar/strategies/ChristoffersenEtAl_NASA-TP-2009-214786_LunarDustEffectsSpacesuitSystems.pdf. [Accessed: 2020].
- [4] S. Spears, "NASA's BIG Idea Challenge," *bigidea.nianet.org*, 2020. [Online]. Available: <http://bigidea.nianet.org/>. [Accessed: 30-Sep-2020].
- [5] L. Lieng-Huang, "Adhesion and cohesion mechanisms of lunar dust on the moon's surface," *Taylor & Francis*, 2012. [Online]. Available: <https://www.tandfonline.com/doi/abs/10.1163/156856195X00932?journalCode=tast20>. [Accessed: 30-Sep-2020].
- [6] T. J. Stubbs, R. R. Vondrak, and W. M. Farrell, "A Dynamic Fountain Model for Lunar Dust," *NASA*, 2005. [Online]. Available: https://www.nasa.gov/centers/johnson/pdf/486013main_Stubbs.pdf. [Accessed: 29-Sep-2020].
- [7] K. K. Manyapu, P. D. Leon, L. Peltz, J. R. Gaier, and D. Waters, "Proof of concept demonstration of novel technologies for lunar spacesuit dust mitigation," *Acta Astronautica*, 18-May-2017. [Online]. Available: <https://www.sciencedirect.com/science/article/pii/S0094576516313029>. [Accessed: 30-Sep-2020].
- [8] Gaier, James & Waters, Deborah & Banks, Bruce & Knox, Khriisaundra & Christopher, Steven. (2011). Evaluation of Lunar Dust Mitigation Strategies for Thermal Control Surfaces. 10.2514/6.2011-5182.
- [9] J. Jiang, Y. Lu, H. Zhao, and L. Wang, "Experiments on dust removal performance of a novel PLZT driven lunar dust mitigation technique," *Acta Astronautica*, 30-Aug-2019. [Online]. Available: https://www.sciencedirect.com/science/article/pii/S009457651931241X?casa_token. [Accessed: 30-Sep-2020].

- [10] D. J. Loftus, "The Chemical Reactivity of Lunar Dust Relevant to Human Exploration of the Moon," *Lunar and Planetary Institute*, 2009. [Online]. Available: <https://www.lpi.usra.edu/decadal/leag/DavidJLoftus.pdf>. [Accessed: 29-Sep-2020].
- [11] S. X. staff, "NASA's dirty secret: Moon dust," *Phys.org*, 26-Sep-2008. [Online]. Available: <https://phys.org/news/2008-09-nasa-dirty-secret-moon.html>. [Accessed: 30-Sep-2020].
- [12] J. Agui, R. Green, and R. Vijayakumar, "NASA Technical Reports Server (NTRS)," *NASA*, 09-Jul-2018. [Online]. Available: <https://ntrs.nasa.gov/citations/20180008634>. [Accessed: 30-Sep-2020].
- [13] "Moon Fact Sheet," *NASA*. [Online]. Available: <https://nssdc.gsfc.nasa.gov/planetary/factsheet/moonfact.html>. [Accessed: 30-Sep-2020].
- [14] "NASA's Lunar Exploration Program Overview." [Online]. Available: https://www.nasa.gov/sites/default/files/atoms/files/artemis_plan-20200921.pdf.
- [15] A. M. Jarvis, "International Space Station ISS EVA Checklist," *Space Ref*, 2001. [Online]. Available: <http://www.spaceref.com/iss/ops/7A.EVA.checklist.pdf>. [Accessed: 29-Sep-2020].
- [16] Victory Complete. 2020. *Professional Cordless Electrostatic Handheld Sprayer – Victory Complete*. [online] Available at: <https://www.victorycomplete.com/product/professional-cordless-electrostatic-handheld-sprayer/> > [Accessed 21 October 2020].
- [17] NASA, 2020. *Twitter*. [Online] Twitter.com. Available at: https://twitter.com/NASA_Technology/status/1186706059718725632 > [Accessed 21 October 2020].
- [18] "3/8 in. x 50 ft. Industrial Grade Air Hose Reel," *Harbor Freight Tools*, 2020. [Online]. Available: <https://www.harborfreight.com/38-in-x-50-ft-industrial-grade-air-hose-reel-64925.html>. [Accessed: 21-Oct-2020].
- [19] "Top Ten NASA Spinoffs," *Zidbits*, 29-May-2017. [Online]. Available: <https://zidbits.com/2010/11/top-ten-nasa-spinoffs/>. [Accessed: 21-Oct-2020].
- [20] University of Texas at Dallas, "University Mourns Loss of Famed Geoscientist, Community Cornerstone," *DiscoverRichardson.com*, 23-Sep-2019. [Online]. Available: <https://www.discoverrichardson.com/colleges/university-mourns-loss-of-famed-geoscientist-community-cornerstone/>. [Accessed: 21-Oct-2020].
- [21] H. Przybyla, "DuPont expediting production of Tyvek hazmat suits for health care workers," *NBCNews.com*, 26-Mar-2020. [Online]. Available:

<https://www.nbcnews.com/health/health-care/dupont-expediting-production-tyvek-hazmat-suits-health-care-workers-n1169031>.

- [22] H. Kawamoto and N. Hara, “Electrostatic Cleaning System for Removing Lunar Dust Adhering to Space Suits,” *Journal of Aerospace Engineering*, vol. 24, no. 4, pp. 442–444, 2011.
- [23] M. R. Johansen et al., “History and flight development of the electrodynamic dust shield,” *AIAA SPACE 2015 Conference and Exposition*, 2015.
- [24] K. Burrage and T. Tian, “A Note On The Stability Of The Euler Methods For Solving Stochastic Differential Equations,” *Journal of Computational and Applied Mathematics*, 1999.
- [25] “LMS-1 Lunar Mare Simulant Fact Sheet,” *UCF Exolith Lab*. Available: https://sciences.ucf.edu/class/wp-content/uploads/sites/58/2019/02/Spec_LMS-1.pdf
- [26] C. R. Buhler, “Current State of the Electrodynamic Dust Shield for Mitigation,” NASA, 2020.
- [27] S. A. Orszag, “Numerical Simulation of the Taylor-Green Vortex,” MIT, 1974.
- [28] American Elements, “Copper Wire,” *American Elements*, 13-Jun-2017. [Online]. Available: <https://www.americanelements.com/copper-wire-7440-50-8>. [Accessed: 09-Dec-2020].
- [29] C. Woodford, “How does Kevlar work?,” *Explain that Stuff*, 25-Feb-2020. [Online]. Available: <https://www.explainthatstuff.com/kevlar.html#pagetop>. [Accessed: 09-Dec-2020].
- [30] ILC Dover (1994). Space Suit Evolution From Custom Tailored To Off-The-Rack. Retrieved December 09, 2020, from https://spaceflight.nasa.gov/outreach/SignificantIncidentsEVA/assets/space_suit_evolution.pdf

APPENDIX A (IMPORTANT SUPPORTING DOCUMENTATION)

Table A1. Manufacturing plan for test box

Manufacturing Plan					
<i>Part Number:</i>	1				
<i>Part Title:</i>	Test Box				
<i>Team Name:</i>	Lunatics				
<i>Raw Material Stock:</i>	6, 12"x12" 0.25" thick Acrylic Sheets				
<i>Step #</i>	<i>Process Description</i>	<i>Machine</i>	<i>Fixture(s)</i>	<i>Tool(s)</i>	<i>Speed (RPM)</i>
1	Laser cut acrylic sheets	Laser Cutter			
2	Transfer punch blanks onto frame in alignment with acrylic sheet holes			Transfer Punch, Bar Clamps	
3	Drill press through holes at transfer punch blanks locations for frame	Drill Press	Bar Clamps	1/4-20 Through Hole Drill Bit, Size F (0.2570) for close fit	1200 or less
4	Remove frame and deburr			Hole deburring tool	

Table A2. Testing plan for sticky mat solution

Test Plan - Sticky Mat				
Step #	Process Description	Equipment/ Tools	Time (min)	Location
1	Cut out 1.6" by 1.6" square swatch of teflon fabric	Scissors, calipers	1	Assembly Room/3rd Floor Tables, Concurrent
2	Place teflon square in test chad dish with lid, weight all together, remove from scale afterwards	Chad Dish, Tweezers, Mettler Toledo XP56	10	Assembly Room/3rd Floor Tables, Poli Lab
3	Cut 10"x10" square sheet of a sticky mat	Scissors, Tape Measuring	1	Assembly Room/3rd Floor Tables
4	Fill dust chad dish with roughly 50mg of LMS-1 and shake to apply charge	Chad Dish, food scale (1st plan), Capsules (2nd plan)	2	Assembly Room/3rd Floor Tables, Concurrent
5	Place dust chad dish with the LMS-1 at the bottom of the test box and secure	Test Box, Chad Dish	1	Assembly Room/3rd Floor Tables
6	Put the teflon square on top of the LMS-1 in test chad	Chad Dish, Test Box	5	Assembly Room/3rd Floor Tables

(1) dish

(1) dish permanent LMS-1 Holder

(1) dish permanent LMS-1 holder

	dish and apply >3.3lbf				
7	Place teflon square with LMS-1 in a new chad dish with lid, and weigh both together	Tweezers, Mettler Toledo XP56	10	Assembly Room/3rd Floor Tables, Poli Lab	
8	Place the sticky mat in the bottom of the test box and secure	Test Box	2	Assembly Room/3rd Floor Tables	
9	Remove chad dish and square from scale, remove square from chad dish	Tweezers	3	Assembly Room/3rd Floor Tables, Poli Lab	
10	Place the dirty teflon square in the test box with the dirty side faced towards the sticky mat. Apply <3.3lbf to the clean side and attempt to remove as much dust as possible	Test Box, Tweezers, Weights	5	Assembly Room/3rd Floor Tables	

11	Remove the newly cleaned teflon circle, place in the original chad dish, and re-weigh both	Tweezers, Mettler Toledo XP56	10	Assembly Room/3rd Floor Tables, Poli Lab	
12	Remove sticky mat from box and dispose	Test Box	1	Assembly Room/3rd Floor Tables, Concurrent	
13	Dispose of teflon square with remaining LMS-1 on it	Tweezers	1	Assembly Room/3rd Floor Tables, Concurrent	

Table A3. Testing plan for boot brush solution

Test Plan - Boot Brush						
Step #	Process Description	Equipment/Tools	Time (min)	Location		
1	Cut out 1.6" by 1.6"square swatch of teflon fabric	Scissors, calipers	B1	Assembly Room/3rd Floor Tables, Concurrent		
2	Place teflon square in test chad dish with lid, weigh all together, remove from scale afterwards	Chad Dish, Tweezers, Mettler Toledo XP56	10	Assembly Room/3rd Floor Tables, Poli Lab		
3	Fill dust chad dish with roughly 50mg of LMS-1 and shake to apply charge	Chad Dish, food scale (1st plan), Capsules (2nd plan)	2	Assembly Room/3rd Floor Tables, Concurrent	(1) dish	
4	Place dust chad dish with the LMS-1 at the bottom of the test box and secure	Test Box, Chad Dish	1	Assembly Room/3rd Floor Tables	(1) dish permanent LMS-1 Holder	
5	Put the teflon square on top of the LMS-1 in test chad dish and apply >3.3lbf	Chad Dish, Test Box	5	Assembly Room/3rd Floor Tables	(1) dish permanent LMS-1 holder	

6	Place teflon square with LMS-1 in a new chad dish with lid, and weigh both together	Tweezers, Mettler Toledo XP56	10	Assembly Room/3rd Floor Tables, Poli Lab		
7	Remove chad dish and square from scale, remove square from chad dish	Tweezers	3	Assembly Room/3rd Floor Tables, Poli Lab		
8	Place the dirty teflon square in the test box with the dirty side faced upwards. Apply force with boot brush for 15 seconds, remove as much dust as possible (must be same person each time)	Test Box, Tweezers, Weights	5	Assembly Room/3rd Floor Tables		
9	Remove the newly cleaned teflon circle, place in the original chad dish, and re-weigh both	Tweezers, Mettler Toledo XP56	10	Assembly Room/3rd Floor Tables, Poli Lab		
10	Clean boot brush (with running water or whatever)	Test Box	1	Assembly Room/3rd Floor Tables, Concurrent		

11	Dispose of teflon square with remaining LMS-1 on it	Tweezers	1	Assembly Room/3rd Floor Tables, Concurrent		
----	---	----------	---	--	--	--

Table A4. Testing plan for EDS efficacy test and verification

Test Plan - EDS				
Step #	Process Description	Equipment/Tools	Time (min)	Location
1	Take a square swatch of EDS sewn on CNT and weigh the sample	Scale	1	Testing Site - Scale
2	Gather a set amount of lunar dust simulant and place into the lunar dust simulant holder (LDSH) and weigh the two	Scale	1	Testing Site - Scale
3	Place swatch with EDS within a vacuum chamber	Vacuum Chamber, Tweezers	2	Testing Site - Vacuum Chamber
4	Place and hold lunar simulant above the EDS using the LDSH and get it ready to be dumped	Vacuum Chamber, Tweezers, LDSH	5	Testing Site - Vacuum Chamber
5	Supply power to EDS and turn it on	Vacuum Chamber, Power Supply	5	Testing Site - Vacuum Chamber

6	Make sure the vacuum chamber is sealed and turn it on. Lower the pressure to 3×10^5 bar	Vacuum Chamber	10	Testing Site - Vacuum Chamber
7	Lower vacuum chamber temperature to at least -49 °C	Vacuum Chamber	10	Testing Site - Vacuum Chamber
8	Dump and shower lunar dust simulant on the EDS	Vacuum Chamber, LDSH	5	Testing Site - Vacuum Chamber
9	Power off vacuum chamber and EDS	Vacuum Chamber	2	Testing Site - Vacuum Chamber
10	Remove LDSH and EDS swatch	Vacuum Chamber, Tweezers	2	Testing Site - Vacuum Chamber
11	Weigh "dirty" EDS swatch	Scale	2	Testing Site - Scale
12	Weigh the previously emptied LDSH.	Scale	2	Testing Site - Scale

Solution Subsystem	Failure Mode	Failure Effect	Severity (S)	Root Cause	Occurrence (O)	Process Control	Detectability (D)	RPN
Power Circuit	EDS circuit overheating	Reduces electrode performance	6	High usage or insufficient cooling	7	Extremely difficult to detect	9	378
Wiring Harness	Entanglement of wires	Increase strain on wires	5	Improper harness placement/organization	8	Extremely difficult to detect	9	360
Electrodes	Electrode short circuit	Danger to EDS power subsystem	8	Electrode proximity from bending joints (elbows and knees)	7	Whole system stops working	5	280
Wiring Harness	Harness breaks	System stops functioning depending on tear location	9	Stretched radially	6	Visualize EDS sleeve failure(s)	5	270
Sleeve Bind	Sleeve bind detaches	EDS electrodes detached from spacesuit area	9	Bad physical adhesion between either end of sleeve	7	Visual inspection of loose bind	4	252
Wiring Harness	Wiring harness short	EDS sleeve failure(s)	8	Physical break in wiring harness	6	Visualize EDS sleeve failure(s)	5	240
Power Circuit	EDS PCB failure	Electrodes fail to be powered	8	Circuit element stops functioning	9	Dust remains on patch	3	216
Sleeve Bind	Opening present in bind	Lunar dust potentially seeps through opening	8	Tear in sleeve or propagation of opening	4	Visual inspection of tear	5	160
Electrodes	Electrode tears	Not all dust removed	8	Stretched radially	5	Visualize dust patch	3	120
Power Circuit	Insufficient power to PCB board	Electrodes fail to be powered	8	Main circuit battery failure	6	Failure warning from suit diagnostics	2	96
Electrodes	Electrode rail breaks	No dust removed from section	9	Stretched axially	5	Visualize too much dust	2	90
Sleeve Bind	Unable to detach sleeve after usage	Cannot re-use sleeve	5	Introduction of other sources of adhesion unaccounted for while manufacturing	3	Absurd amount of force required for detachment	3	45

Figure A1. FMEA spreadsheet used for risk assessment. Failure modes with highest RPN values are highlighted in red.

Solution Subsystem	Failure Mode	Original RPN	Proposed Solution	New S Value	New O Value	New D Value	New RPN	% RPN Reduction
Power Circuit	EDS circuit overheating	378	Include miniature low-power cooling fans activated by temperature sensor in EDS circuit box. Develop diagnostic interface which notifies astronaut of overheating.	6	4	3	72	81
Wiring Harness	Entanglement of wires	360	Enforce wire organization through the use of in-suit pathways. Link wires to strain gauges and notify astronaut of high-strain scenarios using diagnostic interface.	5	3	4	60	83
Electrodes	Electrode short circuit	280	Segment arm and leg EDS sleeves into two halves to limit electrode contact when bending elbows and knees or consider using enameled copper wire electrodes. Place proximity sensors in vicinity of electrodes to notify user of potential short circuiting.	8	5	3	120	57
Wiring Harness	Harness breaks	270	Utilize low-gauge wiring with elastic harness material to reduce risk of snapping. Include in diagnostic interface a feature which detects when the EDS stops functioning.	9	4	2	72	73
Sleeve Bind	Sleeve bind detaches	252	Leverage a system which uses clips and acceptors for linking the two ends of the electrode sleeve.	9	2	4	72	71

Figure A2. Risk mitigation strategies for most risky failure modes (derived from Figure A1 above). Potential risk mitigation strategies are color-coded to indicate which critical number (*S*, *O*, and *D*) is changed with implementation.

Finalized Project BOM						
Item	Category	Quantity	Product Price (Full-Quantity)	Delivery/Service Fees	Total Price	Supplier Link
LMS-1 Simulant	Simulant - lunar dust	1	25.00	10	35.00	https://sciences.ucf.edu/class/simulant_lunarmare/
PTFE Fabric Simulant	Simulant - spacesuit	1	66.99	4.02	71.01	https://rb.gy/iffphvx
Hand-held boot brush	Solution - boot brush	2	8.78	2.5	11.28	https://rb.gy/mcfyoi
Layered sticky mats	Solution - sticky mats	1	19.00	0	19.00	https://rb.gy/xmnpqm
Low-Grade Teflon Replacement	Simulant - spacesuit	2	13.98	0	13.98	https://rb.gy/is0bzv
Plastic Handle	Test box	1	3.90	6.51	10.41	https://www.mcmaster.com/1078A311/
Surface Mount Hinges	Test box	2	3.06	0	3.06	https://www.mcmaster.com/1603A2/
Cast Acrylic Panels	Test box	6	89.88	5.4	95.28	https://rb.gy/rmvzem
Chem-Resistant Glove Pack	Test box	1	8.99	0.54	9.53	https://rb.gy/et8cnp
Neodymium Magnets	Test box	4	6.92	6.93	13.85	https://www.mcmaster.com/5862K105/
Aluminum Tube Stock	Test box	1	0.00	0	0.00	ME Machine Shop
Black-Oxide Alloy Steel Hex Screws (1pk = 25qty)	Test box	1	6.09	0	6.09	https://www.mcmaster.com/91253A083/
Hinge Nuts (1pk = 100qty)	Test box	1	1.00	0	1.00	https://www.mcmaster.com/90480A003/
Phillips Head Screws	Test box	50	15.24	0	15.24	https://www.mcmaster.com/91772A548/
1/4-20 Nuts	Test box	50	4.88	16.92	21.80	https://www.mcmaster.com/95479A111/
3D printer nozzles	Testing apparatus	1	7.99	0	7.99	https://rb.gy/smfde0
PLA spool	Testing apparatus	1	22.99	1.89	24.88	https://rb.gy/0ma6yn
HM4118-ND Transformer	Solution - EDS	1	10.76	0	10.76	https://rb.gy/ivig72
IR2301PBF MOSFET Driver	Solution - EDS	2	6.70	12.04	18.74	https://rb.gy/7dpikp
0.13 mm copper wire	Solution - EDS	1	7.69	0	7.69	https://rb.gy/ukeff6
22 gauge wire	Solution - EDS	1	12.98	0	12.98	https://rb.gy/socswc
47 nF, 400 V Capacitor	Solution - EDS	1	16.99	0	16.99	https://rb.gy/nxtzfs
4800 µF, 16 V Capacitor	Solution - EDS	4	7.99	0	7.99	https://rb.gy/femhxu
10 µF, 16 V Capacitor	Solution - EDS	4	8.49	0	8.49	https://rb.gy/nys9w9
1N4001 Diode	Solution - EDS	100	4.28	0	4.28	https://rb.gy/sfytst
IRFZ44N MOSFETs	Solution - EDS	5	6.75	3.91	10.66	https://rb.gy/aok6kd
TOTAL					\$ 449.99	

Figure A3. Bill of materials for project.

Technology Readiness Level Definitions

TRL	Definition	Hardware Description	Software Description	Exit Criteria
1	Basic principles observed and reported.	Scientific knowledge generated underpinning hardware technology concepts/applications.	Scientific knowledge generated underpinning basic properties of software architecture and mathematical formulation.	Peer reviewed publication of research underlying the proposed concept/application.
2	Technology concept and/or application formulated.	Invention begins, practical application is identified but is speculative, no experimental proof or detailed analysis is available to support the conjecture.	Practical application is identified but is speculative, no experimental proof or detailed analysis is available to support the conjecture. Basic properties of algorithms, representations and concepts defined. Basic principles coded. Experiments performed with synthetic data.	Documented description of the application/concept that addresses feasibility and benefit.
3	Analytical and experimental critical function and/or characteristic proof of concept.	Analytical studies place the technology in an appropriate context and laboratory demonstrations, modeling and simulation validate analytical prediction.	Development of limited functionality to validate critical properties and predictions using non-integrated software components.	Documented analytical/experimental results validating predictions of key parameters.
4	Component and/or breadboard validation in laboratory environment.	A low fidelity system/component breadboard is built and operated to demonstrate basic functionality and critical test environments, and associated performance predictions are defined relative to the final operating environment.	Key, functionally critical, software components are integrated, and functionally validated, to establish interoperability and begin architecture development. Relevant Environments defined and performance in this environment predicted.	Documented test performance demonstrating agreement with analytical predictions. Documented definition of relevant environment.
5	Component and/or breadboard validation in relevant environment.	A medium fidelity system/component breadboard is built and operated to demonstrate overall performance in a simulated operational environment with realistic support elements that demonstrates overall performance in critical areas. Performance predictions are made for subsequent development phases.	End-to-end software elements implemented and interfaced with existing systems/simulations conforming to target environment. End-to-end software system, tested in relevant environment, meeting predicted performance. Operational environment performance predicted. Prototype implementations developed.	Documented test performance demonstrating agreement with analytical predictions. Documented definition of scaling requirements.
6	System/sub-system model or prototype demonstration in an operational environment.	A high fidelity system/component prototype that adequately addresses all critical scaling issues is built and operated in a relevant environment to demonstrate operations under critical environmental conditions.	Prototype implementations of the software demonstrated on full-scale realistic problems. Partially integrate with existing hardware/software systems. Limited documentation available. Engineering feasibility fully demonstrated.	Documented test performance demonstrating agreement with analytical predictions.
7	System prototype demonstration in an operational environment.	A high fidelity engineering unit that adequately addresses all critical scaling issues is built and operated in a relevant environment to demonstrate performance in the actual operational environment and platform (ground, airborne, or space).	Prototype software exists having all key functionality available for demonstration and test. Well integrated with operational hardware/software systems demonstrating operational feasibility. Most software bugs removed. Limited documentation available.	Documented test performance demonstrating agreement with analytical predictions.
8	Actual system completed and "flight qualified" through test and demonstration.	The final product in its final configuration is successfully demonstrated through test and analysis for its intended operational environment and platform (ground, airborne, or space).	All software has been thoroughly debugged and fully integrated with all operational hardware and software systems. All user documentation, training documentation, and maintenance documentation completed. All functionality successfully demonstrated in simulated operational scenarios. Verification and Validation (V&V) completed.	Documented test performance verifying analytical predictions.
9	Actual system flight proven through successful mission operations.	The final product is successfully operated in an actual mission.	All software has been thoroughly debugged and fully integrated with all operational hardware/software systems. All documentation has been completed. Sustaining software engineering support is in place. System has been successfully operated in the operational environment.	Documented mission operational results.

Figure A4. NASA TRL definitions.

NASA Submission Timeline	
September 25, 2020	Deadline to submit a Notice of Intent
October 7, 2020 11:59 AM EST	Deadline to submit questions for Q&A session Click here to submit questions for the Q&A session
October 14, 2020	Q&A Session for interested teams
December 13, 2020	Deadline to submit Project Plan Proposal and Video
January 29, 2021	Teams are notified of their selection status
Early February 2021	First installment of development stipends sent as appropriate
May 20, 2021	Mid-Point Report Deadline
June 10, 2021	Teams are notified of pass/fail status
Late June 2021	Second installment of stipends sent as appropriate (from SG directly to schools)
October 14, 2021	Deadline for Forum Registration & Hotel Reservations
October 27, 2021	Technical Paper and Verification Demonstration Submission Deadline
November 15, 2021	Presentation and Digital Poster File Submission Deadline
November 17 - 19, 2021	2021 BIG Idea Forum (in conjunction with ASCEND 2021)

Figure A5. NASA deliverables timeline for 2021 Big Idea Challenge. Deliverables which have been completed thus far are highlighted in green, and deliverables which are in progress are highlighted in yellow.

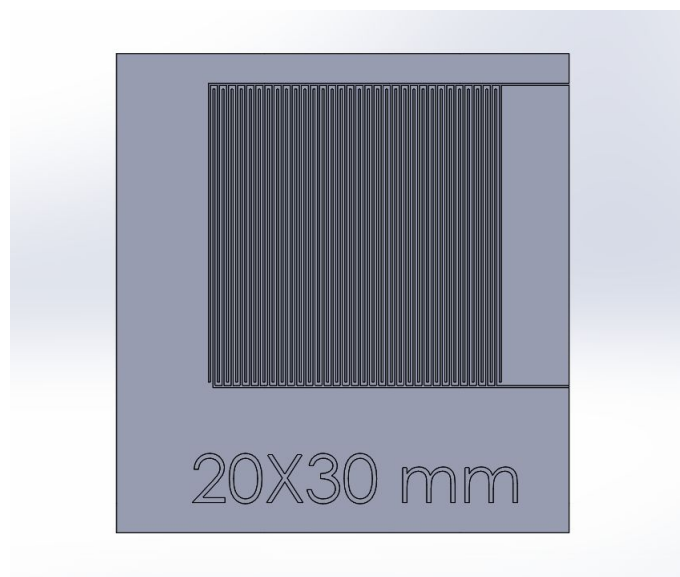


Figure A6. EDS wafer with proposed 0.3 mm electrode gap for prototyping purposes. This was unfortunately unable to be fabricated due to time and resource constraints.

APPENDIX B (SUPPLEMENTAL CONTEXT)

Engineering Standards

The 8000 - NASA standards were the primary standards considered throughout the development of our project. The primary standards considered within the 8000 series were NASA-STD-8739.4, NASA-STD-8739.8, NASA-STD-8739.10, NASA-HDBK-8739.21 and NASA-HDBK-8739.23.

NASA-STD-8739.4, titled “Workmanship Standard for Crimping, Interconnecting Cables, Harnesses, and Wiring” was reviewed when developing the final solution. Since our final proposed solution includes a wiring harness capable of connecting eight independent EDS, the guidelines in this standard will be critical if we are awarded funding to continue working on the 2021 BIG Idea Challenge.

NASA-STD-8739.8, titled “Software Assurance and Software Safety Standard” ensures that all software used and maintained by NASA is tested and meets the highest standards of safety. While our current solution is not yet fully developed, this standard should be met if we continue to develop a full stand-alone EDS system. Since the power supply we propose incorporates the use of a microcontroller, it is critical that all software used in the operation of the EDS sleeves meets this standard.

NASA-STD-8739.10 titled “Electrical, Electronic, and Electromechanical (EEE) Parts Assurance Standard” covers all non-flight systems used by NASA. Since our EDS sleeve is an electrical device in nature, this standard will be critical to verify and test the final solution to make sure it is safe and easily troubleshooted during use on the moon.

NASA-HDBK-8739.21 titled “Workmanship Manual for Electrostatic Discharge Control (Excluding Electrically Initiated Explosive Devices)” describes safe practices for discharging electrostatic devices. Since our proposed final design is an electrostatic device, it is paramount that this standard is considered and factored into the wear plan. It is likely that a plan to ensure all residual electrostatic charge on the surface of the spacesuit is discharged before reentry of the lunar habitat or spacecraft. This will lower the chances of an accidental discharge that could potentially damage sensitive electronics.

Finally, NASA-HDBK-8739.23, titled “NASA Complex Electronics Handbook for Assurance Professionals” while similar to NASA-STD-8739.10, delves more into complex embedded circuits. While our developed prototype was a fairly simple breadboard circuit, going forward it is likely that it will be adapted to a PCB and an integrated microcontroller will replace the arduino. If this is the case, our circuit must follow the guidelines laid out in this standard.

Engineering Inclusivity

Our EDS solution will encompass factors that will make it comfortable, accessible, and operable for all astronauts. The xEMU spacesuit is designed to be flexible and one-size-fits-all. The spacesuit is adaptable to different body types and all genders, and has an adjustable feature in the shoulder that makes it easier to wear. Our EDS solution which will be attachable to the xEMU spacesuit will not hinder any of these qualities that make the spacesuits adaptable to different body types.

More information about the spacesuits inclusivity for different body types can be found here:

<https://phys.org/news/2019-10-nasa-unveils-flexible-one-size-fits-all-space.html>

<https://www.marieclaire.com/fashion/a32033537/nasa-spacesuit-artemis-generation-astronauts/>

Environmental Context Assessment

To determine the environmental footprint and costs of our EDS sleeve solution, CES EduPack, an eco-audit software, was used. Firstly, several hand calculations were performed to determine the amount of mass of each material required with a bundle of EDS sleeves. Remember that each bundle consists of eight EDS sleeves, where each sleeve consists of several buckles, a layer of ortho-fabric, and two sets of electrodes. For this analysis, copper electrodes were considered for simplicity. To further simplify our analysis, we also excluded any effects from the PCB circuit, wiring harness, and power supply. In fact, the usage of our EDS sleeve solution would not occur on Earth, so therefore including the electronics isn't necessary. Furthermore, computing the carbon footprint from transportation of these EDS sleeves using spacecraft is not possible through CES EduPack and will therefore not be considered. Hence, only the material and manufacturing product phase for the non-electronic components were considered in this analysis.

Based on the above eco-audit model simplifications, the only information required to generate CO₂ footprint plots were the masses of copper wire, Kevlar ortho-fabric, and plastic buckles required for eight EDS sleeve assemblies. The corresponding materials used in EduPack are shown in Table B1 below.

Table B1. EduPack materials used for carbon footprint analysis of EDS sleeve solution

Component	CES EduPack Material
Electrodes and electrode rails	Copper, cast (h.c. copper)
Buckles	ABS+PVC (flame retarded)
Ortho-fabric	Kevlar 149 aramid fiber

The length of copper wire in feet required for eight EDS sleeves is provided in Table 10 in the main section of the report. The copper wire which we purchased from Amazon was used as the reference for other dimensions required to compute a total wire mass. From this table we see that roughly 7796 ft of copper wire is required. The wire's diameter is roughly 0.0049 inches in diameter. Then, using the equation for the volume of a cylinder, the wire's volume was found to be roughly 1.763 in³. A value for

enamel copper density was determined to be roughly 8.96 g/cm³ [28]. Multiplying this density with the volume provided us with a total wire mass of roughly 259 g, or around 9 oz.

A similar calculation was done for the ortho-fabric. The density of Kevlar ortho-fabric in particular was determined to be roughly 1.44 g/cm³ [29]. Then, the values in the below table were utilized for estimating the area of ortho-fabric required for each body segment (upper arm, forearm, thigh, and calf). Note that these values are simply estimates and wouldn't greatly affect the final eco-audit results.

Table B2. Diameter and height values for appendage areas which require EDS sleeves.

Appendage Area	Diameter [in]	Height [in]
Upper arm	6	9
Forearm	4	8
Thigh	8	12
Calf	4.5	12

Then, using the above values, surface areas were calculated for each appendage type (using the surface area formula for a cylinder). It must additionally be noted that there are two of each appendage present, meaning the total area can be found by computing the sum of twice each appendage surface area. The resulting value, 1483 in², is the total area of ortho-fabric required for eight EDS sleeves. A volume was then determined by finding the thickness for the outer layer of a representative xEMU spacesuit (~0.017 in) and multiplying it by the surface area [30]. Finally, taking the density of Kevlar ortho-fabric found above and multiplying it by the resulting fabric volume provided us with a total ortho-fabric mass of roughly 21 oz, or ~1.3 lb.

The above mass values for all materials are summarized in the EduPack image below.





Qty.	Component name	Material	Recycled content	Mass (lb)	Primary process	Secondary process	% removed	End of life	% recovered
1	electrodes	 Copper, cast (h.c. copper)	Virgin (0%)	0.5625	Casting		0	Reuse	100
1	buckles	 ABS+PVC (flame retar... 	Virgin (0%)	0.25	Polymer extrusion		0	Landfill	100
1	orthofabric	 Kevlar 149 aramid fiber	Virgin (0%)	1.3	Fabric production		0	Landfill	100

Figure B1. Eco-audit parameters for materials and manufacturing phase of product. Note that well-established manufacturing processes were chosen for each material.

The results from the EduPack simulation are shown in the figure below.

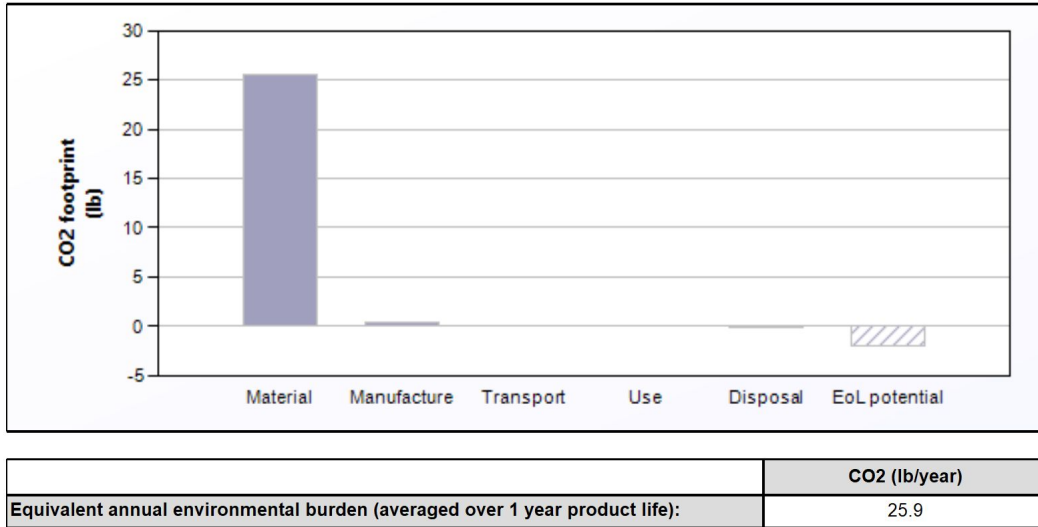


Figure B2. Annual carbon footprint of EDS sleeve bundle for single astronaut.

We can see from the figure above that the product phase which contributes the largest to increasing carbon footprint on Earth is the material phase. Coupled with the other product phases, each EDS sleeve bundle (eight sleeves) is expected to result in an environmental burden of roughly 25.9 lb of CO₂ per year. If these bundles are to be mass produced, then one can expect a rise compounding of this annual value; however, with a smaller CO₂ footprint on Earth for a single bundle, it is safe to say that our EDS sleeve solution is fairly environmentally sustainable.

It should once again be noted that the results from this EduPack analysis are solely underestimates of the actual environmental impact of our proposed solution. The limitations of EduPack prevent us from performing a more realistic analysis. Furthermore, several of the product phases would be inappropriate to include in the analysis for planet Earth, which makes this EduPack analysis even more limited.

Social Context Assessment

Socially, the main issue people have with space travel is that it is extremely costly and seems to be unnecessary and unessential for the common person. While it is true that our project will cost quite a bit, the technology is not limited to space travel. The EDS that we develop could also be used on earth and could have various useful applications. The EDS could have medical applications where it can be used to keep surfaces clean of dust.

Ethical Decision Making

The design process for the EDS solution and the implications of a finalized EDS solution encompasses ethical decision making. During the design process, Team 4 was in contact with the stakeholders to determine the requirements and specifications, as well as other details that were necessary for the ME450 senior design project and the NASA submission. The EDS solution was designed such that it would be safe for astronauts to use on Artemis missions while also having a high efficiency rate for mitigating lunar dust off of xEMU spacesuits. It was also designed so that there would be minimal hindrance to movement

while wearing the spacesuits. For the future finalized EDS solution and potential continuation of work with NASA on this challenge, if Team 4 is to be selected, we would continue to keep a constant stream of communication with NASA and other stakeholders so that all parties involved would be informed of details and changes of the solutions, to avoid problems with lack of communication or irresponsible management.

APPENDIX C (NUMERICAL SIMULATION CODE)

```
import os
import numpy as np
import matplotlib.pyplot as plt
# from mpl_toolkits.mplot3d import Axes3D
import imageio as im

SAVE_FOLDER = 'autosim' # for images

# define functions for E, dE/dx, dE/dy, and dE/dz
def efield(x, y, z):
    ex = np.multiply(np.sin(2*np.pi*x), np.cos(2*np.pi*y))
    ey = -1*np.multiply(np.cos(2*np.pi*x), np.sin(2*np.pi*y))
    ez = 0
    return ex, ey, ez

def efield2_grad(x, y, z, gradfac):
    dex2 = gradfac*4*np.pi*np.multiply(np.power(np.cos(2*np.pi*y), 2),
np.multiply(np.sin(2*np.pi*x), np.cos(2*np.pi*x)))
    dey2 = -gradfac*4*np.pi*np.multiply(np.power(np.cos(2*np.pi*x), 2),
np.multiply(np.sin(2*np.pi*y), np.cos(2*np.pi*y)))
    dez2 = 0
    return dex2, dey2, dez2

def create_plot(xp, yp, eps, Lx, Ly, mode, save_folder, imgname):
    plt.clf()
    plt.scatter(xp, yp, s=5)
    plt.xlim((0-eps, Lx+eps))
    plt.ylim((0-eps, Ly+eps))
    plt.xlabel('x')
    plt.ylabel('y')
    plt.title('Particle Trajectory')
    plt.gca().set_aspect('equal', adjustable='box')
    if mode == 'show':
        plt.show()
    elif mode == 'save':
```



```

plt.savefig('{0}/{1}'.format(save_folder, imgname),
bbox_inches='tight')

def main():
    # define 3D domain
    Lx = 1
    Ly = 1
    Lz = 1
    tfinal = 2000 # final simulation time (CHANGEABLE)
    dt = 0.005 # time step (CHANGEABLE)
    numiter = np.ceil(tfinal/dt)
    numimg = 100 # number of images in gif (CHANGEABLE)
    interv = np.ceil(numiter/numimg)
    npart = 100 # number of particles

    # define constants
    eps_m = 8.85e-12
    eps_p = 8.85e-11
    sig_m = 0
    sig_p = 6e-15
    freq = 10 # changeable (Hz)
    w = freq*2*np.pi
    gz = 1.62
    tau_mw = (eps_p + eps_m)/(sig_p + 2*sig_m)
    appendterm = 3*(eps_m*sig_p -
eps_p*sig_m)/(tau_mw*(sig_p+2*sig_m)**2*(1+tau_mw**2*w**2))
    ReKw = (eps_p - eps_m)/(eps_p + 2*eps_m) + appendterm
    # print(ReKw)

    # allocate particles
    xp = np.zeros(npart)
    yp = np.zeros(npart)
    zp = np.zeros(npart)
    up = np.zeros(npart)
    vp = np.zeros(npart)
    wp = np.zeros(npart)

```

```

# particle properties (see if can be done pseudo-randomly as per
distribution)
dp = 63e-6
rp = dp/2
rho_p = 1.56/1000000
rho_q = 3.3e-6
Vp = 4/3*np.pi*rp**3
Sp = 4*np.pi*rp**2
mp = rho_p*Vp # kind of like Stokes number in this case
qp = rho_q*Sp
# print(2*np.pi*eps_m*rp**3/mp)

# randomly allocate particles on grid
x0 = Lx/2
y0 = Ly/2
r = 0.1
i = 0
while i < npart:
    xp[i] = Lx * np.random.rand(1,1)[0,0]
    yp[i] = Ly * np.random.rand(1,1)[0,0]
    if np.sqrt((xp[i] - x0)**2 + (yp[i] - y0)**2) <= r:
        # up[0,i], vp[0,i] = taylor_green(xp[0,i], yp[0,i])
        i = i+1

# plot the electric field function
nx = 200
ny = 200
x = np.linspace(0, Lx, num=nx)
y = np.linspace(0, Ly, num=ny)
Ex = np.zeros((nx, ny))
Ey = np.zeros((nx, ny))
for i in range(nx):
    for j in range(ny):
        Ex[i,j] = np.sin(2*np.pi*x[i])*np.cos(2*np.pi*y[j])
        Ey[i,j] = -1*np.cos(2*np.pi*x[i])*np.sin(2*np.pi*y[j])
[XG, YG] = np.meshgrid(x, y)

```

```

    # plt.streamplot(XG, YG, np.transpose(Ex[0:nx, 0:ny]),
np.transpose(Ey[0:nx, 0:ny]), color='r', linewidth=0.2)

# implemented scheme (Euler)
images = [] # stores images for final gif
t = 0
coun = 0
imgname = 'plot_{0}.png'.format(np.round(t, 0))
create_plot(xp, yp, 0.03, Lx, Ly, 'save', SAVE_FOLDER, imgname) #
plot initial condition
while t < tfinal:
    if t != 0:
        # perform boundary checks at each iteration (TODO:check
boundaries)
        # ex, ey, ez = efield(xp, yp, zp)
        gradfac = 1 # changeable
        dex2, dey2, dez2 = efield2_grad(xp, yp, zp, gradfac)
        xp = xp + dt*up
        yp = yp + dt*vp
        # zp = zp + dt*wp
        up = up + dt*(2*np.pi*eps_m*rp**3/mp*ReKw*dex2)
        vp = vp + dt*(2*np.pi*eps_m*rp**3/mp*ReKw*dey2)
        # zp = wp + dt*()
    t = t+dt
    # print(t)
    if coun != 0 and coun % interv == 0:
        imgname = 'plot_{0}.png'.format(np.round(t, 0))
        create_plot(xp, yp, 0.03, Lx, Ly, 'save', SAVE_FOLDER,
imgname) # images for gif
        images.append(im.imread(os.path.join(SAVE_FOLDER, imgname)))
    coun += 1

count_left = 0
for i in range(len(xp)):
    if (xp[i] <= 1 and xp[i] >= 0) and (yp[i] <= 1 and yp[i] >= 0):
        count_left += 1

```

```
effective = (npart-count_left)/npart*100
print(effective)

# save movie
im.mimsave(os.path.join(SAVE_FOLDER, 'particlesim.gif'), images,
fps=100)

if __name__ == '__main__':
    main()
```

APPENDIX D (CONCEPT SCREENING DOCUMENTATION)

Eliminated through gut check

Eliminated through practicality

Eliminated through monetary restrictions

Eliminated through complexity/scope

Eliminated based on foreseeable effectiveness

Eliminated based on ease of use

Eliminated based on durability/robustness

Also look at alignment with requirements and specifications

Post EVA Removal (generated in brainstorming)

1. Vacuum Cleaner
2. Dust Brushes
3. Scrubs
4. Electromagnetic Dust Removal
5. Microwave Dust
6. Electric + Air Dust Removal
7. Cleaning Liquid
8. Ultrasonic Vibrations
9. Sticky Mats
10. Licking Technology
11. Electromagnetic Storage Locker
12. Internal Vacuum + Wind Technology in Locker

Real Time Mitigation (generated in brainstorming)

1. EDS
 - a. Nano Circuits
 - b. Copper w/ Shielding
 - c. Carbon Nanotubes
 - i. Topmost Surface of Suits
 - ii. Wearable Non-Embedded Weave
 - iii. Nanotube suit add-ons/sleeves
2. Kevlar
 - a. Nanotubes
 - b. Laminate clip-on sleeves
3. Zorb balls
 - a. Encasing umbrella attached to back of spacesuit
 - b. Encasing umbrella held up by compressed air drone
4. Magnetic field repulsion
 - a. Wearable magnetic suit that creates invisible repulsive barrier

Eliminated through gut check

Eliminated through practicality

Eliminated through monetary restrictions

Eliminated through complexity/scope

Eliminated based on foreseeable effectiveness

Eliminated based on ease of use

Eliminated based on durability/robustness

Also look at alignment with requirements and specifications

5. Bunny adhesive suit
 - a. Worn above spacesuit before conducting EVA
6. Hand-held device that removes dust
 - a. Remove dust on suit
 - i. Air hose
 - ii. EM wave generator
 - iii. Microwave radiation generator
 - iv. Vibration generator
 1. Ultrasonic waves
 - b. Remove dust from surroundings
 - i. Impinging jets
 - ii. Magnetic repulsion
 - c. Reverse photoionization dust removal technology
7. External aid
 - a. Surrounding robots that follow astronaut and clear dust from path
8. Removable Dust Storage Containers: Utilizing Electrostatic Attraction
 - a. Utilizing Electrostatic Attraction
 - b. Suction Technology
9. Nonwoven Fabric
 - a. Really Fine Weave
 - b. Low Fidelity Removal
 - c. Nonwoven

Post Concept Development Ideas

1. EDS (Design Heuristics)

- a. Incorporate on/off switch on EDS circuit to activate and deactivate mechanism on demand
- b. Make a full-body EDS circuit that spans over entire spacesuit
- c. Make EDS mats/sleeves that are appendable to various portions of spacesuit which require high lunar dust mitigation
- d. Integrate EDS circuit chains into the actual weave of the spacesuits
- e. Stacked EDS circuit layers for more effectiveness

Eliminated through gut check

Eliminated through practicality

Eliminated through monetary restrictions

Eliminated through complexity/scope

Eliminated based on foreseeable effectiveness

Eliminated based on ease of use

Eliminated based on durability/robustness

Also look at alignment with requirements and specifications

~~f. Consider use of different materials for the EDS circuit components (carbon nanotubes, Kevlar?, copper, polypeptide nanotubes)~~

~~g. Potentially attach EDS to inside and outside of spacesuit to increase effectiveness~~

2. Realtime Dust Storage Canisters

a. Button that can be pressed to activate canister storage system

b. Instead of mini-canisters attached to various parts of the spacesuit for storage, we use a backpack or larger container at the back to store all the sucked dust

~~c. Dust canisters are made of adhesive materials which capture dust from the outside well~~

d. Canisters attach to spacesuit with some plug-socket configuration

~~e. Canisters can be daisy-chained to one another to increase lunar dust storage capacity if needed~~

~~3. e "Shiver-like" vibration for dust removal~~

4. Layered dust trap in locker

5. Storage Locker + Electrostatics + Vibration

a. Automated removal of suit with control interface

b. Smaller sub-lockers for glove/helmets/detachable space suit equipment

~~c. Centrifugal rotation for dust removal~~

~~d. High frequency, low amplitude~~

e. Locker coated in material that attracts dust particles

f. Some surfaces of locker generate electric field, others produce vibrations

6. Bunny adhesive suit

a. Detachable, jumper-like suit

b. Bunny suit sleeves for high dust accumulation areas on suit - arms, legs

~~c. Roll on bunny suit material~~

d. Use natural adhesives

~~e. See #'s 1,2,3~~

f. Multiple layers of bunny suits

g. Bunny suit with dust resistant coating

~~h. Reversible bunny suits~~

Eliminated through gut check

Eliminated through practicality

Eliminated through monetary restrictions

Eliminated through complexity/scope

Eliminated based on foreseeable effectiveness

Eliminated based on ease of use

Eliminated based on durability/robustness

Also look at alignment with requirements and specifications

Real Time Mitigation (generated in brainstorming)

16. EDS

- a. Nano Circuits
- b. Copper w/ Shielding
- c. Carbon Nanotubes
 - i. Topmost Surface of Suits
 - ii. Wearable Non-Embedded Weave
 - iii. Nanotube suit add-ons/sleeves

17. Kevlar

- a. Nanotubes
- b. Laminate clip-on sleeves

18. Zorb balls

- a. Encasing umbrella attached to back of spacesuit
- b. Encasing umbrella held up by compressed air drone

19. Magnetic field repulsion

- a. Wearable magnetic suit that creates invisible repulsive barrier

20. Bunny adhesive suit

- a. Worn above spacesuit before conducting EVA

21. Hand-held device that removes dust

- a. Remove dust on suit
 - i. Air hose
 - ii. EM wave generator
 - iii. Microwave radiation generator
 - iv. Vibration generator
 1. Ultrasonic waves
- b. Remove dust from surroundings
 - i. Impinging jets
 - ii. Magnetic repulsion
- c. Reverse photoionization dust removal technology

Eliminated through gut check

Eliminated through practicality

Eliminated through monetary restrictions

Eliminated through complexity/scope

Eliminated based on foreseeable effectiveness

Eliminated based on ease of use

Eliminated based on durability/robustness

Also look at alignment with requirements and specifications

Real Time Mitigation (generated in brainstorming)

10. EDS

a. Nano Circuits

b. Copper w/ Shielding

c. Carbon Nanotubes

i. Topmost Surface of Suits

ii. Wearable Non-Embedded Weave

iii. Nanotube suit add-ons/sleeves

11. Kevlar

a. Nanotubes

b. Laminate clip on sleeves

12. Zorb balls

a. Encasing umbrella attached to back of spacesuit

b. Encasing umbrella held up by compressed air drone

13. Magnetic field repulsion

a. Wearable magnetic suit that creates invisible repulsive barrier

14. Bunny adhesive suit

a. Worn above spacesuit before conducting EVA

15. Hand-held device that removes dust

a. Remove dust on suit

i. Air hose

ii. EM wave generator

iii. Microwave radiation generator

iv. Vibration generator

1. Ultrasonic waves

b. Remove dust from surroundings

i. Impinging jets

ii. Magnetic repulsion

c. Reverse photoionization dust removal technology

APPENDIX E (EDS CIRCUIT CONTROLLER CODE)

```
0 ,0 ,0 ,0 ,0 ,0 ,0 ,0 ,0 ,0 ,
0 ,0 ,0 ,0 ,0 ,0 ,0 ,0 ,0 ,0 ,
0 ,0 ,0 ,0 ,0 ,0 ,0 ,0 ,0 ,0 ,
0 ,0 ,0 ,0 ,0 ,0 ,0 ,0 ,0 ,0 ,
0 ,0 ,0 ,0 ,0 ,0 ,0 ,0 ,0 ,0 ,
0 ,0 ,0 ,0 ,0 ,0 ,0 ,0 ,0 ,0 ,
0 ,0 ,0 ,0 ,0 ,0 ,0 ,0 ,0 ,0 ,
0 ,0 ,0 ,0 ,0 ,0 ,0 ,0 ,0 ,0 ,
0 ,0 ,0 ,0 ,0 ,0 ,0 ,0 ,0 ,0 ,
50 ,100 ,151 ,201 ,250 ,300 ,349 ,398 ,446 ,494 ,
542 ,589 ,635 ,681 ,726 ,771 ,814 ,857 ,899 ,940 ,
981 ,1020 ,1058 ,1095 ,1131 ,1166 ,1200 ,1233 ,1264 ,1294 ,
1323 ,1351 ,1377 ,1402 ,1426 ,1448 ,1468 ,1488 ,1505 ,1522 ,
1536 ,1550 ,1561 ,1572 ,1580 ,1587 ,1593 ,1597 ,1599 ,1600 ,
1599 ,1597 ,1593 ,1587 ,1580 ,1572 ,1561 ,1550 ,1536 ,1522 ,
1505 ,1488 ,1468 ,1448 ,1426 ,1402 ,1377 ,1351 ,1323 ,1294 ,
1264 ,1233 ,1200 ,1166 ,1131 ,1095 ,1058 ,1020 ,981 ,940 ,
899 ,857 ,814 ,771 ,726 ,681 ,635 ,589 ,542 ,494 ,
446 ,398 ,349 ,300 ,250 ,201 ,151 ,100 ,50 ,0};
```

```
void setup(){
    // Register initilisation, see datasheet for more detail.
    TCCR1A = 0b10100010;
        /*10 clear on match, set at BOTTOM for compA.
        10 clear on match, set at BOTTOM for compB.
        00
        10 WGM1 1:0 for waveform 15.
        */
    TCCR1B = 0b00011001;
        /*000
        11 WGM1 3:2 for waveform 15.
        001 no prescale on the counter.
        */
    TIMSK1 = 0b00000001;
        /*0000000
        1 TOV1 Flag interrupt enable.
        */
```

```

0 ,0 ,0 ,0 ,0 ,0 ,0 ,0 ,0 ,0 ,
0 ,0 ,0 ,0 ,0 ,0 ,0 ,0 ,0 ,0 ,
0 ,0 ,0 ,0 ,0 ,0 ,0 ,0 ,0 ,0 ,
0 ,0 ,0 ,0 ,0 ,0 ,0 ,0 ,0 ,0 ,
0 ,0 ,0 ,0 ,0 ,0 ,0 ,0 ,0 ,0 ,
0 ,0 ,0 ,0 ,0 ,0 ,0 ,0 ,0 ,0 ,
0 ,0 ,0 ,0 ,0 ,0 ,0 ,0 ,0 ,0 ,
0 ,0 ,0 ,0 ,0 ,0 ,0 ,0 ,0 ,0 ,
50 ,100 ,151 ,201 ,250 ,300 ,349 ,398 ,446 ,494 ,
542 ,589 ,635 ,681 ,726 ,771 ,814 ,857 ,899 ,940 ,
981 ,1020 ,1058 ,1095 ,1131 ,1166 ,1200 ,1233 ,1264 ,1294 ,
1323 ,1351 ,1377 ,1402 ,1426 ,1448 ,1468 ,1488 ,1505 ,1522 ,
1536 ,1550 ,1561 ,1572 ,1580 ,1587 ,1593 ,1597 ,1599 ,1600 ,
1599 ,1597 ,1593 ,1587 ,1580 ,1572 ,1561 ,1550 ,1536 ,1522 ,
1505 ,1488 ,1468 ,1448 ,1426 ,1402 ,1377 ,1351 ,1323 ,1294 ,
1264 ,1233 ,1200 ,1166 ,1131 ,1095 ,1058 ,1020 ,981 ,940 ,
899 ,857 ,814 ,771 ,726 ,681 ,635 ,589 ,542 ,494 ,
446 ,398 ,349 ,300 ,250 ,201 ,151 ,100 ,50 ,0};

```

```

void setup(){
    // Register initilisation, see datasheet for more detail.
    TCCR1A = 0b10100010;
        /*10 clear on match, set at BOTTOM for compA.
        10 clear on match, set at BOTTOM for compB.
        00
        10 WGM1 1:0 for waveform 15.
        */
    TCCR1B = 0b00011001;
        /*000
        11 WGM1 3:2 for waveform 15.
        001 no prescale on the counter.
        */
    TIMSK1 = 0b00000001;
        /*0000000
        1 TOV1 Flag interrupt enable.
        */
}

```

```

    ICR1    = 1600;      // Period for 16MHz crystal, for a switching
frequency of 100KHz for 10 subdivisions per 10Hz sin wave cycle.
    sei();              // Enable global interrupts.
    DDRB = 0b00000110; // Set PB1 and PB2 as outputs.
    pinMode(13,OUTPUT);
}

void loop(){; /*Do nothing . . . . forever!*/}

ISR(TIMER1_OVF_vect){
    static int num;
    // change duty-cycle every period.
    OCR1A = lookUp1[num];
    OCR1B = lookUp2[num];

    if(++num >= 200){ // Pre-increment num then check it's below
200.
        num = 0;      // Reset num.
    }
}

```